AD-A174 492 HIGH SPEED LOW POWER NONLINEAR OPTICAL SIGNAL PROCESSING(U) GTE LABS INC WALTHAM MA M DAGENAIS ET AL 15 SEP 86 AFOSR-TR-86-1093 1/2

UNCLASSIFIED F490620-84-C-0052 F/G 20/6 NL

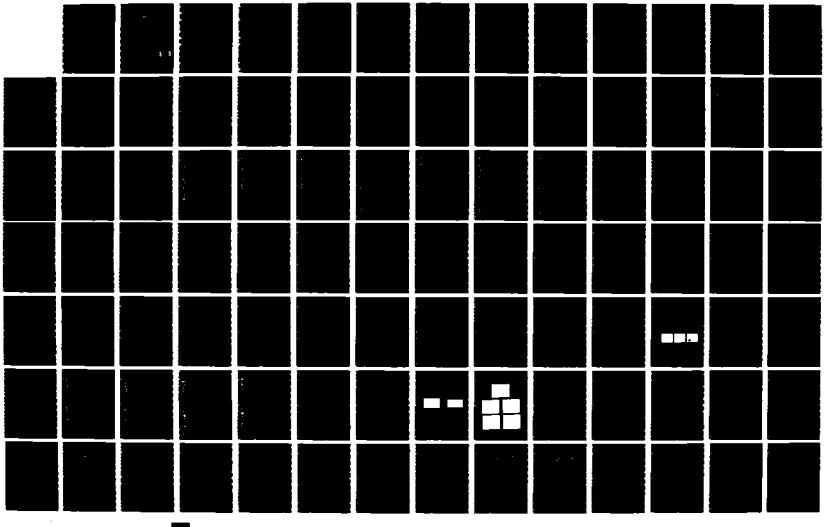

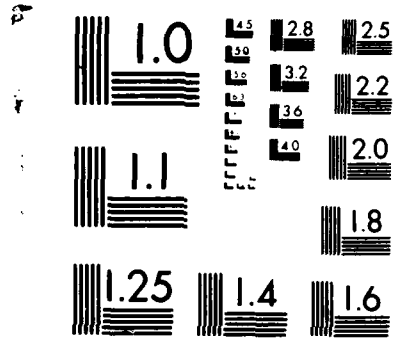

Research and Development

(2)

AFOSR-TR- 86-1093

R|D

High Speed Low Power Nonlinear Optical Signal Processing

Air Force Office of Scientific Research
Contract No. F49620-84-C-0052

Final Report
May 1984 through May 1986

M. Dagenais
W.F. Sharfin

September 1986

GTE Laboratories Incorporated
40 Sylvan Road
Waltham, MA 02254

GTE

UNCLASSIFIED
SECURITY CLASSIFICATION OF THIS PAGE

AD-A174 492

REPORT DOCUMENTATION PAGE

1a REPORT SECURITY CLASSIFICATION: UNCLASSIFIED	1b RESTRICTIVE MARKINGS
2a SECURITY CLASSIFICATION AUTHORITY	3 DISTRIBUTION/AVAILABILITY OF REPORT: Approved for public release; distribution unlimited.
2b DECLASSIFICATION/DOWNGRADING SCHEDULE	
4 PERFORMING ORGANIZATION REPORT NUMBER(S)	5 MONITORING ORGANIZATION REPORT NUMBER(S): AFOSR-TR- 86-1093
6a NAME OF PERFORMING ORGANIZATION: GTE LABORATORIES, INC. / 6b OFFICE SYMBOL (If applicable)	7a NAME OF MONITORING ORGANIZATION: AFOSR
6c ADDRESS (City, State and ZIP Code): 40 Sylvan Road, Waltham, MA 02254	7b ADDRESS (City, State and ZIP Code): same as 8c
8a NAME OF FUNDING/SPONSORING ORGANIZATION: Air Force Office of Scientific Research / 8b OFFICE SYMBOL (If applicable): AFOSR/NE	9. PROCUREMENT INSTRUMENT IDENTIFICATION NUMBER: F49620-84-C-0052
8c ADDRESS (City, State and ZIP Code): Building 410, Bolling AFB, DC 20332-6448	10 SOURCE OF FUNDING NOS: PROGRAM ELEMENT NO. 61102F; PROJECT NO. 2305; TASK NO. B4; WORK UNIT NO.
11. TITLE (Include Security Classification): High Speed Low Power Nonlinear Optical Signal Processing (Unclassified)	
12. PERSONAL AUTHOR(S): Dagenais, Mario and Sharfin, Wayne F.	
13a TYPE OF REPORT: Final Technical Report / 13b. TIME COVERED: FROM 5/26/84 TO 7/26/86	14 DATE OF REPORT (Yr., Mo., Day): September 15, 1986 / 15. PAGE COUNT
16. SUPPLEMENTARY NOTATION	

17 COSATI CODES		
FIELD	GROUP	SUB GR

18 SUBJECT TERMS (Continue on reverse if necessary and identify by block number): Excitons, Nonlinear Optics, Quantum Dots, Modulators, Polaritons, Exciton Damping, Optical Bistability, Optical Switching, Quantum Confined Stark Effect, Bound Exciton

19 ABSTRACT (Continue on reverse if necessary and identify by block number)

During the two-year period of this contract, substantial progress was made in the understanding of both the linear and the nonlinear optical properties of direct gap semiconductors and in the implications for high speed, low power, nonlinear optical signal processing. In particular, the detuning and the temperature dependence of the damping of an exciton-polariton was obtained for the first time. The lowest single beam switching energy (< 4 pJ) and the fastest reported ON/OFF switching (< 1 ns) bistable device with clearly resolved stable states was demonstrated using the nonlinearity associated with bound excitons in CdS. Thermal effects on the millisecond and microsecond time scales were experimentally studied. Optical bistability due to induced absorption near the free and bound exciton was experimentally studied with and without a Fabry-Perot cavity. Large degenerate four-wave mixing signals were observed near free and bound excitons in CdS at cryogenic temperatures. Nonlinear transmission signals were studied at different detunings below the free exciton resonance and at temperatures up to 120 K. These signals were interpreted in terms of a broadening of

20 DISTRIBUTION AVAILABILITY OF ABSTRACT: UNCLASSIFIED/UNLIMITED ☒ SAME AS RPT ☐ DTIC USERS ☐	21 ABSTRACT SECURITY CLASSIFICATION: UNCLASSIFIED
22a NAME OF RESPONSIBLE INDIVIDUAL: Dr. Lee Giles	22b TELEPHONE NUMBER (Include Area Code): 202-767-4931 / 22c OFFICE SYMBOL: NE

DD FORM 1473, 83 APR EDITION OF 1 JAN 73 IS OBSOLETE.

SECURITY CLASSIFICATION OF THIS PAGE

19. ABSTRACT (Continued)

the free exciton resonance by exciton-exciton collisions. The quantum confined Stark shifting of a quantum dot was performed for the first time. A new generation of efficient optical modulators is envisioned.

Research Objectives

Some of the largest optical nonlinearities in nature have been observed in direct-gap semiconductors exhibiting excitonic effects. Because these large nonlinearities open new possibilities in the field of all-optical signal processing, they have recently attracted much attention. So far, the main efforts in this field have been devoted to minimizing the switching energy of semiconductor optical bistable devices or optical logic elements for low or room temperature operation. A good physical understanding of the role of phonons, impurities, carriers, and carrier-exciton interactions on the switching energy of bistable devices is still required. The study of the resonant nonlinearities associated with free and bound excitons in CdS is a very fruitful area of research. For these reasons, we have proposed a comprehensive research program that has three major thrusts.

1. To characterize the optical nonlinear response of bound excitons in CdS and to demonstrate the fast and low power operation of an all-optical bistable device (p. 3 of our proposal);

2. To demonstrate novel electro-optical and all-optical signal processing functions (pp. 3-4 of our proposal);

3. Study the temperature and the density dependence of the free exciton broadening and determine implications for other semiconductor systems.

NB. The third research thrust is different from the one in the original proposal. Both parties agreed on this change in prior correspondences.

CONTENTS

1. INTRODUCTION

During the two-year period of this contract, substantial progress was made in the understanding of both the linear and the nonlinear optical properties of direct gap semiconductors and in the implications for high speed, low power, nonlinear optical signal processing. In particular, the detuning and the temperature dependence of the damping of an exciton-polariton was obtained for the first time. The lowest single beam switching energy (< 4 pJ) and the fastest reported ON/OFF switching (< 1 ns) bistable device with clearly resolved stable states was demonstrated using the nonlinearity associated with bound excitons in CdS. Thermal effects on the millisecond and microsecond time scales were experimentally studied. Optical bistability due to induced absorption near the free and bound exciton was experimentally studied with and without a Fabry-Perot cavity. Large degenerate four-wave mixing signals were observed near free and bound excitons in CdS at cryogenic temperatures. Nonlinear transmission signals were studied at different detunings below the free exciton resonance and at temperatures up to 120 K. These signals were interpreted in terms of a broadening of the free exciton resonance by exciton-exciton collisions. The quantum confined Stark shifting of a quantum dot was performed for the first time. A new generation of efficient optical modulators is envisioned.

The report is divided in the following way. We first discuss both theoretically and experimentally the linear transmission characteristics of a good optical quality CdS platelet near the band gap. We then present the experimental measurements of the nonlinear optical properties of both bound and free excitons. We then conclude and make suggestions for further research directions.

2. LINEAR PROPERTIES OF FREE AND BOUND EXCITONS: THEORY

2.1 EXCITON-POLARITON

Some of the largest optical nonlinearities in nature have been observed in direct-gap semiconductors exhibiting excitonic effects. Since cadmium sulfide (CdS) exhibits very strong excitonic effects at low temperatures and can be grown in very good optical quality, high purity platelets, it was chosen as an ideal candidate for the study of optical nonlinear interactions in direct gap semiconductors[1]. But in order to have a good understanding of nonlinear interactions in semiconductors, it is absolutely necessary to obtain a deep understanding of the linear optical properties of the material. As will be seen, even though there is a substantial amount of information already available in the literature, not all the linear properties of CdS are understood. We have, in particular, contributed substantially to the present understanding of exciton dephasing in semiconductors. The linear optical properties of CdS near the band gap will now be reviewed.

In CdS, the valence-band and the conduction-band extrema are located at $K = 0$. The valence band of CdS is split by spin-orbit and crystal-field effects into three nearly degenerate p-like bands (Figure 1). This leads to three separate intrinsic exciton series, A, B, and C. Series A, occurring at the lowest photon energies, is strongly active only for light polarized with its E vector perpendicular to the c axis of the hexagonal crystal. Series B and C are active for both modes of polarization of the light. To a large extent, our studies concentrated on the ($n = 1$) A and B exciton using mostly light polarized perpendicular to the c-axis. The samples used for the studies were high-optical-quality platelets with low impurity concentration ($\leq 1 \times 10^{15}$/cc) grown from vapor phase with thicknesses varying between 1 and

SKETCH OF THE BAND EXTREMA IN CdS

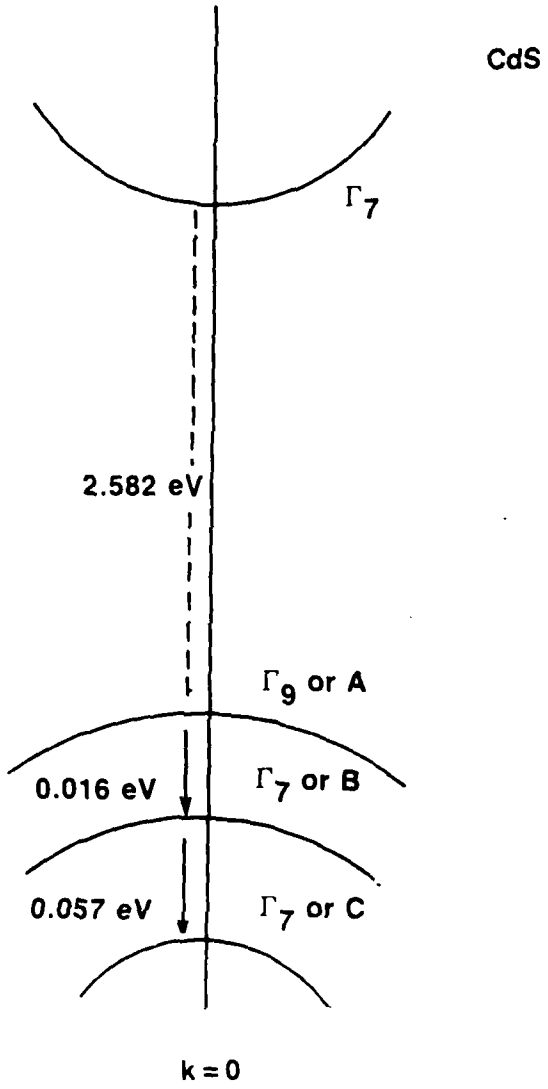

- Γ_9 Valence Band Is Strongly Active for $E \perp c$
- Γ_7 Valence Bands Are Strongly Active for both $E \perp c$ and $E \| c$

Figure 1

35 μm. They were generously supplied to us by Dr. D. C. Reynolds from Wright-Patterson Air Force Base, who grew them more than 15 years ago. At cryogenic temperatures, excitonic effects in CdS dominate the linear optical properties. Their properties are now discussed.

Excitons are electronic excitations of semiconductors and insulators consisting of Coulomb-correlated electron-hole pairs. Exciton polaritons are composite quasi-particles formed by the coupling of light and dipole-active excitons.

The dispersion relation, expressed by the dielectric constant $\varepsilon(K, \omega)$, is given in the single-exciton-band approximation as

$$\varepsilon(K, \omega) = \frac{c^2K^2}{\omega 2(K)} = (n+i\kappa)^2 = \varepsilon_b + \frac{4\pi\beta\omega_n^2(K)}{\omega_n^2(K) - \omega^2(K) - i\omega(K)\Gamma}, \quad (1)$$

where $\omega_n(K)$ is given by the following expression in the parabolic and nondegenerate band case:

$$h\omega_n(K) = E_{n,T} + \frac{h^2K^2}{2M_x}, \quad (2)$$

and κ is related to the absorption coefficient α by:

$$\frac{2\omega}{c} \kappa = \alpha \quad (3)$$

$E_{n,T}$ is the nth transverse exciton energy, and $h^2K^2/2M_x$ represents the translational kinetic energy of the exciton as a function of its wave vector K and translational mass $M_x = m_e + m_h$. β is the exciton polarizability, ε_b is the background dielectric constant, which contains contributions from all interactions except the exciton in question, and Γ describes the damping of the polariton. The polariton dispersion curves are obtained by solving Eq. (1) for $\omega(K)$ and are shown in Figure 2 for the case of the A and B excitons in CdS. Table 1 gives the value of relevant CdS parameters. For energies far below $E_{n,T}$ the exciton polariton (known as the lower polariton) is fundamentally photonlike. As the frequency increases, the polariton takes on more of an exciton character, until at and above $\omega_{n,T}$, it is primarily excitonlike. At a frequency identified as ω_{nL} a new inner polariton branch (known as the upper polariton) arises, which quickly takes on a predominantly photon character. These modes exist simultaneously because the effective exciton mass M_x is finite. The strength of the exciton-photon interaction can be described equivalently by a number of interrelated quantities, such as the total oscillator strength per unit cell f_{exc}, the exciton polarizability β, and the longitudinal-transverse splitting $E_{nLT} = h(\omega_{nL} - \omega_{nT})$. In the spherical hydrogenic approximation for the 1s-exciton ground state, we have

$$f_{exc} \simeq \frac{3P^2}{E_G} \frac{\Omega}{\pi a_B^3} \tag{4}$$

More generally, for an anisotropic crystal, we can write

$$f_{exc} \equiv \sum_{i=x,y,z} f^i_{exc} , \tag{5a}$$

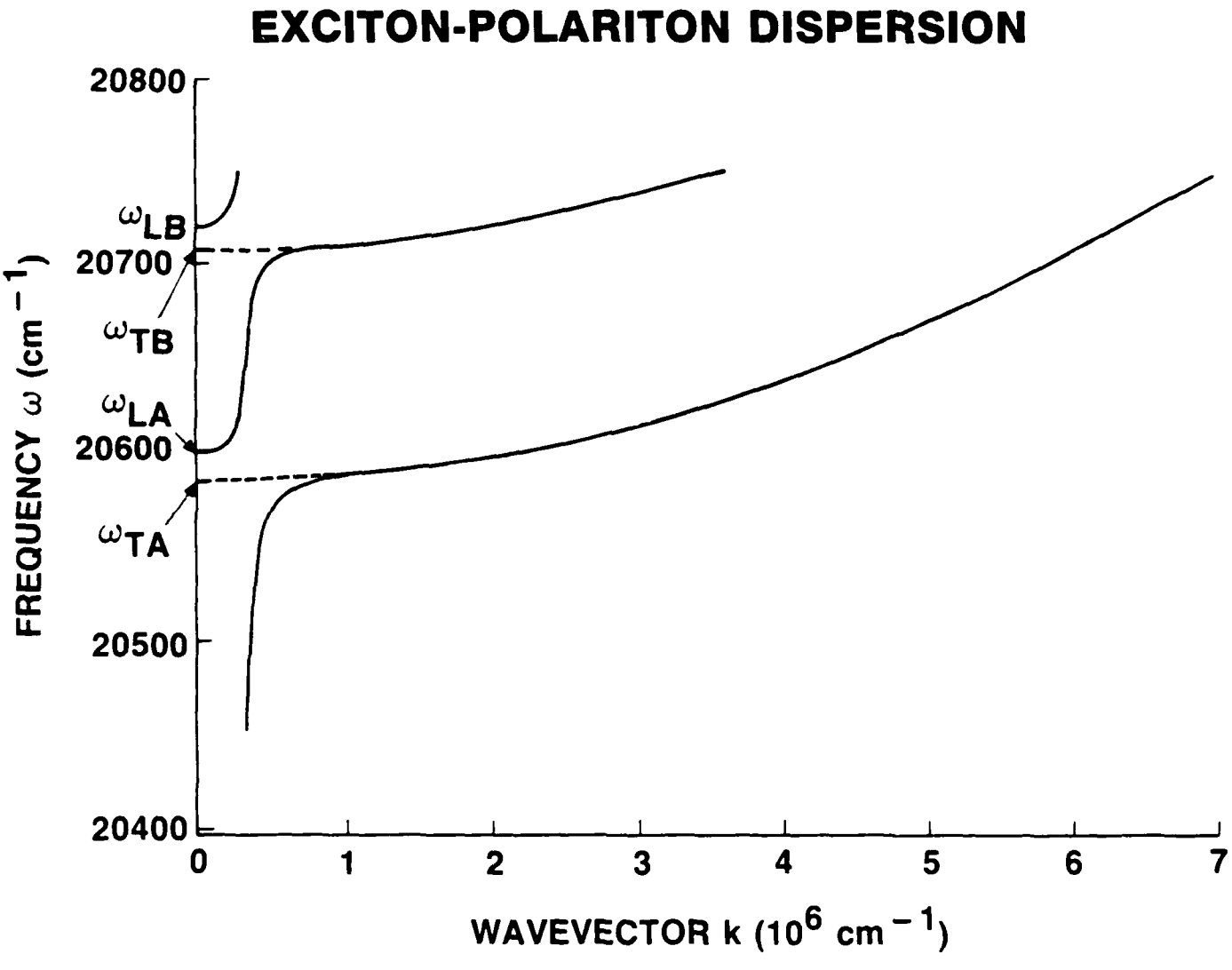
EXCITON-POLARITON DISPERSION
20800
ω_{LB}
20700
ω_{TB}
ω_{LA}
20600
ω_{TA}
20500
20400
FREQUENCY ω (cm^{-1})
0
1
2
3
4
5
6
7
WAVEVECTOR k (10^6 cm^{-1})

Figure 2

Table 1. Properties of CdS Near the A and B Free Excitons

$$f^{\perp}_{Aexc} = 2.3 \times 10^{-3}$$

$$f^{z}_{Aexc} = 0$$

$$f^{\perp}_{Bexc} = 1.68 \times 10^{-3}$$

$$m_{e|A_{exc}} = m_{e|B_{exc}} = 0.20m_0$$

$$m_{h\perp|A_{exc}} = m_{h\perp/B_{exc}} = 0.69m_0$$

$$m_{h/\!/|A_{exc}} = m_{h/\!/B_{exc}} = 2.65m_0$$

$$E_{TA} = 20583.8 \text{ cm}^{-1}$$

$$= 2.5521 \text{ eV}$$

$$E_{TB} = 20706.0 \text{ cm}^{-1}$$

$$= 2.5672 \text{ eV}$$

$$E_{b_{(I2)}} \simeq 52 \text{ cm}^{-1} = 6.4 \times 10^{-3} \text{ eV}$$

$$\Omega = 4.98 \times 10^{-29} \text{ m}^3$$

$$n_{b_{Aexc}} = \varepsilon_{b|Aexc}^{1/2} = 2.52$$

$$n_{b|_{Bexc}} = \varepsilon_{b|_{Bexc}}^{1/2} = 2.22$$

$$a_B = 3.0 \times 10^{-9} \text{ m}$$

$$E_{LT|_{Aexc}} = 15.8 \text{ cm}^{-1}$$

$$= 1.96 \times 10^{-3} \text{ eV}$$

$$E_{LT|_{Bexc}} = 14.5 \text{ cm}^{-1}$$

$$= 1.80 \times 10^{-3} \text{ eV}$$

$$E_G(T = 2K) = 20817 \text{ cm}^{-1}$$

$$= 2.581 \text{ eV}$$

NB: The c axis is taken along the z direction. Both the x and z axes are taken in the plane of the sample.

$$4\pi\beta^i = \frac{2E_{LT}\epsilon_b^i}{E_G} = \frac{e^2}{\epsilon_0 m_o}\frac{\hbar^2}{\Omega}\frac{f_{exc}^i}{E_G^2}, \qquad (5b)$$

where i = x,y,z refers to the polarization of the incident beam of light. P^2 is the reduced interband matrix element ($P^2 = 2|\langle c|P|v\rangle|^2/m_o$) between conduction-band states c and valence-band states v, Ω is the volume of the unit cell, m_o is the free-electron mass, and a_b is the Bohr radius of the exciton. The exciton admixture is almost total for a wide range around the resonance determined by $h\omega_c = (E_{LT}E_T)^{1/2}$. In CdS, ω_c is 574 cm^{-1} around the A and B excitons. For $\Gamma << \omega_{LT}$, the polariton description is the appropriate description for describing the propagation of a strongly coupled exciton-photon system. In this case, the polariton is the only allowed mode of propagation in the crystal. In samples of extremely high purity (impurity concentration < 10^{14} cm^{-3}), near liquid-He temperatures, it is predicted that polaritons can traverse a sample with relatively little absorption. At low temperatures, the integrated absorption [$\int_0^\infty \alpha(\omega)\, d\omega$] in such samples decreases with a decrease in temperature. This situation occurs when the time between collisions with phonons (acoustical or optical) or impurities is longer than the lifetime τ extracted from the full free exciton oscillator strength f_{Exc} [$\equiv(\pi a_B^3/\Omega)\, f_{exc}$]:

$$\tau = \frac{6\pi m_0 \epsilon_0 c^3}{e^2\omega^2 f_{Exc} n_b} \qquad (6)$$

In practice, this occurs only in the purest samples with few defects. In a more typical good-quality sample, the integrated absorption does not significantly vary with temperature. For an incident beam with its polarization along the i axis and for sufficient detuning (or at high temperatures), the

absorption and the index of refraction can conveniently be represented by the following two expressions:

$$a^i(\omega) \approx \frac{\pi e^2 f^i_{exc}}{2\varepsilon_0 m_0 c\Omega n_b} \frac{T_2/\pi}{1 + (\omega_T - \omega)^2 T_2^2} , \tag{7}$$

$$n^i(\omega) \approx n_b + \frac{\lambda e^2 f^i_{exc}}{8\pi\varepsilon_0 m_0 c\Omega n_b} \frac{(\omega_T - \omega) T_2^2}{1 + (\omega_T - \omega)^2 T_2^2} , \tag{8}$$

with i = x,y,z.

These expressions predict the group velocity v_g away from resonance:

$$v_g \approx \frac{c}{n_b} \left[1 + \frac{\omega_c^2}{(\omega_T - \omega)^2} \right]^{-1} \tag{9}$$

They also correctly predict the spacing $\Delta\lambda$ between two Fabry-Perot transmission peaks:

$$\Delta\lambda = \frac{\lambda^2}{2L\left(n_b - \lambda \frac{dn}{d\lambda}\right)} = \frac{\lambda^2 v_g}{2Lc} \tag{10}$$

where L is the sample thickness, n_b is the background index of refraction excluding, of course, the contribution from the considered exciton, and λ is the wavelength of light in vacuum. In these expressions, T_2 can be interpreted as the time between the collision of a polariton with another polariton, a phonon (acoustical or optical), or an impurity. T_2 is energy dependent. The polariton interacts with phonons through its exciton component and is scattered into other polaritons.

If a polariton collides inelastically with an impurity, it can get trapped. This process directly affects the lifetime of a polariton. Polaritons are trapped through their exciton components and may become bound excitons. Before they are scattered by phonons or impurities, the polaritons travel in the crystal at the group velocity v_g. However, after a few collisions, it is more appropriate to describe their propagation as a random walk in the crystal. In this description, the polariton constantly changes direction under the effects of phonons or elastic collisions on impurities (T_2 process). Occasionally, they are trapped and form bound excitons (T_1 process).

2.2 BOUND EXCITONS

In the absorption spectra of pure direct-gap semiconductors at low temperature, a number of narrow and weaker lines occur at energies just below the exciton bands. They have been observed in many semiconductors (CdS, CdSe, GaAs, InP, CuCl, etc.). In luminescence experiments on pure samples, most of the emitted light comes from these lines. In 1962, Rashba and Gurgenishivili[2] were the first to interpret correctly the physical origin of these lines in terms of radiative decay of a weakly bound exciton. They pointed out that excitons, weakly bound to impurities, have giant oscillator strengths that are many orders of magnitude larger than the oscillator strength per molecule of the free exciton. Their reasoning is reproduced below[3].

Let $\psi(\vec{r}_e,\vec{r}_h)$ be the envelope function for an exciton (free or bound). The oscillator strength of an allowed transition is given by

$$f = C^2 \left| \int d\vec{x}\psi(\vec{x},\vec{x}) \right|^2, \qquad (11)$$

where C is a constant of proportionality including the electric-dipole matrix element. For an exciton of wave vector $\vec{K}$, the envelope function is given by

$$\psi(\vec{r}_e,\vec{r}_h) = V^{-1/2}\exp(i\vec{K} \cdot \vec{R})\ \phi_{ex}(\vec{r}_e - \vec{r}_h), \tag{12}$$

where R is the center-of-mass coordinate:

$$\vec{R} = \frac{m_e}{M}\ \vec{r}_e + \frac{m_h}{M}\ \vec{r}_h, \tag{13}$$

ϕ_{ex} describes the relative motion of the electron and the hole, and V is the volume of the crystal. Transitions are allowed only for K = 0. The oscillator strength of the free exciton per molecule becomes

$$f_{exc} = C^2|\phi_{ex}(0)|^2\Omega, \tag{14}$$

where Ω is the volume of one CdS molecule. From Eqs. (11) and (14), we deduce that

$$f = f_{exc}\left[\frac{|\int dx\psi(\vec{x},\vec{x})|^2}{|\phi_{ex}(0)|^2\Omega}\right] \tag{15}$$

When an exciton is weakly bound to a center, it may be regarded as a quasiparticle moving in the field of the center as a single entity, the radius of this state exceeding that of the internal motion in the exciton. Using the

deuteron approximation in which the wave function is completely determined by the coupling energy, we write

$$\psi(\vec{r}_e,\vec{r}_h) = \phi_{ex}(\vec{r}_e - \vec{r}_h)F(R) = \phi_{ex}(\vec{r}_e - \vec{r}_h)\ \frac{e^{-R/\sigma}}{(2\pi\sigma)^{1/2}R}\ , \tag{16}$$

where

$$\sigma = \left(\frac{\hbar^2}{2M_x E_B}\right)^{1/2} .$$

E_B is the binding energy of the exciton bound to the impurity. For ellipsoidal bands, M_x is given by $M_x = [(m_e + m_{h\perp})^2 (m_e + m_{h/\!/})]^{1/3}$. $m_{h\perp}$ and $m_{h/\!/}$ are the hole masses when light propagates perpendicular and parallel, respectively, to the c axis. Using Eq. (16) in Eq. (15), we find that

$$f = f_{exc}\left|\int F(\vec{x})d\vec{x}\right|^2/\Omega \tag{17}$$

We then get

$$f = 8f_{exc}\ \frac{\pi\sigma^3}{\Omega} \tag{18}$$

$$f = 8f_{exc}\left(\frac{\mu_x E_{exc}}{M_x E_B}\right)^{3/2}\frac{\pi a_B^3}{\Omega}\ , \tag{19}$$

where μ_x is the exciton reduced mass. The factor $8\pi\sigma^3/\Omega$ is the bound-exciton oscillator strength-enhancement factor over the free-exciton oscillator strength per molecule of the crystal. The enhancement factor for neutral donors or acceptors is of the order of 1000, and for ionized donors it is of the order of 10,000. In this context, we speak of giant oscillator strengths for these systems. The wave function of the exciton weakly bound to the defect involves a large region around the defect, and the oscillations of the electronic polarization are coherent over the whole region. More-detailed calculations[4] indicate that Eqs. (18) and (19) are more accurate for describing excitons bound to neutral acceptors than to neutral or ionized donors. Associated with the large oscillator strengths is a short radiative lifetime given by

$$\tau_{spont} = \frac{6\pi m_0 \varepsilon_0 c^3}{e^2 \omega^2 f n_b} , \qquad (20)$$

The spontaneous lifetime of a direct-gap bound exciton is typically less than 1 nsec.

In addition to decaying radiatively, excitons bound to neutral donors or acceptors can decay nonradiatively by means of Auger processes. In the latter, an electron and a hole recombine, and the energy of the bound exciton is transferred to the other electron on the donor or the hole in the acceptor. The electron or hole is ejected from the impurity with a large kinetic energy. The Auger lifetime has been measured for the case of excitons bound to neutral donors in indirect-gap semiconductors[5]. There it was found to be larger than 10 nsec. There appears to be no fundamental reason why the Auger decay rate should be much different in a direct-gap semiconductor. For this reason, it

is believed that bound excitons in direct-gap semiconductors decay mostly radiatively. This is not to say that no heat is generated in the crystal when light is absorbed by bound excitons. Multiple internal surface reflections followed by tail absorption from the free excitons and nonradiative decay may generate heat. Heating can be alleviated by using a sharp focusing geometry, enabling the heat to diffuse away rapidly from the small focal region. In CdS, we have only observed excitons bound to neutral (the I_2 line) and ionized donors.

3. LINEAR PROPERTIES OF FREE AND BOUND EXCITONS: EXPERIMENTAL RESULTS

3.1 LINEAR TRANSMISSION MEASUREMENTS NEAR THE BAND GAP AT 2 K

Our linear measurements on CdS samples consist mostly of optical transmission measurements. The experimental apparatus is shown in Fig. 3. A krypton ion pumped cw ring dye laser (Spectra Physics model 380) with coumarin 102 dye operating near 487 nm is used as the source. The laser has a multimode linewidth of 20 GHz. Since the A free exciton resonance is only dipole active for E c, a half-wave plate is used to orient the electric field vector until maximum absorption is obtained at the A free exciton resonance. The crystal c axis is in the plane of the platelet. The light is focused to a 30-μm-diam spot ($1/e^2$) on the sample with a 10.0-cm focal length lens. A photodiode monitors a small fraction of the input light and another photodiode placed about 20 cm beyond the sample monitors the whole transmitted beam. The laser is scanned continuously with a computer controlled stepping motor that turns the birefringent filter inside the dye beam cavity. The wavelength of the light is accurately monitored by a Burleigh wavemeter and this number is stored in

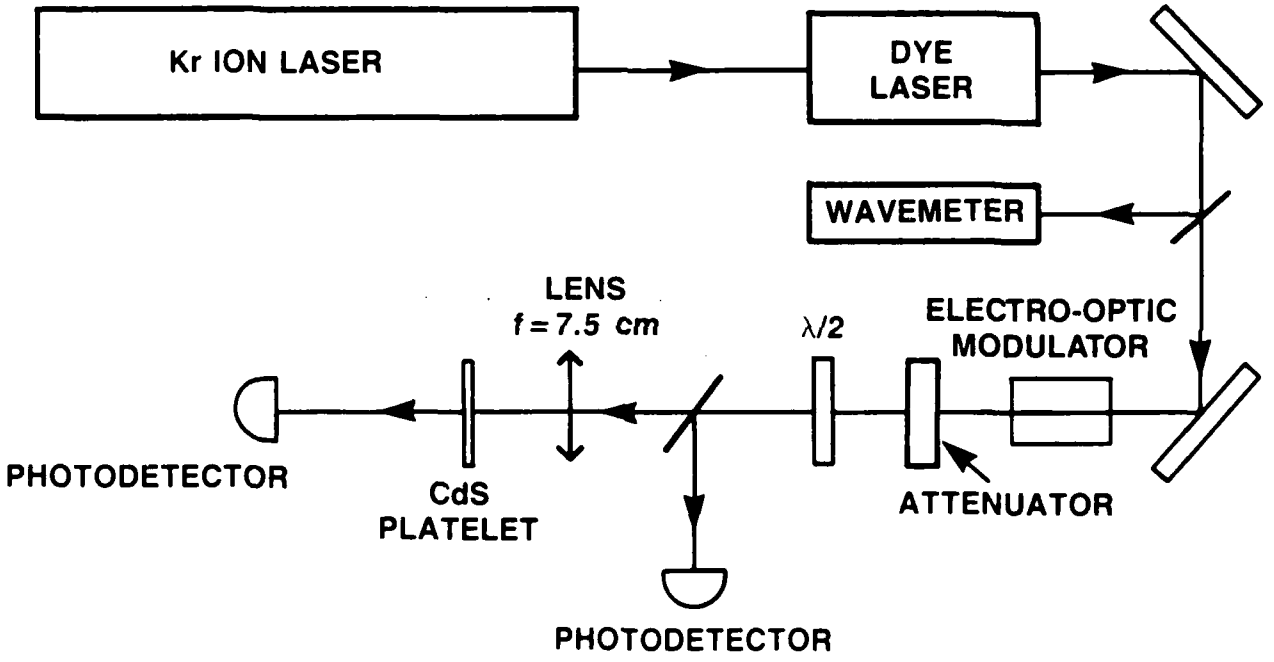

Figure 3. Block diagram of the experimental setup.

memory at the same time as the transmission is read and stored in memory. An attenuator is used to attenuate the light without beam deflection. The good optical quality CdS samples that were studied vary in thickness between 1 and 35 μm. They are typically about 2 mm x 4 mm in dimensions. The thinner samples are usually smaller since they can easily be broken. They are positioned inside a tiny cavity formed by a 25 or 50 μm spacer and two transparent glass substrates. This assembly is cooled to cryogenic temperature in a Janis Supervaritemp dewar. A typical transmission spectrum of a good quality 1.21 μm sample taken at 2K in superfluid helium is shown in Fig. 4. One clearly sees the Fabry-Perot oscillations and the A and B free exciton absorption peaks located at 20583.8 cm^{-1} and 20706 cm^{-1} respectively.

It can be shown that the transmission T of Fabry-Perot is given by

$$T = \frac{I_{out}}{I_{in}} = \frac{G}{1 + F \sin^2\left(\frac{2\pi L n}{\lambda_{vac}}\right)} \tag{21}$$

where

$$G = \frac{(1 - R)^2 \exp(-\alpha L)}{\left[1 - R \exp(-\alpha L)\right]^2} \tag{22}$$

and

$$F = \frac{4 R \exp(-\alpha L)}{\left[1 - R \exp(-\alpha L)\right]^2} \tag{23}$$

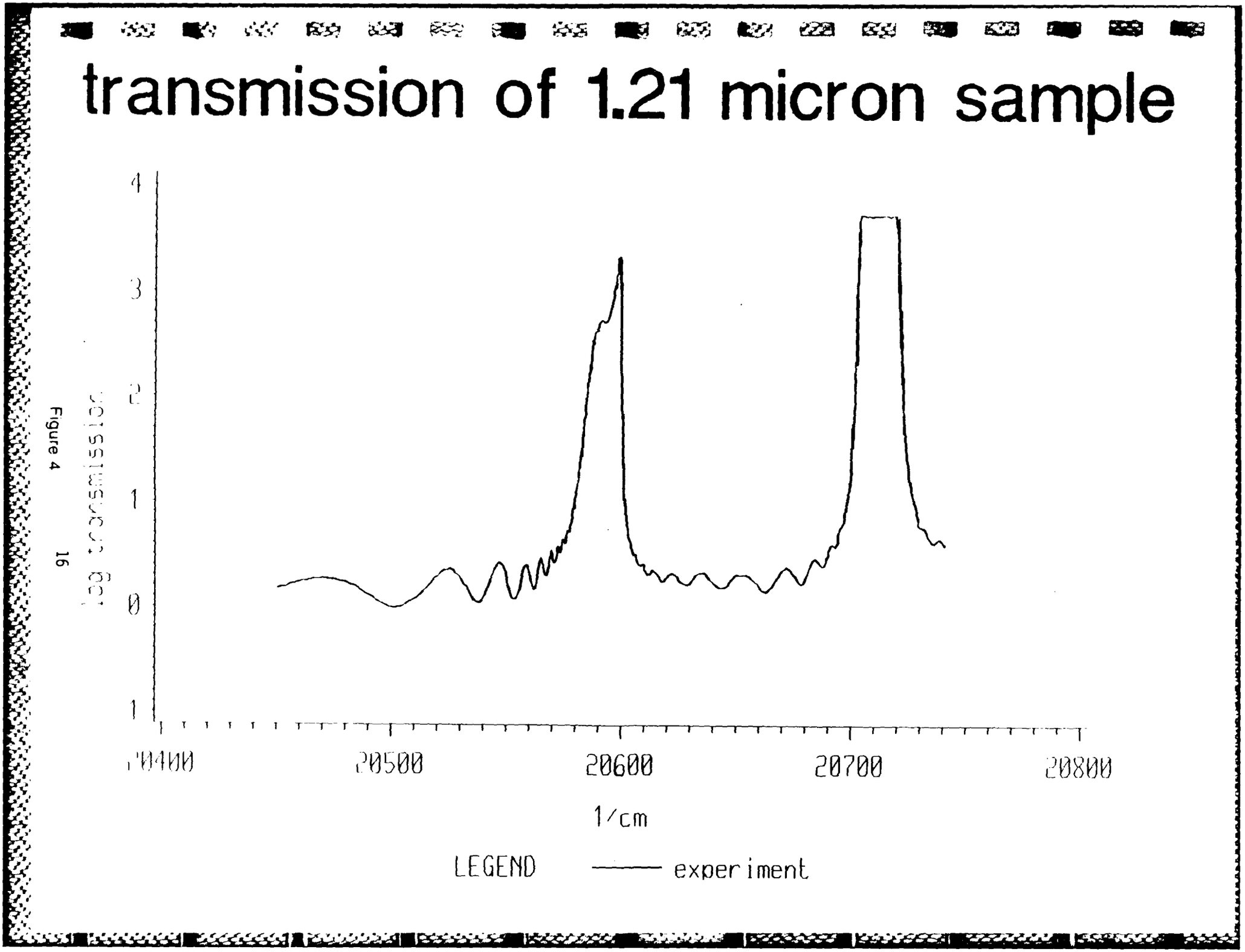
transmission of 1.21 micron sample
4
3
0
1
20500
20600
20700
20800
1/cm
LEGEND
experiment

Figure 4

where n and α are the index of refraction and the absorption coefficient of the CdS platelet and L and R are the thickness and reflectivity of the sample respectively. n and α are extracted from a fit to the transmission using Eqs. (1), (3) and (21) to (23). Eq. (1) is modified to include the contributions from both the A and B n=1 excitons. The reflection coefficient R is taken to be:

$$R = \frac{(n-1)^2 + \kappa^2}{(n+1)^2 + \kappa^2} \tag{24}$$

The damping Γ is related to the dephasing time via the following relationship:

$$\Gamma = \frac{2}{T_2} \tag{25}$$

In general, Γ(or T_2) is energy dependent and varies according to the scattering mechanism (e.g. exciton-phonon, exciton-impurities) responsible for the interaction. Figure 5 shows a fit to the experimental data assuming two fixed (detuning independent) dephasing coefficients for describing the A exciton above and below the resonance and two more fixed (detuning independent) dephasing coefficients for describing the B exciton above and below the resonance. The position of the transmission peaks over the whole spectrum and the total transmission below the A free exciton resonance can be modeled accurately. Above the A free exciton, the dephasing time is found to be energy dependent. When this dependence was chosen such that the dephasing rate increases linearly with the detuning, a very good fit was obtained (cf. Figure 6). A dephasing speed v_ϕ was then defined:

FIXED DEPHASING COEFFICIENTS

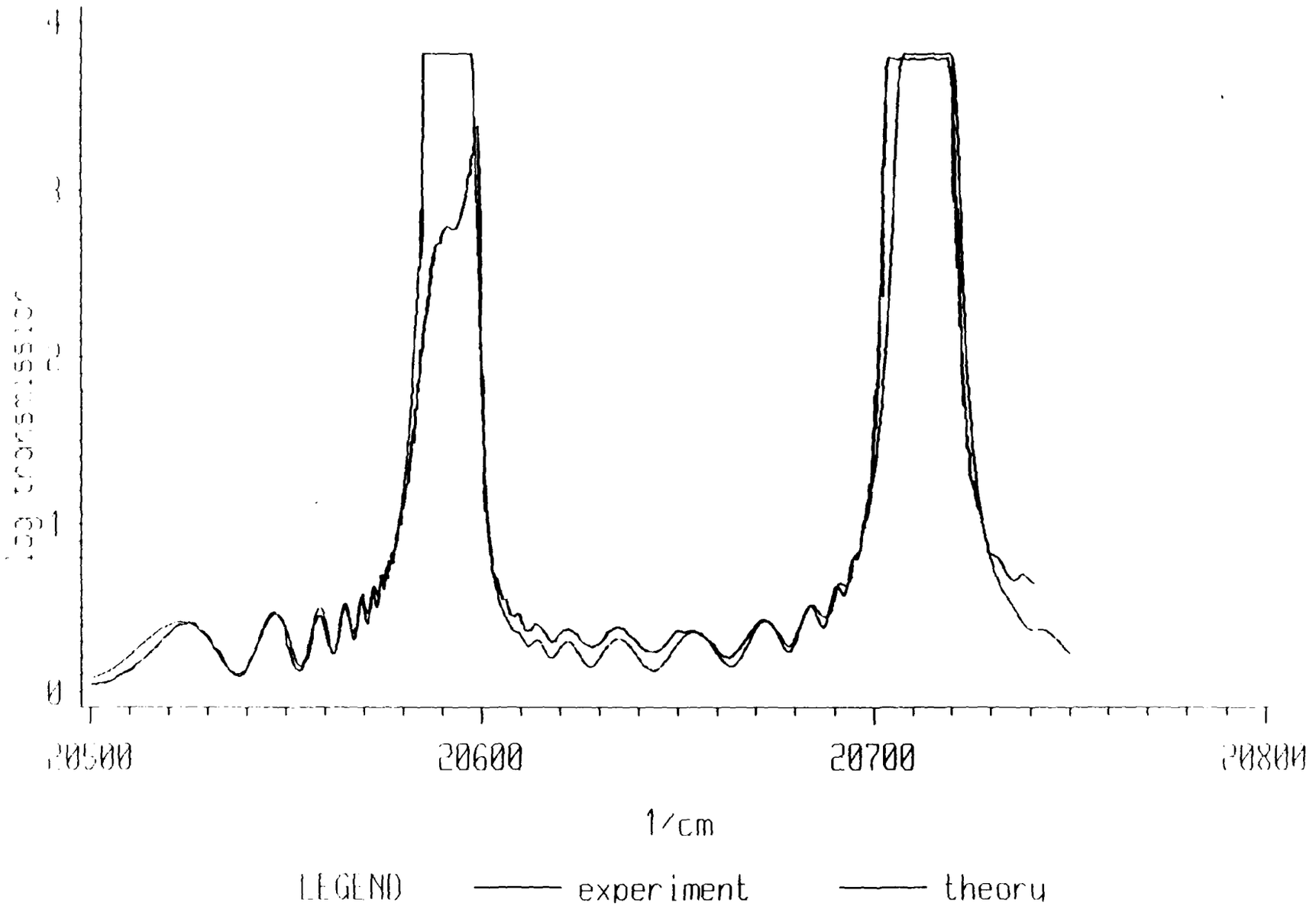

Figure 5

fit using dephasing speed

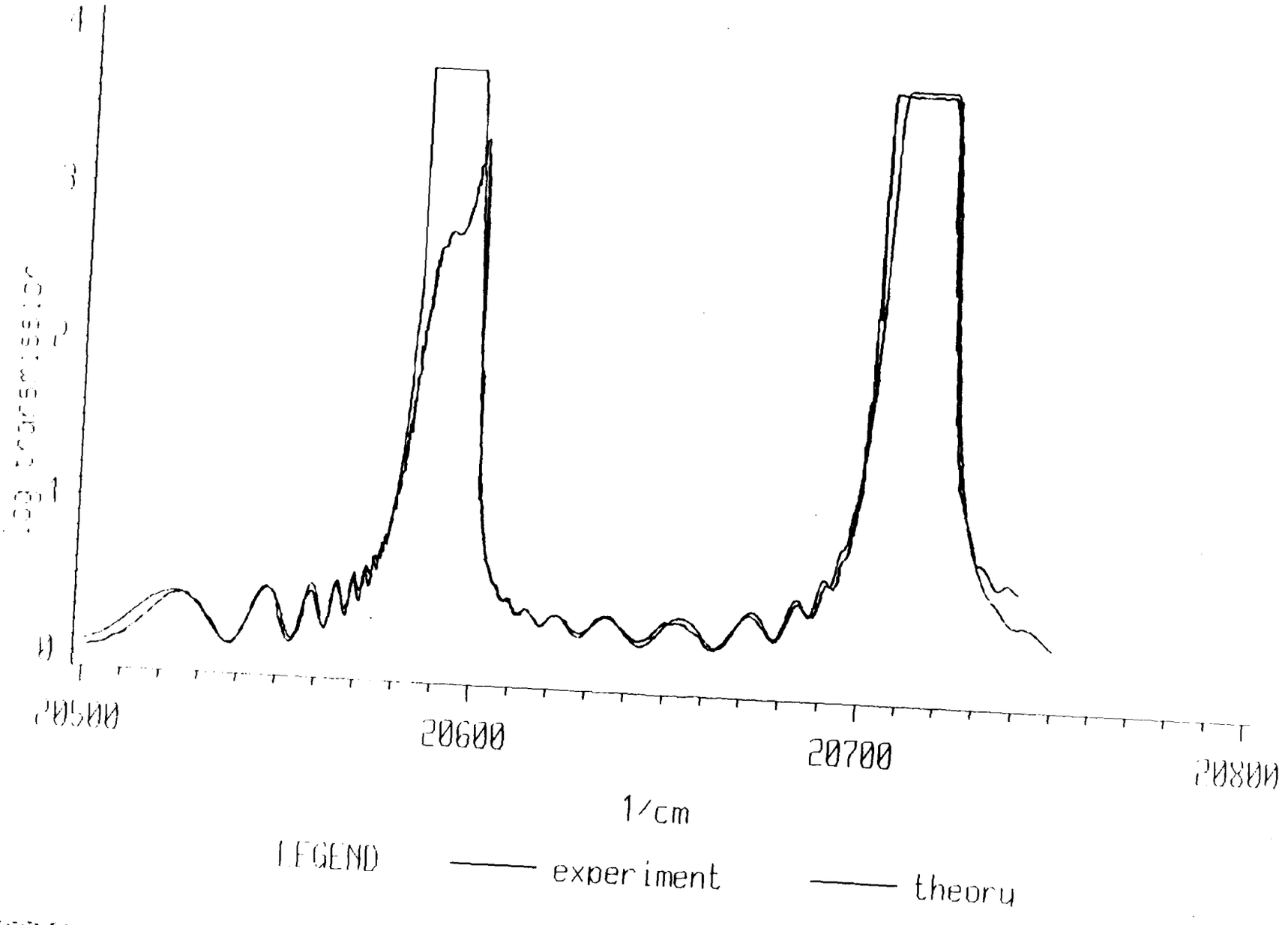

Figure 6

$$\frac{1}{T_2} \approx v_\phi \, \Delta\sigma \qquad (26)$$

where $\Delta\sigma$ is the detuning in cm^{-1}. One of the likely candidates for dephasing polaritons above the ω_L resonance is the scattering of the inner branch polariton to the outer branch by emission of an acoustical phonon[6]. We remind the reader that above the ω_L frequency, the inner branch polariton is mostly responsible for the absorption process. Figure 7 is an illustration of the proposed exciton-phonon scattering process. Since the density of final states depends on the wavevector of the scattered polariton and since it increases with k, we expect this mechanism to be a likely mechanism. Other possible sources of exciton-polariton dephasing are impurity and defect scattering. Contrary to the first dephasing mechanism considered, these sources of dephasing should be very sample dependent. Since the density of states is very low for polaritons with energy less than ω_T, we expect that the first source of dephasing to play a minimal role compared to the role played by impurity and defect scattering for detunings below the A free exciton resonance. Table 2 shows a study of the dephasing speed of exciton polaritons for various samples. Below the ω_{TA} resonance, the dephasing rate is very much sample dependent and is well described by a unique dephasing time for each sample. Above the ω_{TA} resonance, there appears to be little variation of the dephasing rate from sample to sample (if we exclude the 1.2 μm data). This is in agreement with what is expected. Our recent theoretical calculations predict the observed detuning dependence of the damping for frequencies above the A free exciton resonance.

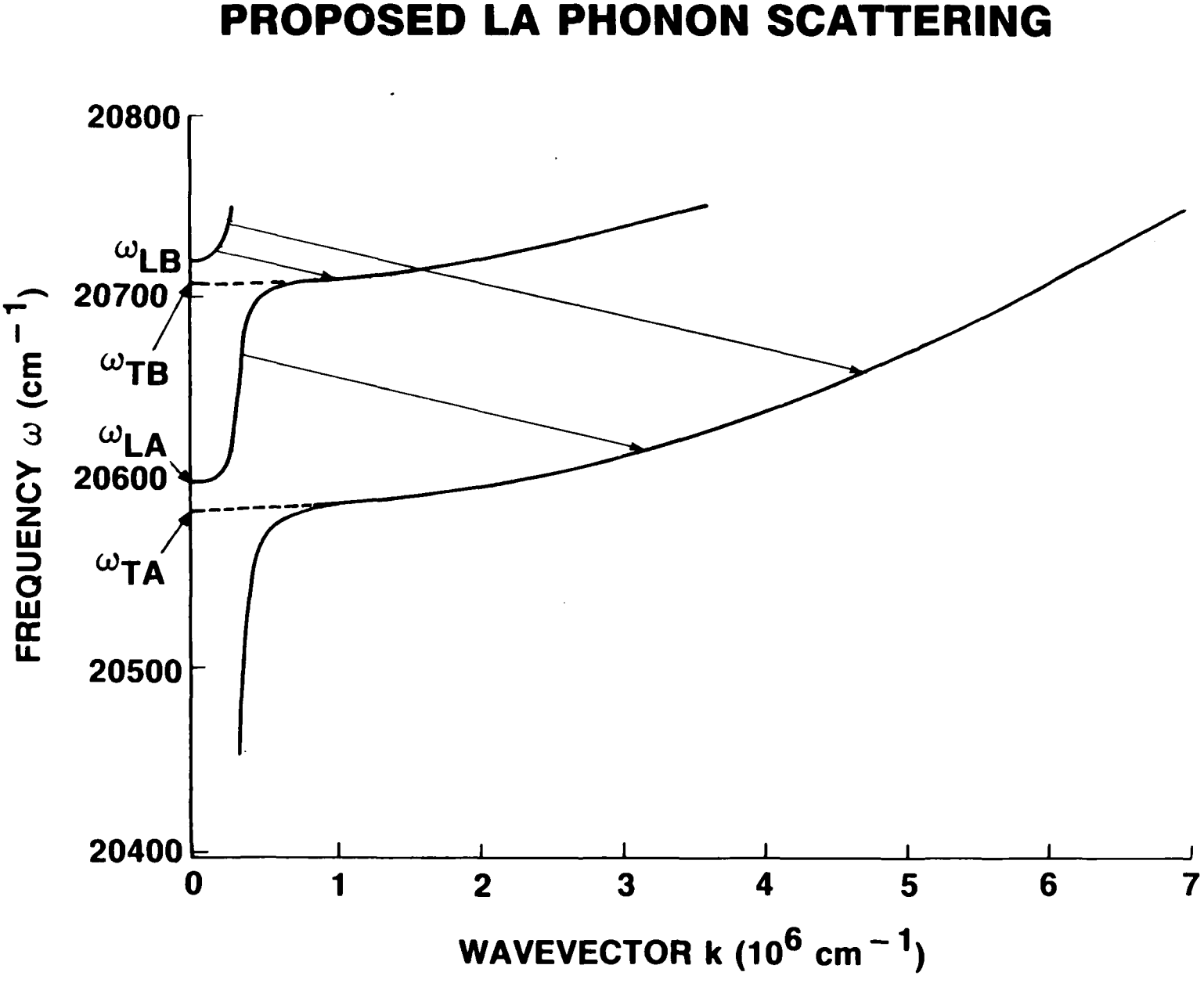
PROPOSED LA PHONON SCATTERING
20800
ω_{LB}
20700
ω_{TB}
ω_{LA}
20600
ω_{TA}
20500
20400
FREQUENCY ω (cm^{-1})
0
1
2
3
4
5
6
7
WAVEVECTOR k (10^6 cm^{-1})

Figure 7

Table 2

Sample Thickness	Dephasing Time Below A Exciton	Dephasing Speed (cm/s) of the A exciton above the A exciton resonance	Dephasing Speed (cm/s) of the B exciton below the B exciton resonance	Product of Concentration(cm^{-3}) of bound excitons by their oscillator strength (f)
12.5 μm	60 ps	1.9×10^9	9×10^8	9×10^{15}
2.8 μm	28 ps	2.1×10^9	8×10^8	$\approx 5 \times 10^{15}$
15.6 μm	80 ps	1.8×10^9	7×10^8	5×10^{15}
1.21μm	40 ps	3.8×10^9	1×10^9	$< 1 \times 10^{16}$

It should be mentioned that our study is the first detailed study of the energy dependence of the polariton dephasing over a wide frequency range. This is made possible by the high quality of the transmission data obtained with the automated data acquisition system. In addition, the transmission data analysis permits the precise extraction of the longitudinal and transverse exciton frequencies, the background index of refraction and the A and B free-exciton oscillator strengths. These parameters are shown in Table I. We believe that we have significantly increased the accuracy with which these important parameters are presently known. Figures 8 and 9 show the energy dependence of both the index of refraction and the absorption coefficient in a typical good quality CdS sample. Our measurements do not permit the accurate extraction of the variation of the index of refraction and absorption coefficient within the ω_{LT} region of the A and B excitons.

3.2 TEMPERATURE DEPENDENCE OF THE TRANSMISSION NEAR THE BAND GAP

In order to obtain additional information on the different scattering mechanisms acting on the polariton, the temperature dependence of the dephasing was studied on the 1.21 μm sample. Figures 10 to 15 show the sample transmission at different temperatures between 2 and 100 K. Below the ω_{TA} frequency, no temperature dependence is observed for the dephasing coefficient. This is exactly what we expect for impurity-polariton scattering when acoustic or optical phonons do not play any role. We suspect that this impurity-polariton scattering is mostly elastic in nature (purely dephasing collisions). The polariton under a collision just changes its direction of motion without losing much energy. The momentum difference is absorbed by the lattice. Once in a while, the collision will be inelastic and the whole pho-

index of refraction

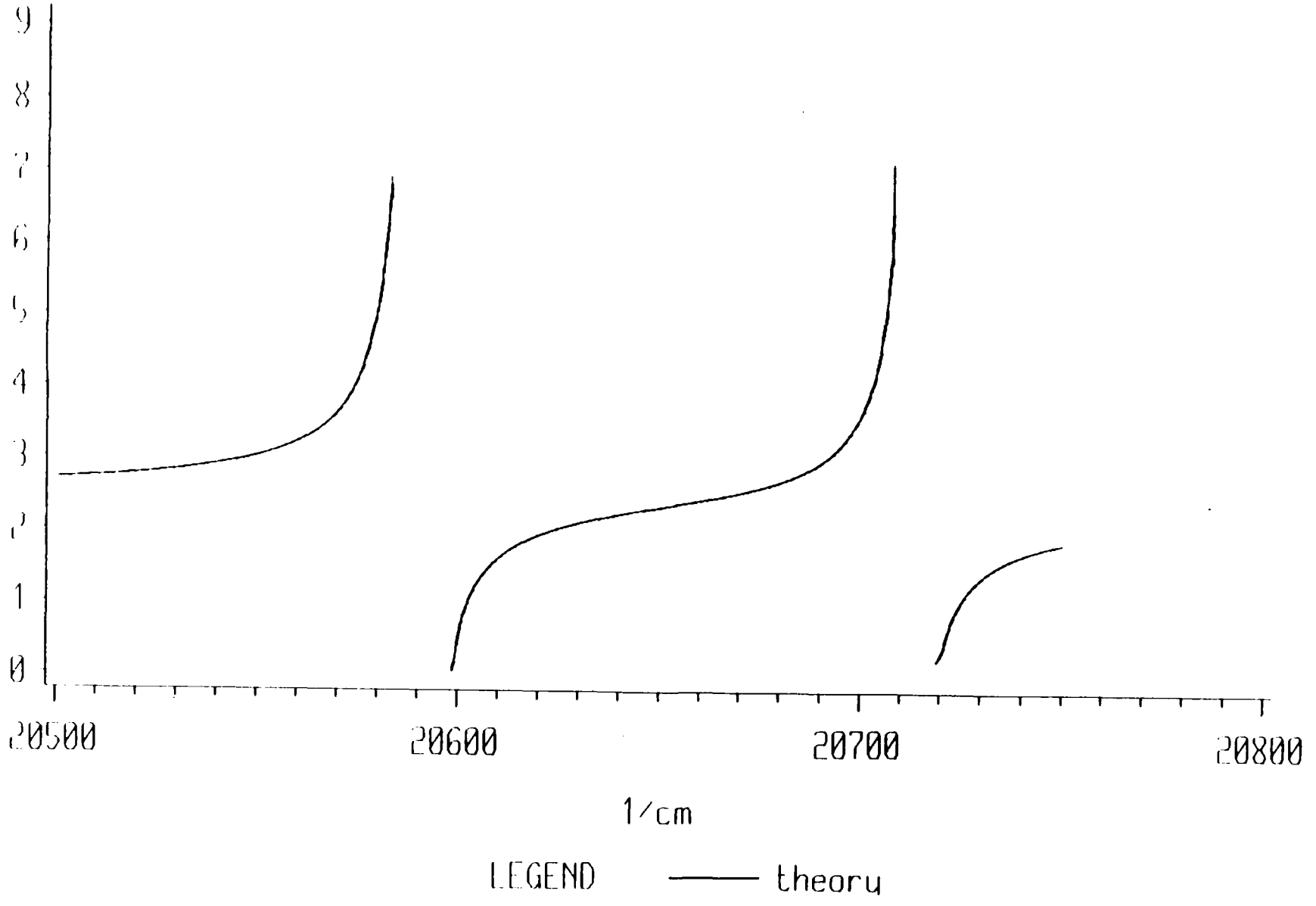

Figure 8

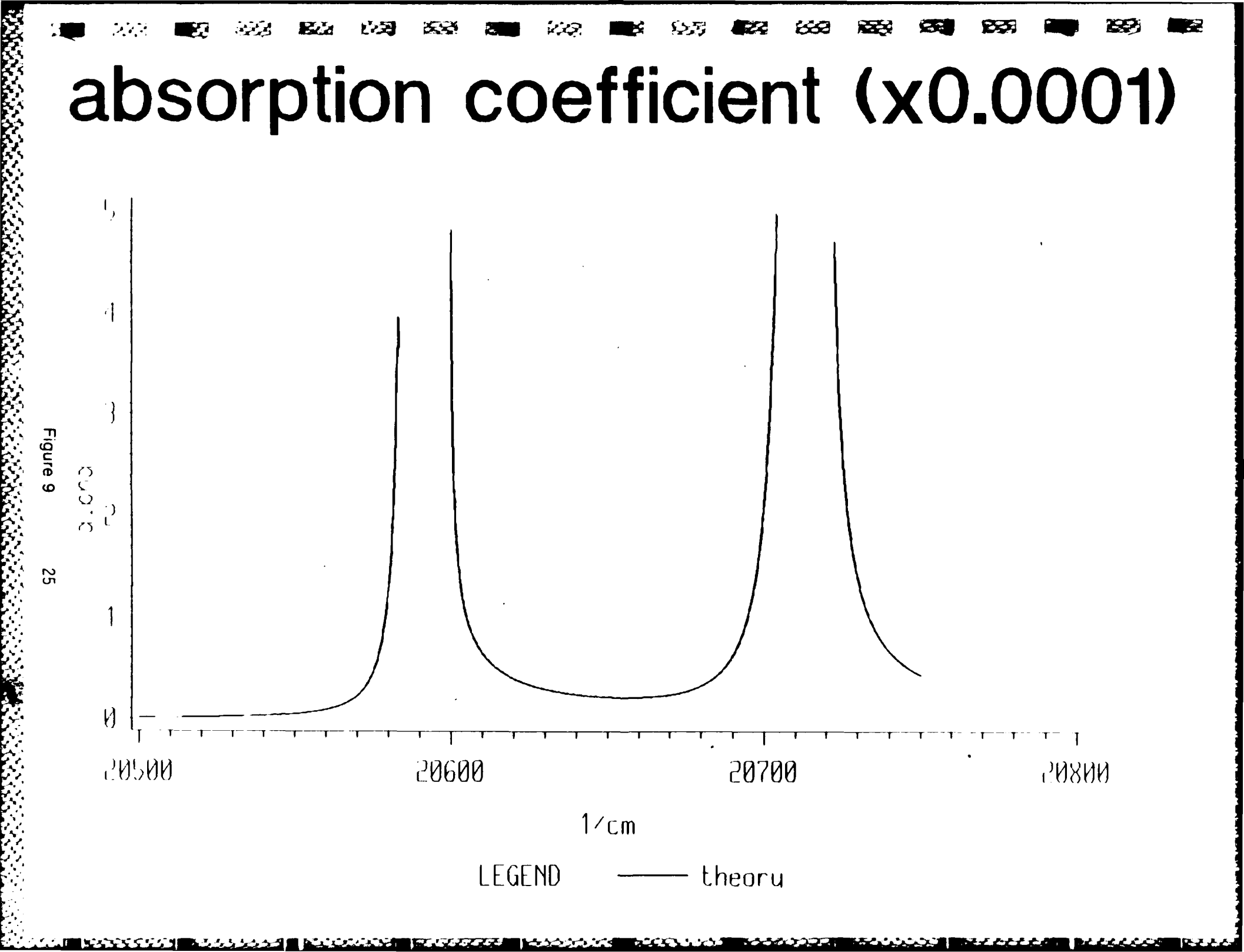
absorption coefficient (x0.0001)
0
1
3
20500
20600
20700
20800
1/cm
LEGEND
theoru

Figure 9

linear transmission at 2 k

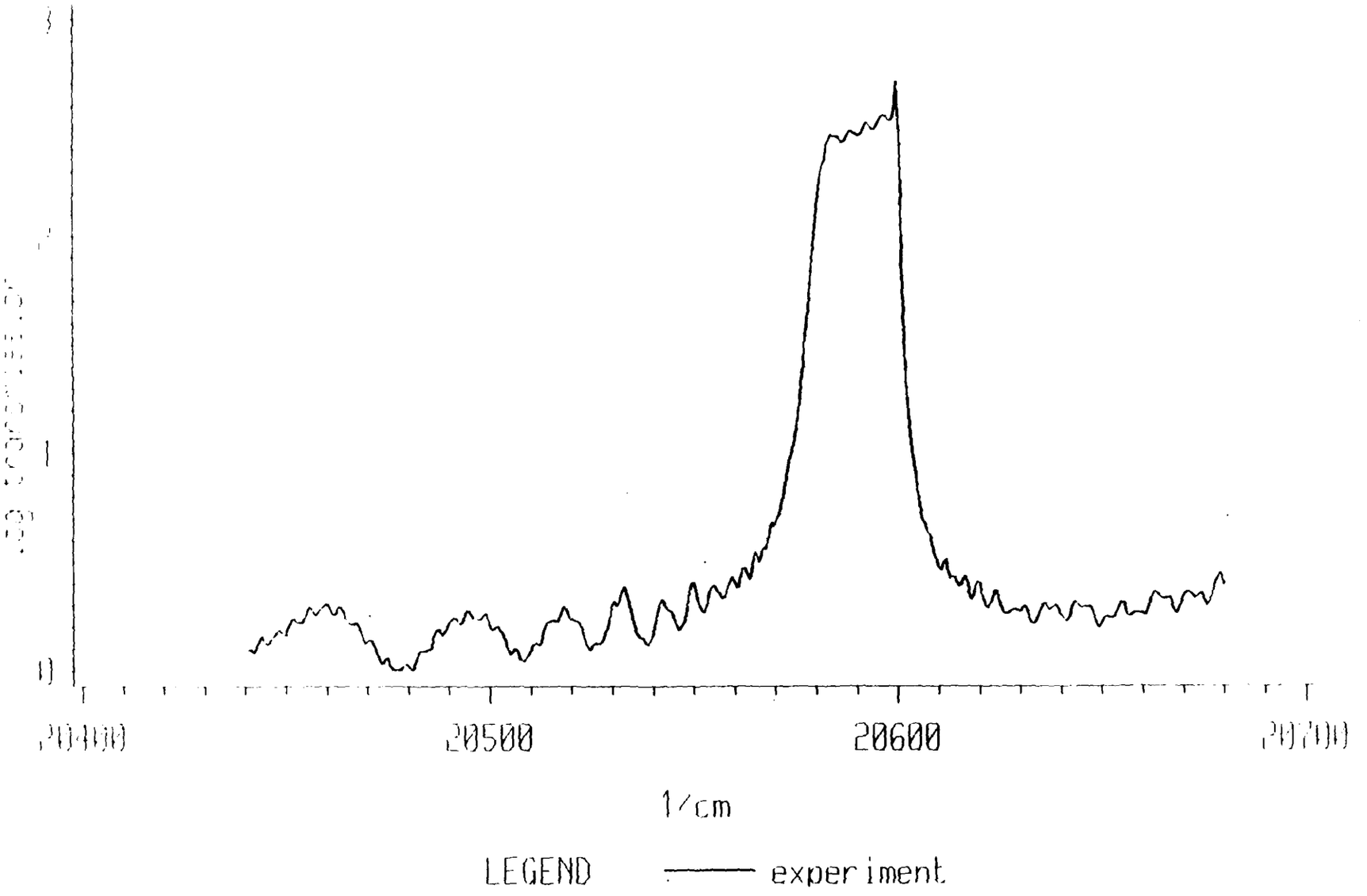

Figure 10

linear transmission at 25 k

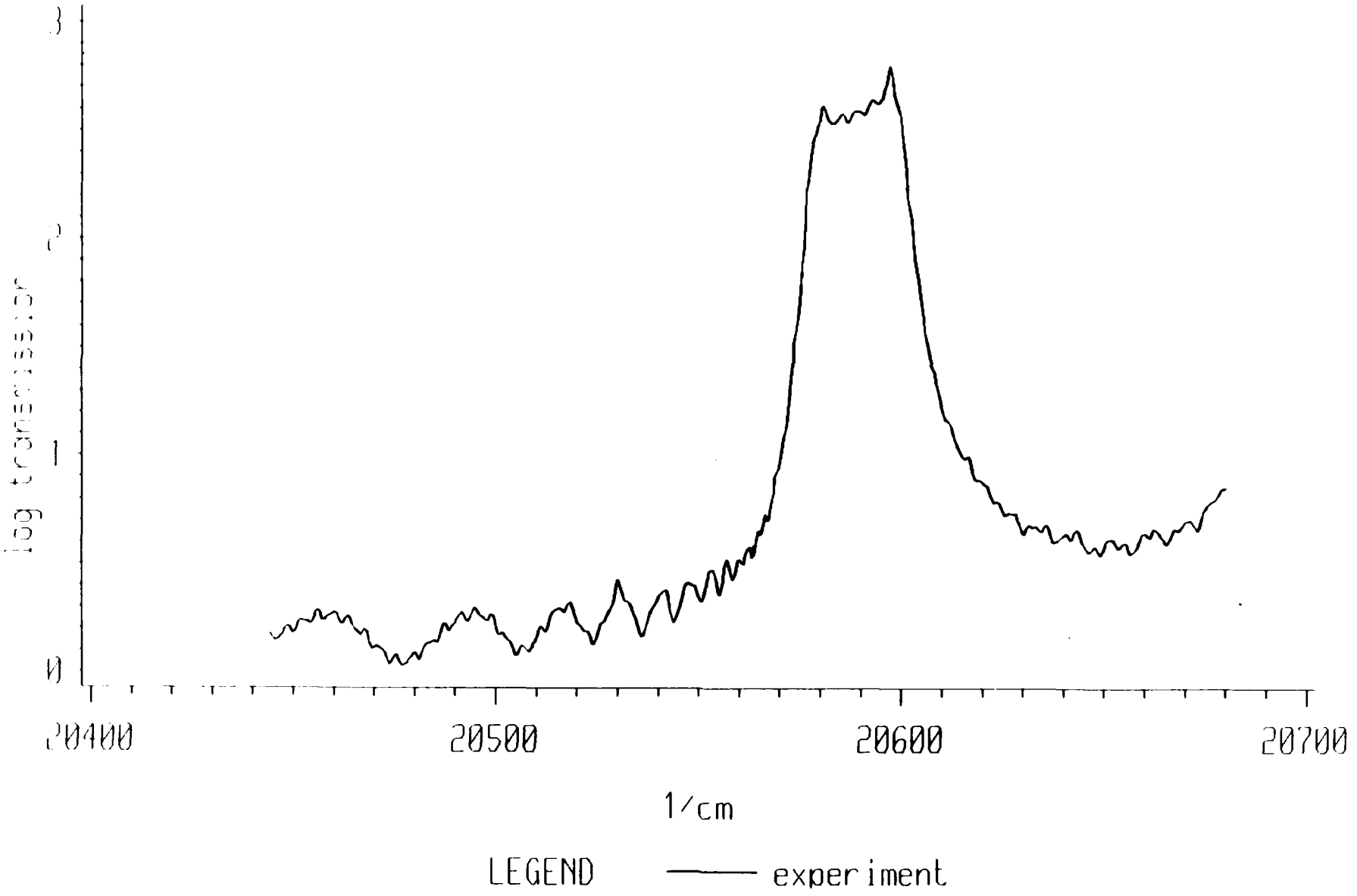

Figure 11

linear transmission at 40 k

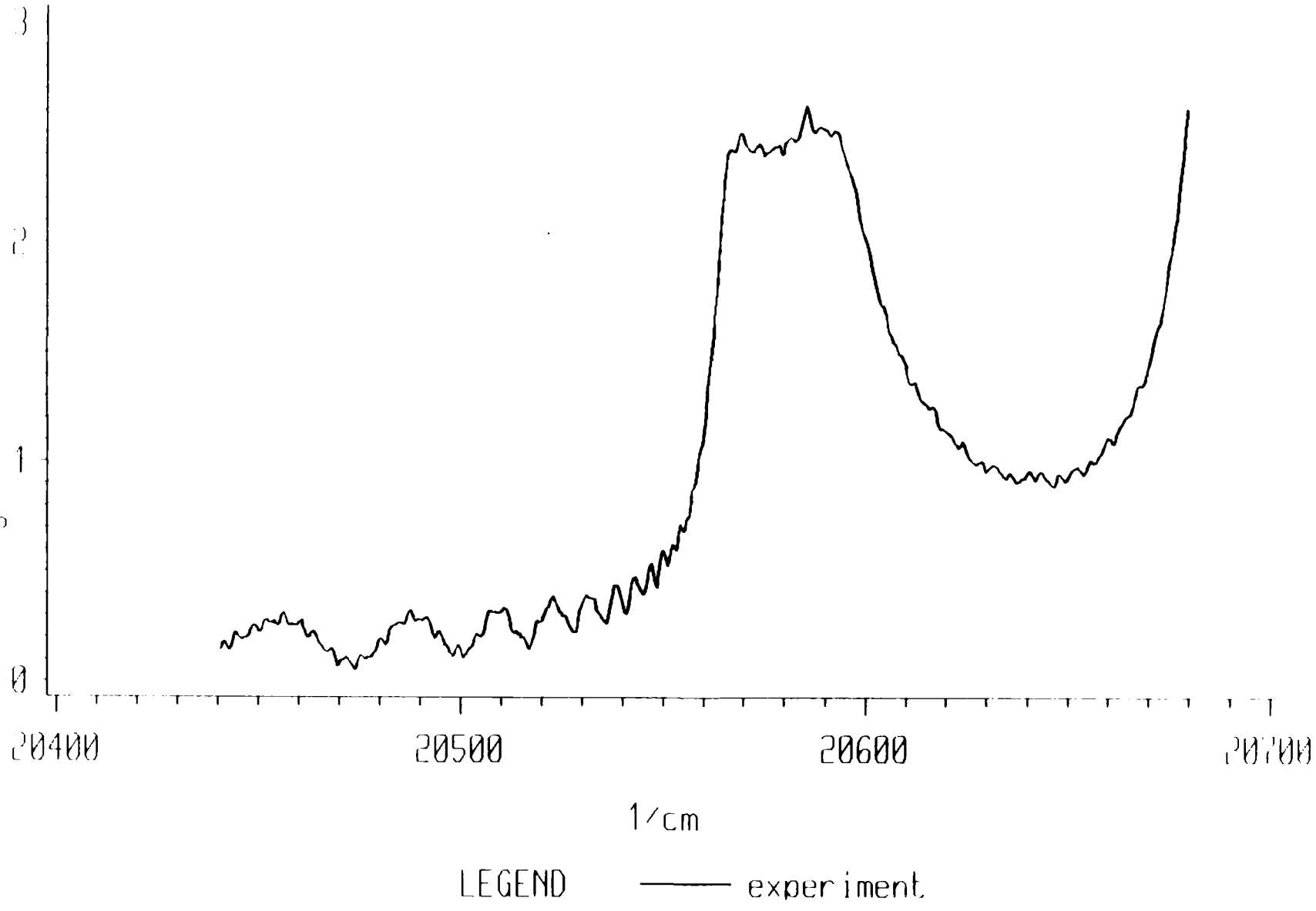

Figure 12

linear transmission at 50 k

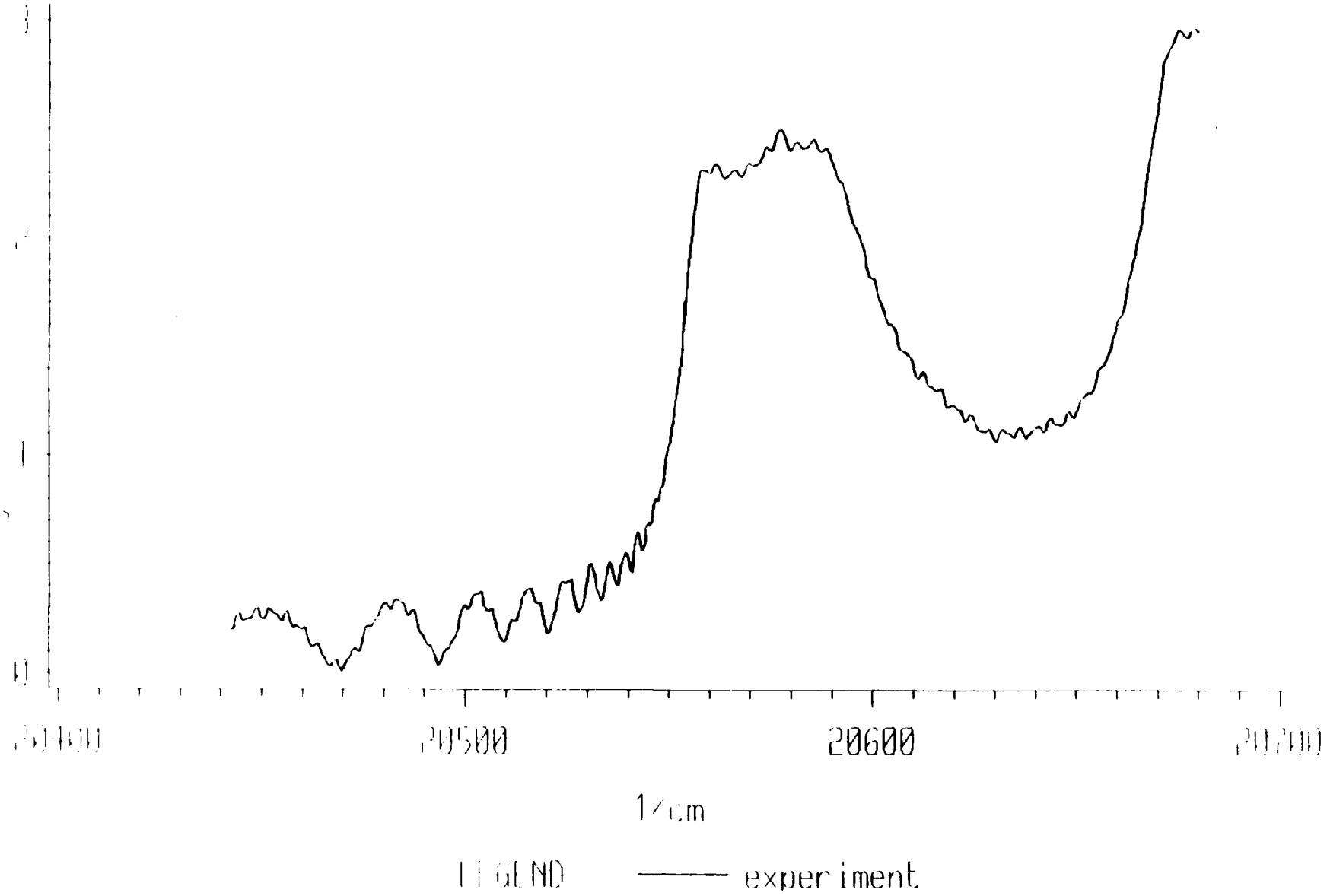

Figure 13

linear transmission at 80 k

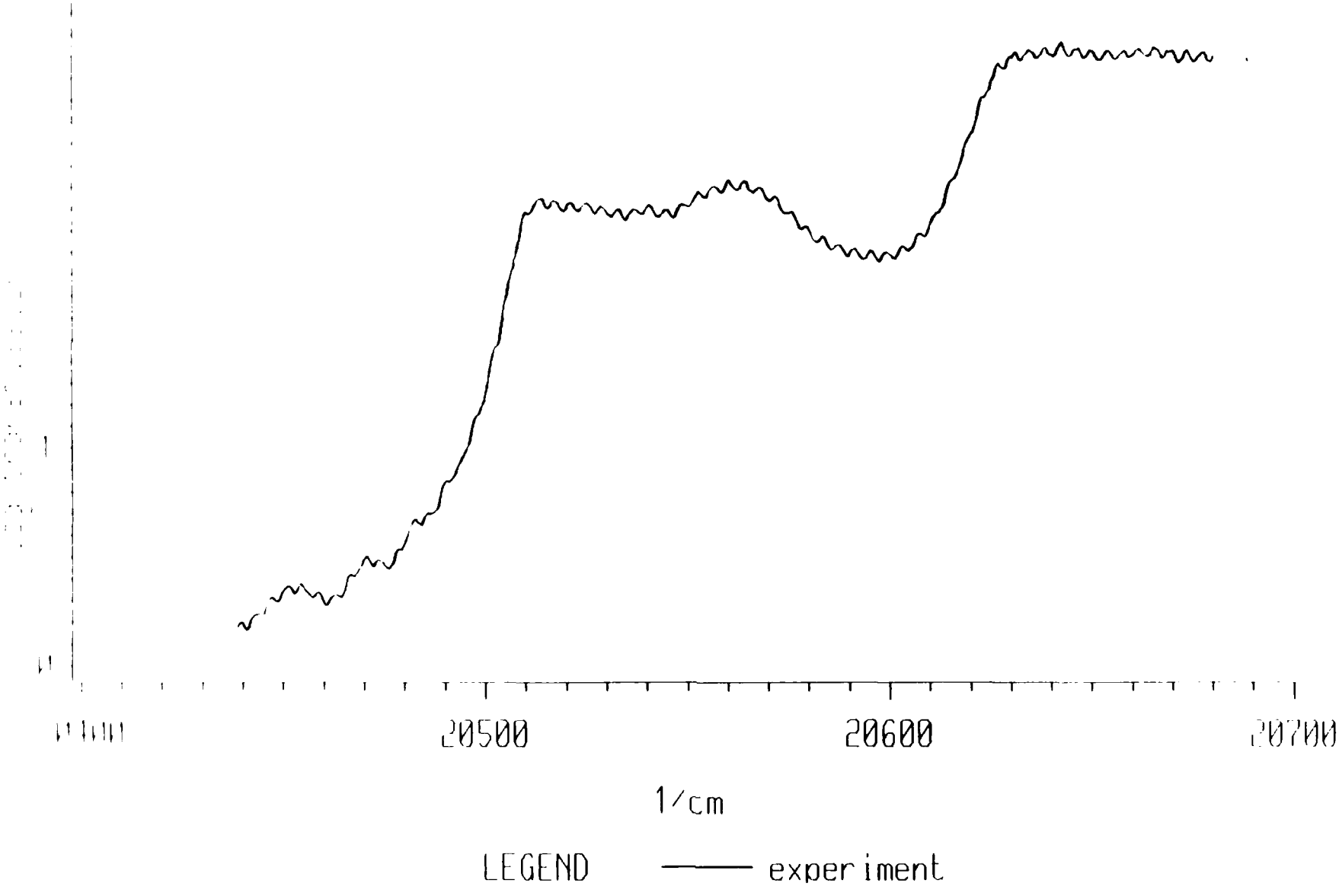

Figure 14

linear transmission at 100 k

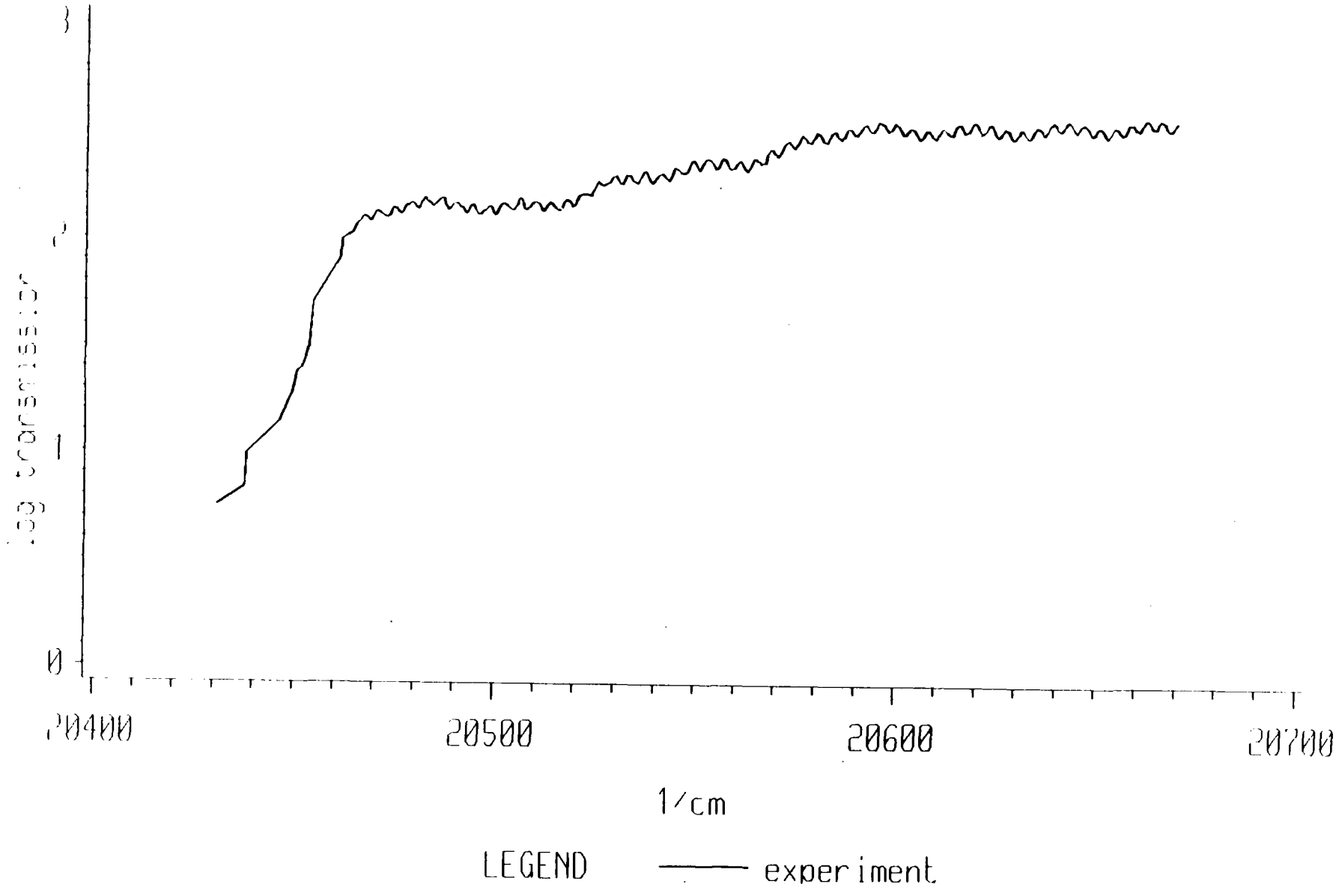

Figure 15

ton energy will disappear as heat to the lattice. In other instances the exciton energy will be used to form a bound exciton. When the temperature is increased above 50 K, the exciton-polariton scatters off LO-phonons. In the process of doing so, the exciton gets dissociated because the LO-phonon energy (38 meV) is much larger than the A free-exciton binding energy (29 meV). A lifetime broadening of the free exciton is then observed. The temperature dependence of the A free exciton broadening parameter below the resonance is shown in Fig. 16. One clearly sees the dramatic rise of the damping coefficient when LO-phonons appear. The following expression describes the temperature broadening of the A free exciton below the resonance:

$$(1/T_2) = 5.2 \times 10^{13} \exp(-441/T) + 3.70 \times 10^{10}, \text{ for } \omega < \omega_{TA}. \quad (27)$$

Later, we will see that this mechanism is responsible for explaining the sharp reduction of the nonlinear signal due to exciton self-broadening as the temperature is increased. For frequencies above the ω_{TA} resonance, the dephasing speed increases dramatically as the temperature is increased from 2 K. This can be seen from Fig. 17. Above 100 K, we expect that the dephasing rate due to LO-phonon scattering will be the dominant scattering mechanism above the ω_{TA} resonance and that the difference between the dephasing rate for above and below the A resonance will vanish. Figure 18 shows the temperature dependence of the position of the A free exciton. This was obtained by carefully monitoring the position of the ω_L resonance. Since some of the linearly polarized input light is converted to elliptically polarized light by stray birefringence in the windows of the dewar or in the sample itself, part of the light can be absorbed by resonances which are dipole active in the other polariza-

dephasing rate below a exciton

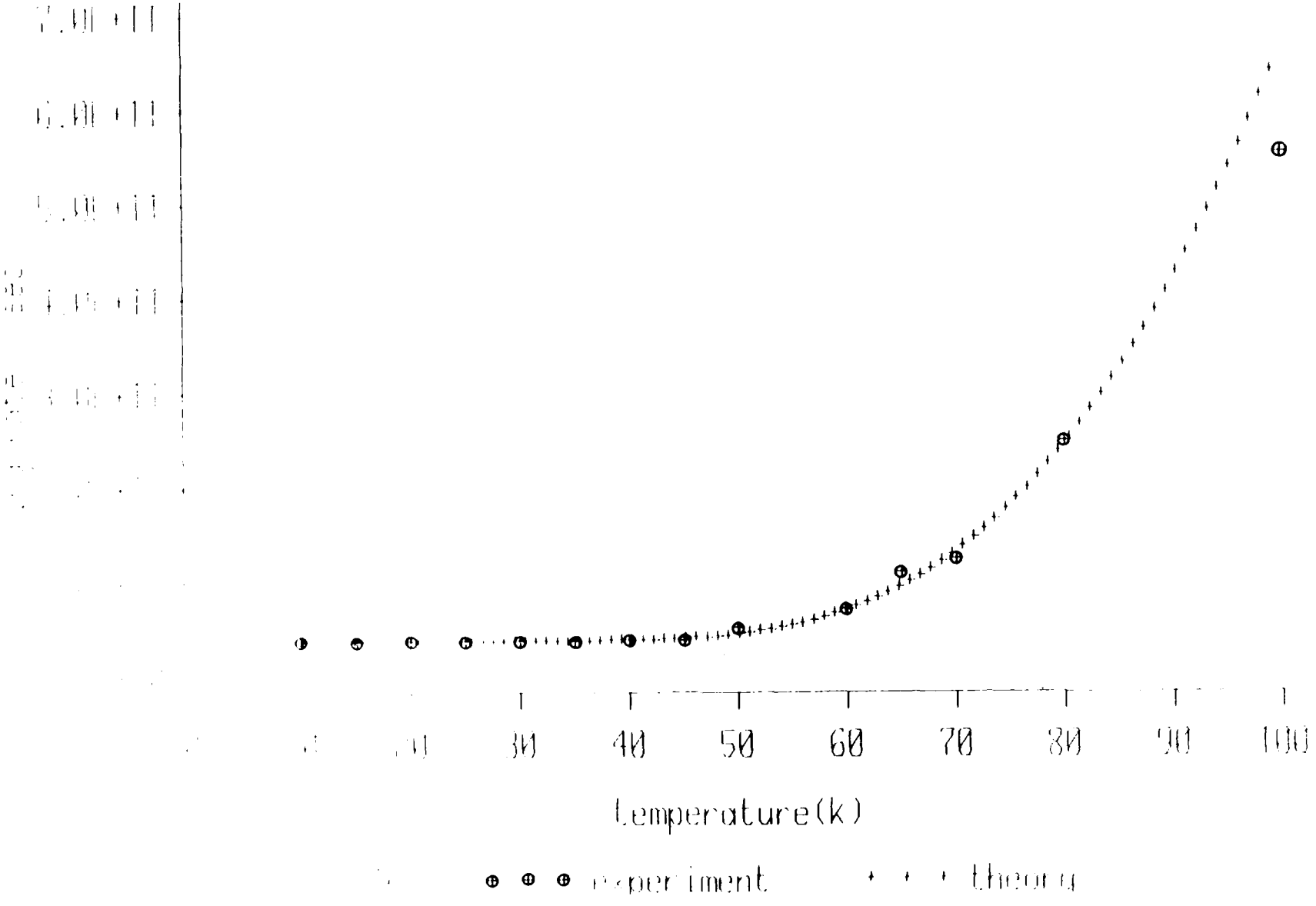

Figure 16

dephasing speed above A exciton

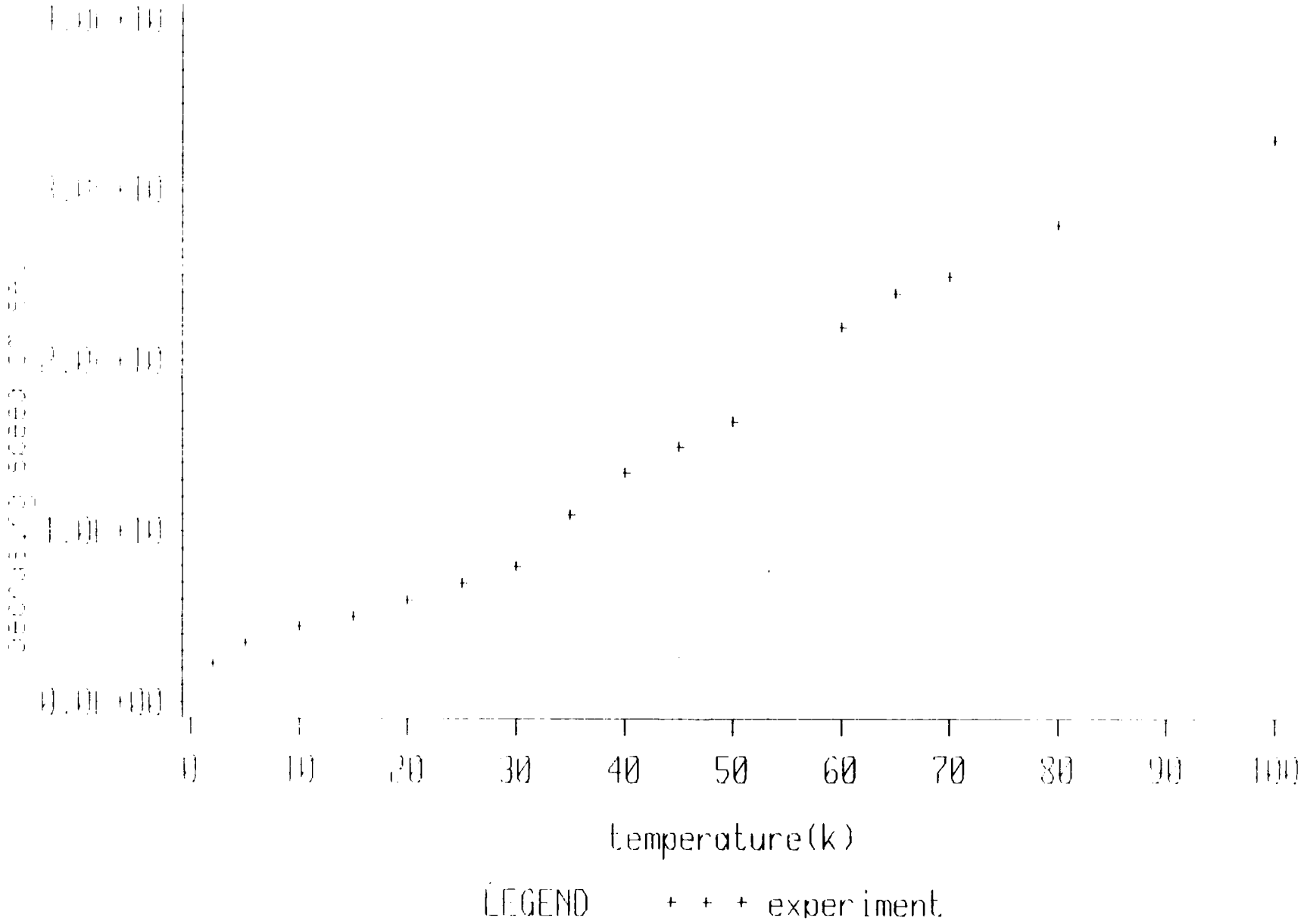

Figure 17

position of a exciton vs temperature

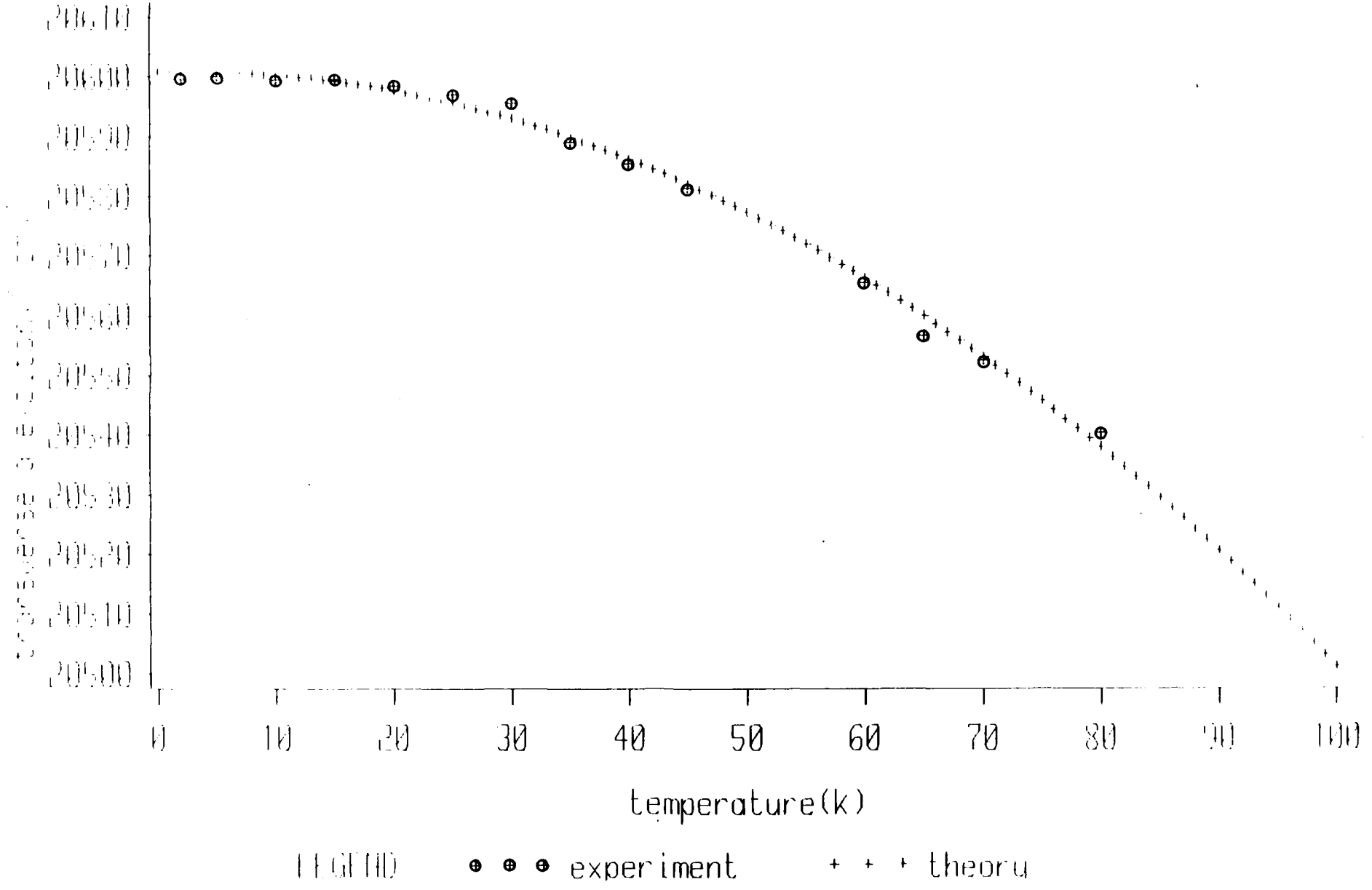

Figure 18

tion perpendicular to the input polarization. For this reason, the ω_L resonance appears on top of the A exciton absorption peak. The major inaccuracy in plotting the A free exciton resonance position vs temperature comes from an inaccurate knowledge of the sample temperature. Experimentally, we find that the following analytical expression describes reasonably well the variation of the free exciton position with temperature:

$$\omega_{TA}(cm^{-1}) = -0.010526\ T^2 + 0.05667T + 20600.6 \qquad (28)$$

3.3 LI IMPLANTATION OF CDS

In order to further increase the understanding of the role played by impurities on broadening the free exciton resonance and in order to demonstrate new optical switching concepts, good optical quality Cds samples were implanted with Li ions[7]. Li was chosen because it is known to act both as a substitutional acceptor and an interstitial donor in CdS. These donors and acceptors can in turn bind free excitons and form bound excitons. Since bound excitons are known to have a very large oscillator strength and since their transition linewidth is very narrow, they are ideal candidates for the study of optical nonlinear interactions in CdS and for the demonstration of optical switching. Since the position of the implanted Li ions can be controlled accurately by using standard mask techniques, a very good spatial control on the position of the nonlinearity is obtained and two-dimensional arrays of optical switches can be envisioned. One CdS sample ($\simeq$ 13 μm) was Li implanted at energies of 280, 160, and 105 keV and fluences of 1.4×10^{12}, 1×10^{12}, and 5.7×10^{11} cm^2, respectively. This corresponds to an estimated impurity density of

$\approx 3 \times 10^{16}$ cm^{-3}. Another CdS sample ($\approx$ 12 μm) was Li implanted at the same three energies, but at three different fluences: 4.5×10^{12}, 3.4×10^{12}, and 1.9×10^{12} cm^{-2}. This corresponds to an estimated impurity concentration of $\approx 1 \times 10^{17}$ cm^{-3}. In order to determine the exact implantation profile, a secondary ion mass spectroscopy (SIMS) analysis was performed. The results are shown in Fig. 19. This indicates that the Li ions are distributed over a thickness of 0.6 to 0.7 μm inside the sample. The samples were implanted from both sides. The absorption spectra of both of these samples are shown in Figs. 20 and 21. The unimplanted portion of the sample shows two sharp lines at 20529.5 (weak) and 20531.8 cm^{-1} (strong). They probably correspond to excitons bound to Li interstitial neutral donors (the I_2 line). Comparing the spectra obtained from the implanted and the unimplanted areas of the same sample, we make the following observations. First, the free exciton absorption peaks substantially broadened following Li implantation, but within the accuracy of our measurements, did not shift. Second, we did not detect any absorption due to excitons bound to neutral acceptors (the I_1 line located around 20450 cm^{-1}). This indicates that very few of the implanted ions go substitutionally in the lattice. Third, after implantation, four distinct absorption peaks are seen. They are located at 20529.5, 20531.8, 20534.6, 20537.8 cm^{-1}. The bound exciton contribution to the absorption increases by a factor of about 2 when the flux of implantation is increased by about a factor of 3.

We expect that the absolute accuracy on the flux of implantation is better than a factor of two and that the relative accuracy is probably better than 20 %. Since the I_2 bound exciton oscillator strength ($f = 9 \pm 1$) is known with relatively good accuracy in CdS[3,8], we will use the experimentally measured surface under the bound exciton absorption curve to deduce the concentration of bound excitons. This will allow us to cross check the accuracy

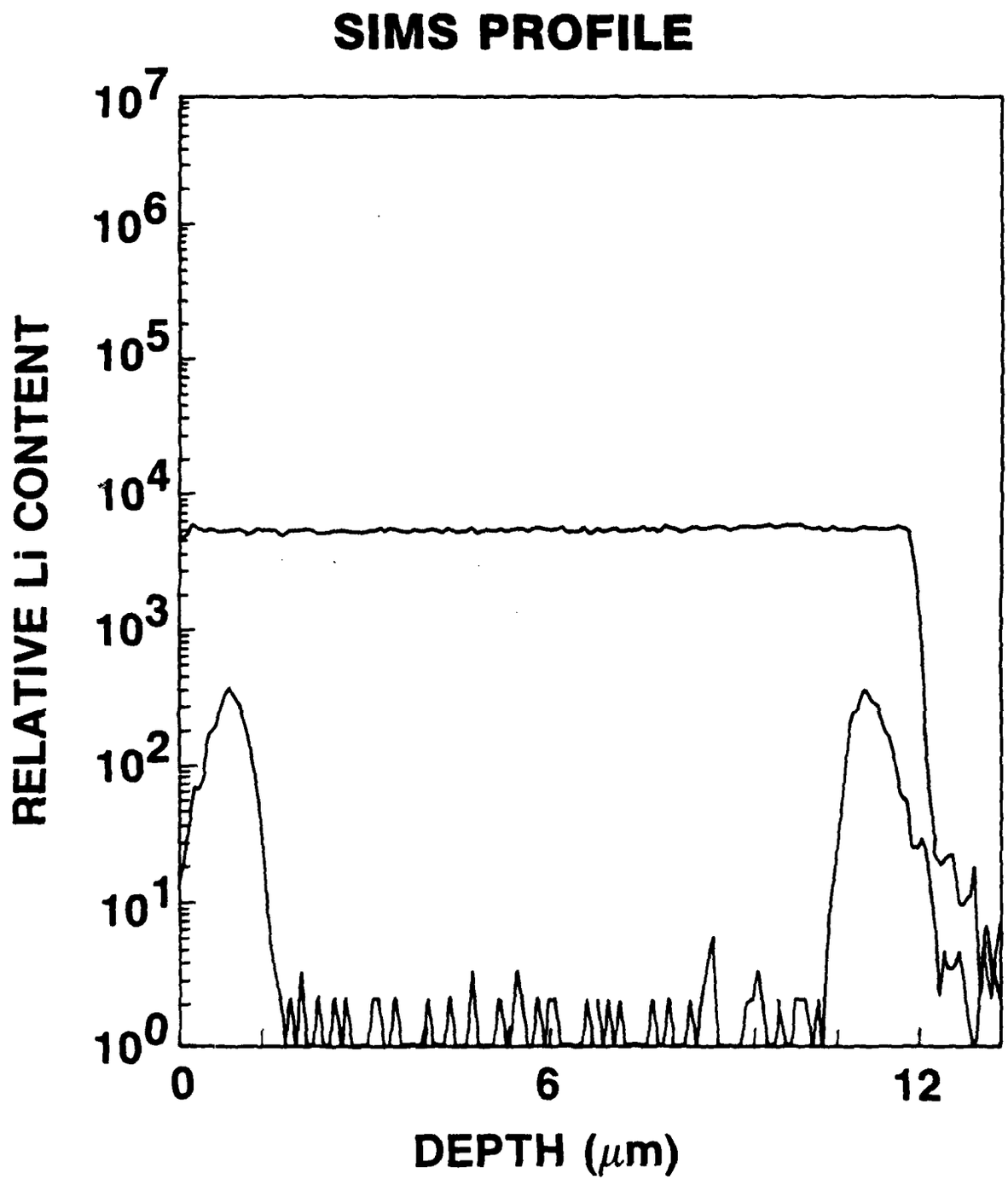
SIMS PROFILE
RELATIVE Li CONTENT
10^7
10^6
10^5
10^4
10^3
10^2
10^1
10^0
0
6
12
DEPTH (μm)

Figure 19

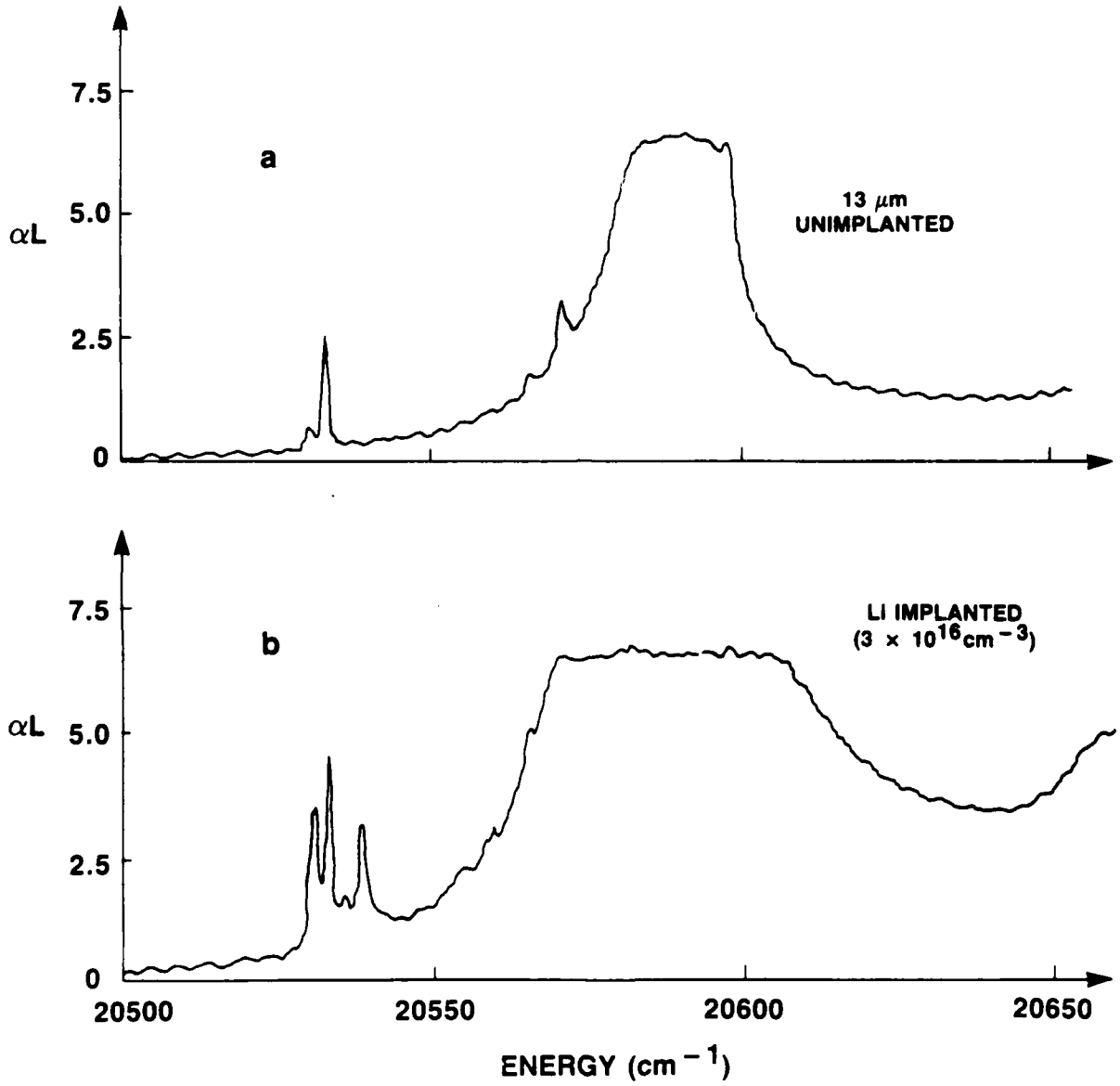
7.5
5.0
2.5
0
αL
a
13 μm
UNIMPLANTED
7.5
5.0
2.5
0
αL
b
LI IMPLANTED
(3 × 10^16cm^-3)
20500
20550
20600
20650
ENERGY (cm^-1)

Figure 20

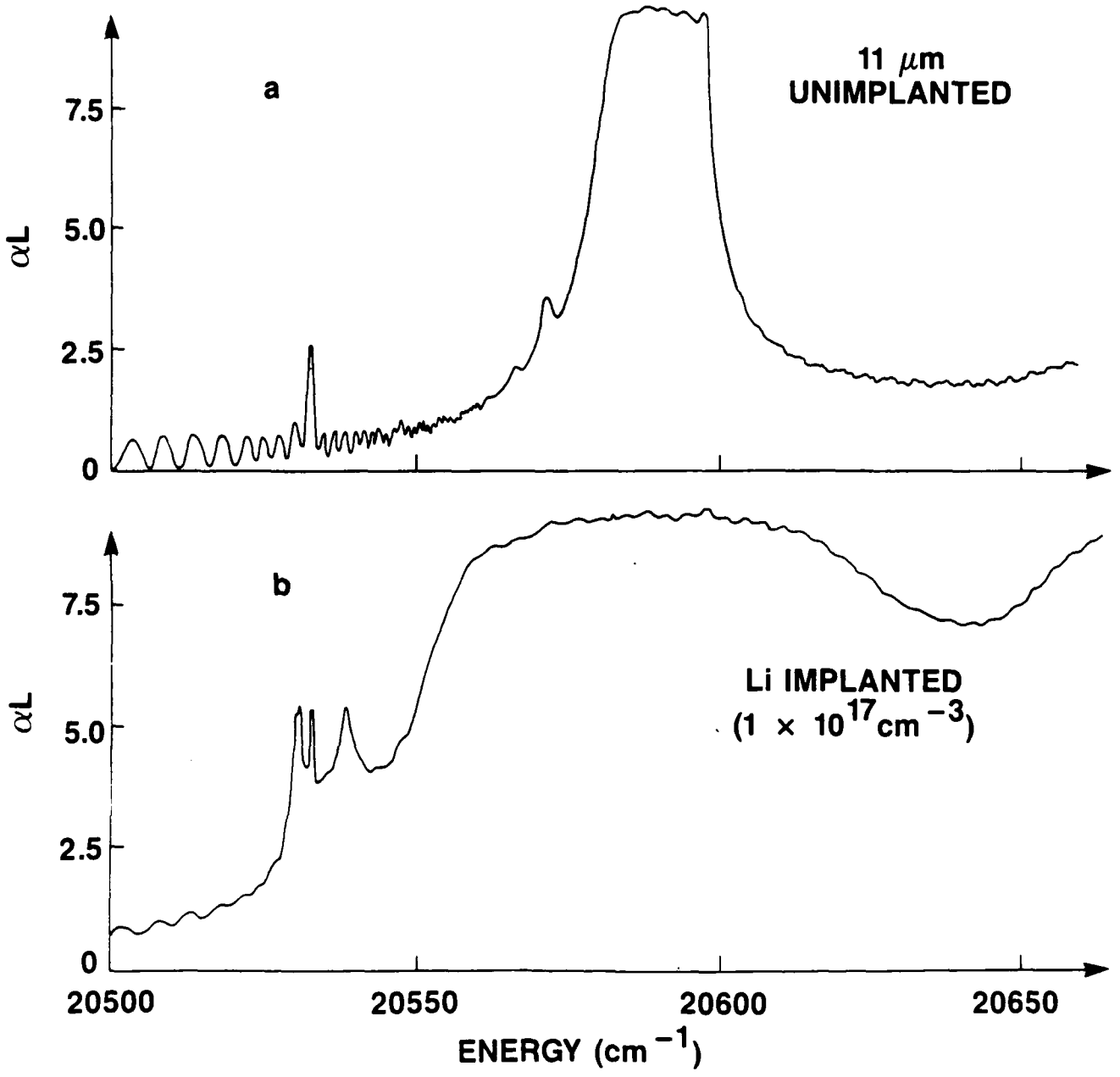
a
11 μm
UNIMPLANTED
αL
7.5
5.0
2.5
0
b
Li IMPLANTED
(1 × 10^17 cm^-3)
αL
7.5
5.0
2.5
0
20500
20550
20600
20650
ENERGY (cm^-1)

Figure 21

of our measurements. Doing so with the $1x10^{17}$/cc Li implanted sample, we deduce a bound exciton impurity concentration of ≈ $4\text{-}6x10^{17}$/cc, much higher than what we expected and also much higher than the inaccuracy of our measurements would allow us. This confusing result can be explained if one assumes that the impinging Li ion can generate many other donors as it slows down in the sample. For instance, these new donors can be sulfur vacancies (point or cluster defects). Even though it is known that much of the damage in CdS can be annealed at room temperature, it is not unreasonable to assume that some types of damage (like the cluster defects) cannot. Annealing at high temperatures might be desirable to eliminate the extra donors. Using the donor concentrations as deduced from the measurement of the bound exciton absorption coefficient and assuming that all the free exciton dephasing comes from these donors, we extract a free exciton dephasing coefficient that varies in the following way as the donor concentration is changed.

$$T_2(\text{sec}) \approx \frac{6 \times 10^5}{N} \tag{29}$$

where N is the donor concentration per cm^3. Since the donor-binding energy in CdS is similar to the exciton-binding energy, it is assumed that Eq. _29_ also provides an order-of-magnitude estimate of the broadening that is due to polariton-polariton scattering. As a simple check of this hypothesis, one can calculate the density of polaritons required to broaden the A free exciton resonance by a quantity equal to the free exciton absorption linewidth. In the case of exciton-polaritons, this linewidth is simply given by the ω_{LT} splitting of the A free exciton which is 15.4 cm^{-1} This implies:

$$\frac{1}{\pi T_2} = \frac{N}{6\times10^5 \times \pi} \simeq c\omega_{LT}. \qquad (30)$$

This gives an exciton concentration of 8.7×10^{17}/cc. On the other hand, it is well known that, in GaAs, saturation effects connected with the generation of free excitons come into play at an exciton concentration of about $1/\frac{4}{3}\pi(2a_B)^3$, where a_B is the exciton Bohr radius[9]. Such a criterion predicts that an exciton concentration of $\simeq 1\times10^{18}$ cm^{-3} would lead to dramatic changes of the absorption coefficient. This is in remarkably good agreement with our previous estimate.

Using ion implantation and modern mask technology, complicated two-dimensional patterns can be written with good accuracy. This opens completely new possibilties in all-optical parallel signal processing applications.

By using thinner unimplanted samples ($\simeq 2\mu m$), no absorption lines in the vicinity of the bound exciton transition frequency would be observed. Using such samples and a mask, we would be able to use the ion implantation process to create a two-dimensional absorption pattern. The large and fast nonlinearity associated with the I_2 bound exciton would only appear at particular spatial sites. Such possibilities will be useful in some all-optical two-dimensional signal processing applications. Furthermore, the use of thinner samples with strong bound exciton absorption lines will allow us to build nonlinear Fabry-Perot bistable devices that work with lower switching energies since a sharper focusing geometry would then be possible.

4. OPTICAL NONLINEARITIES NEAR THE BOUND EXCITONS

4.1 OPTICAL SATURATION OF THE BOUND EXCITON RESONANCE

For these measurements[10], we have used a similar apparatus as shown in Fig. 3. The laser was focused to a measured spot diameter of 4 μm ($1/e^2$ point) on a high optical quality cadmium sulfide platelet of 20 μm thickness mounted strain free in a cryogenic dewar. A sharp focusing geometry also minimizes any thermal effects. Our saturation measurements are shown in Fig. 22 and are representative of the different undoped samples we have tried. They were done by making 30-Ghz single mode scans over the bound exciton resonance at different laser intensities and at the same time monitoring the transmission through the sample. The sample was immersed in superfluid helium. Remarkably, we observe a transition linewidth of only 7.9 GHz full width at half-maximum quite comparable to other sharp resonances in atomic physics. We notice that the width of the resonance is quite constant up to the largest intensities used. As the intensity is increased, we do not observe any shift of the resonance position. We take this as evidence that thermal effects play a minor role at the bound exciton resonance. At low temperature, we expect that the transition linewidth will be inhomogeneously broadened since excitons bound at different locations see different environments. If the line is inhomogeneously broadened, we expect that the absorption coefficient monitored at different points within the absorption line shape will have the same functional dependence on the laser intensity. Qualitatively, this is what we observe experimentally. We describe the saturation of bound excitons right at the peak of the resonance as a saturable, inhomogeneously broadened two-level system. The following equation describes the attenuation of a plane wave as it propagates through an inhomogeneously broadened system:

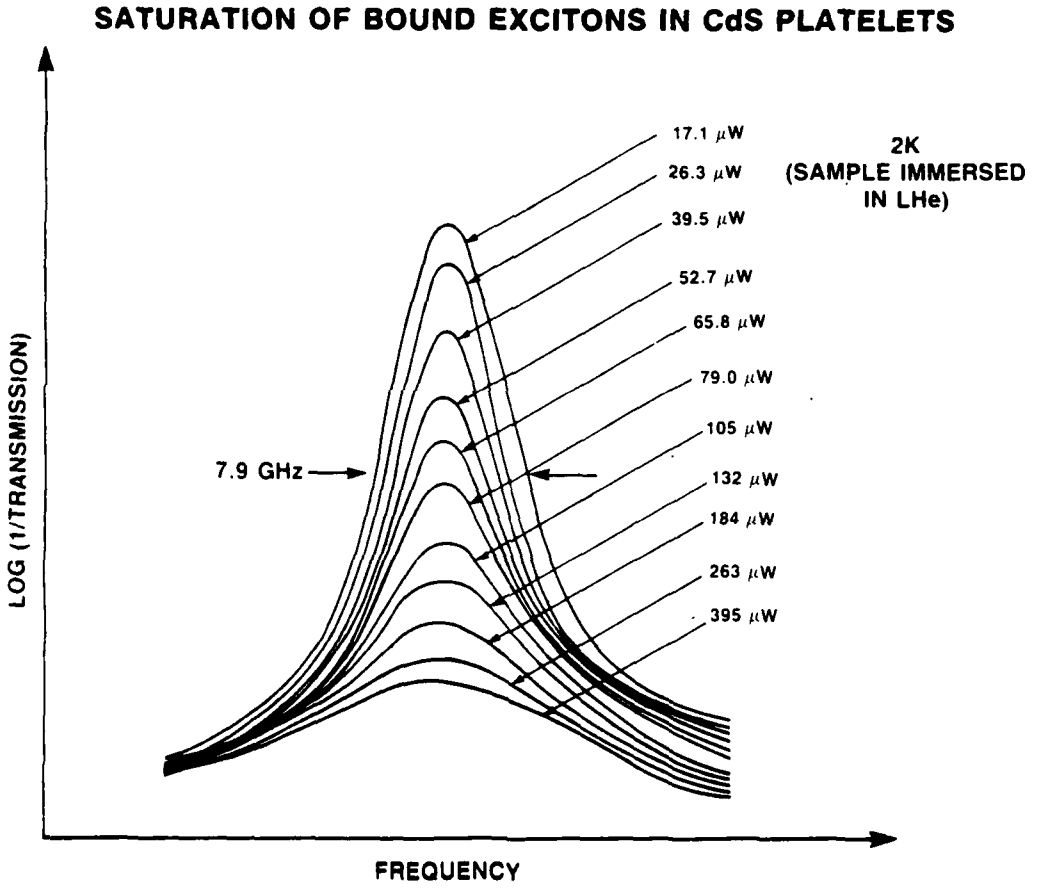
SATURATION OF BOUND EXCITONS IN CdS PLATELETS
17.1 μW
26.3 μW
39.5 μW
52.7 μW
65.8 μW
79.0 μW
105 μW
132 μW
184 μW
263 μW
395 μW
2K
(SAMPLE IMMERSED
IN LHe)
7.9 GHz
LOG (1/TRANSMISSION)
FREQUENCY

Figure 22

$$\frac{dI}{I} = \frac{-\gamma_o}{(1 + I/I_s)^{1/2}}\, dz, \tag{31}$$

γ_o is the linear absorption coefficient and I_s is the saturation intensity. Integrating the above equation yields the following transcendental equation:

$$\frac{(1 + P_{out}/P_s)^{1/2} - 1}{(1 + P_{out}/P_s)^{1/2} + 1} \frac{(1 + P_{in}/P_s)^{1/2} + 1}{(1 + P_{in}/P_s)^{1/2} - 1}$$

$$= \frac{e^{-\gamma_o L}\, e^{2\sqrt{1 + P_{in}/P_s}}}{e^{2\sqrt{1 + P_{out}/P_s}}}, \tag{32}$$

where P_{in} is the incident power inside the crystal right at the input interface, P_{out} is the transmitted power just before leaving the crystal at the output interface, and L is the crystal thickness. Taking the Gaussian nature of the incident beam into account, we obtain the fit shown in Fig. 23. Here we have implicitly assumed that the size of the laser beam is unchanged as it propagates through the sample. In other words, we believe that self-focusing and self-defocusing can be neglected in these particular measurements. For our fit, we have also neglected the effect of feedback which is small right at the peak of the absorption curve. An excellent fit is obtained if one uses as an adjustable parameter a saturation power of only 3.6 μW, which corresponds to a saturation intensity of 58 W/cm^2. The fit describes the experimental results for powers up to 100 times the saturation power. On the basis of a two-level analysis and assuming the measured radiative lifetime of 500 psec and a dipole-dephasing lifetime of 3.2×10^{-10} sec owing to spontaneous decay and

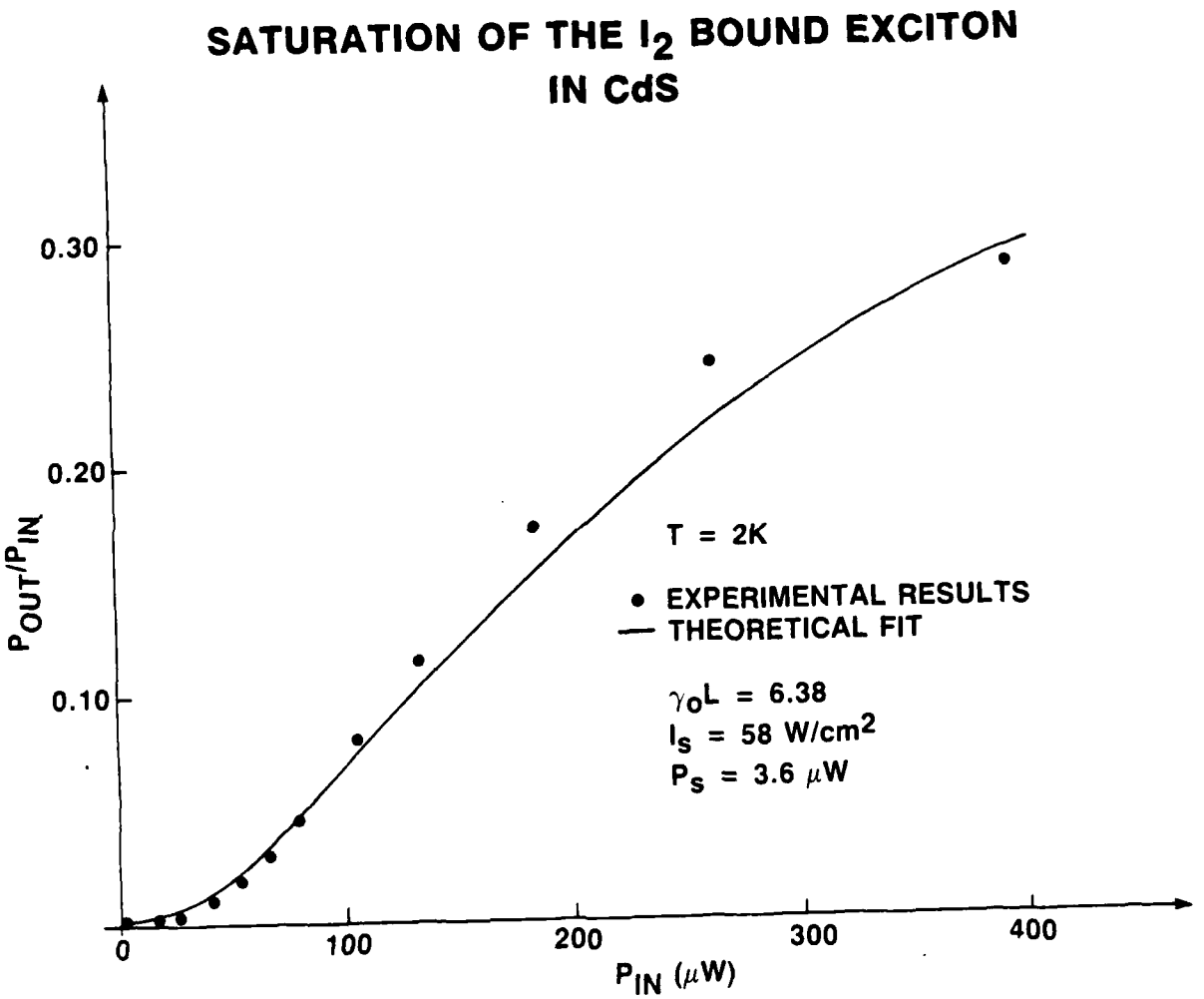
SATURATION OF THE I_2 BOUND EXCITON IN CdS
0.30
0.20
0.10
P_{OUT}/P_{IN}
T = 2K
• EXPERIMENTAL RESULTS
— THEORETICAL FIT
$\gamma_o L$ = 6.38
I_s = 58 W/cm^2
P_s = 3.6 μW
0
100
200
300
400
P_{IN} (μW)

Figure 23

acoustic phonons at 2 K (cf Figure 24), we calculate a theoretical saturation of 42 W/cm^2 using the following expression[11]:

$$I_s = 2\pi n_b^2 hc/\lambda^3 T_2. \qquad (33)$$

The excellent agreement with experiment is somewhat fortuitous since we do not expect that such a measurement can give us the saturation intensity with an accuracy better than a factor of 2 or 3 from the real value. Equation (33) and Fig. 24 show the importance of working at low temperature in reducing the saturation intensity of the bound exciton.

4.2 DEGENERATE FOUR-WAVE MIXING NEAR BOUND EXCITONS

Single-mode forward degenerate four-wave mixing experiments near the I_{2A} bound exciton were conducted to measure the resonant enhancement of the giant bound excitonic nonlinearity. The results are shown in Fig. 25, with the beam geometry that was used in the experiment. If one represents the incident fields by the following expression:

$$E_g(\vec{r},t) = 1/2\ E_g^o(r,j)\ \exp\ i(\omega t - \vec{k} - \vec{r}) \quad + c.c., \quad i=1,2,3, \qquad (34)$$

and if one assumes that $E_3^o << E_2^o << E_1^o$, the following propagation equation for the electric fields are deduced:

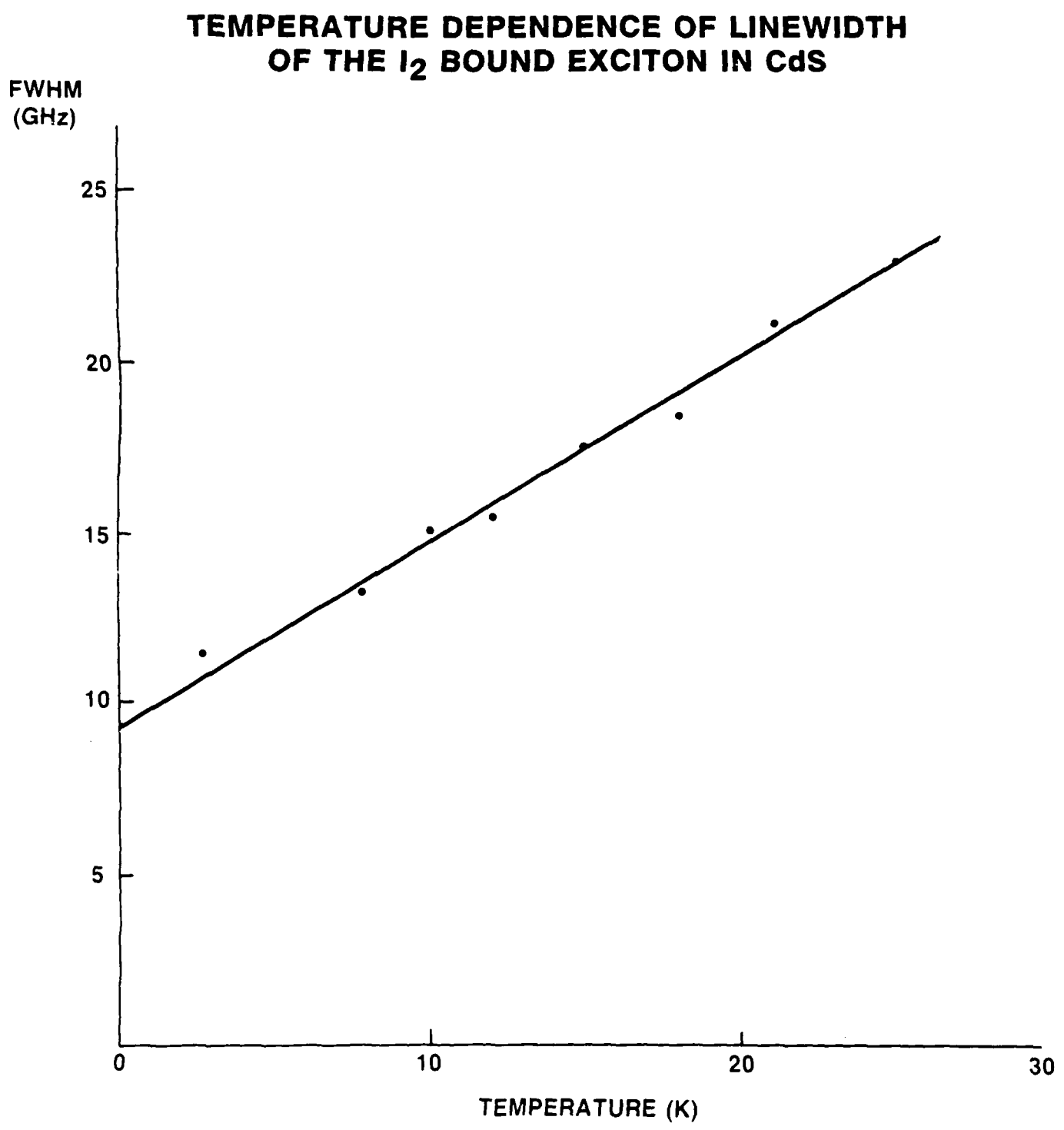
TEMPERATURE DEPENDENCE OF LINEWIDTH
OF THE I_2 BOUND EXCITON IN CdS
FWHM
(GHz)
25
20
15
10
5
0
10
20
30
TEMPERATURE (K)

Figure 24

(a)

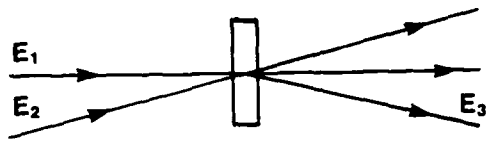
E1
E2
E3

(b)

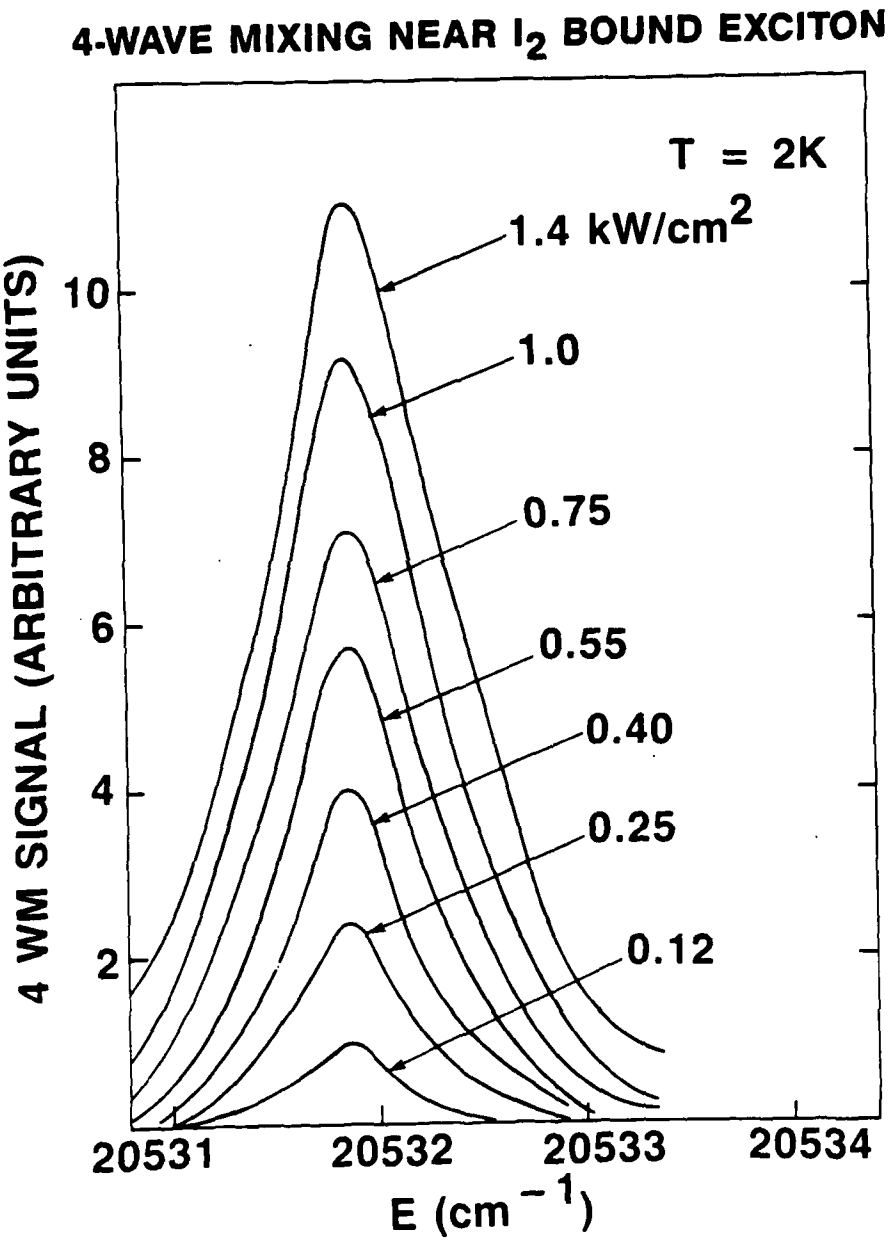
4-WAVE MIXING NEAR I2 BOUND EXCITON
T = 2K
1.4 kW/cm2
1.0
0.75
0.55
0.40
0.25
0.12
4 WM SIGNAL (ARBITRARY UNITS)
10
8
6
4
2
20531
20532
20533
20534
E (cm-1)

Figure 25

$$\frac{dE_1^o}{dz} = -ik X_o \frac{E_1^o}{2} ,$$

$$\frac{dE_2^o}{dz} = -ik X_o \frac{E_2^o}{2} + \frac{ik X_o}{|E_S|^2 (1 + \delta^2 + \left|\frac{E_1^o}{2E_S}\right|^2)} \left|\frac{E_1^o}{2}\right|^2 \frac{E_2^o}{2} , \quad (35)$$

$$\frac{dE_3^{(o)}}{dz} = -ik X_o \frac{E_3^o}{2} + \frac{ik X_o}{|E_S|^2 (1 + \delta^2 + \left|\frac{E_1^o}{2E_S}\right|^2)} \left(\frac{E_1^o}{2}\right)^2 \frac{E_2^o}{2} ,$$

where

$$X_o = -\frac{2\alpha_o}{k} \frac{(1 + \delta)}{(1 + \delta^2 + \left|\frac{E_1^o}{2E_S}\right|^2)} . \quad (36)$$

In these expressions, we have assumed that the bound exciton resonance can be modelled as a saturable homogeneously broadened two-level system. We expect that the inhomogeneous component will be negligible at high intensities. Both the absorptive and the refractive contributions are considered. At low input intensities, one can easily show that the four-wave generated signal is proportional to $I_1^2 I_2$. For input intensities above the saturation level and for an optically thick sample, it can be shown that the four-wave mixing signal at resonance is proportional to the input intensity. This is what is experimentally observed. We have, of course, verified that the four-wave mixing signal originates in the phase-matching direction and that it disappears when any of the two incident beams is blocked. Saturation of the four-wave mixing signal is already apparent at 100 W/cm^2 Since the I_2 bound exciton saturates with only 58 W/cm^2, we can define a nonlinear index of refraction of 1 x 10^{-4}cm^2/W (given an impurity concentration of 2 x 10^{15}/cc). This is the largest nonlinear index that has so far been reported in the literature. Furthermore, this nonlinear index recovers in 500 ps. The change of the index of refraction per optically generated bound exciton per unit volume is as large as 10^{-17} cm^3

near the bound exciton resonance. As we have seen, the impurity content in the sample can be artificially controlled by the technique of ion implantation.

4.3 CAVITYLESS OPTICAL BISTABILITY DUE TO LIGHT-INDUCED ABSORPTION IN CDS

For these measurements[12], Kr-ion-pumped cw ring dye laser is used with Coumarin 102 dye operating near 487 nm as the source. The laser has a multimode linewidth of 20 GHz. The light is focused to a 20-μm-diameter spot ($1/e^2$ points) on the sample with a 7.5-cm focal-length lens. A photodiode monitors a small fraction of the input light, and another photodiode placed about 20 cm beyond the sample monitors the whole transmitted beam. The good-optical-quality CdS sample is about 10 μm thick and has a surface area of less than 0.01 cm^2. It is held electrostatically to a glass slide of 150-μm thickness and then mounted in a cryogenic dewar. At low input intensity, about 90-95% of the incident light is absorbed when the multimode laser is tuned to the bound-exciton resonance. When the laser is detuned a few wavenumbers below the resonance and the total transmitted light is monitored as the input intensity is varied slowly (cw situation), we observe large hysteresis loops with contrast ratios between the on and off states greater than 10. Only a few milliwatts of input power are required for bistability to be observed. As the detuning below the bound-exciton resonance is increased, larger hysteresis loops are observed, and higher input intensities are required for optical bistability to be observed. For small detunings below the resonance and for detunings above the resonance, we do not observe any steady-state bistability.

Our results are shown in Fig.[26-27]. Bistability is observed for detunings as large as 20-30 cm^{-1} below the resonance and at input intensities up to about 20 mW. Figure 6 shows some large detuning results. For these large de-

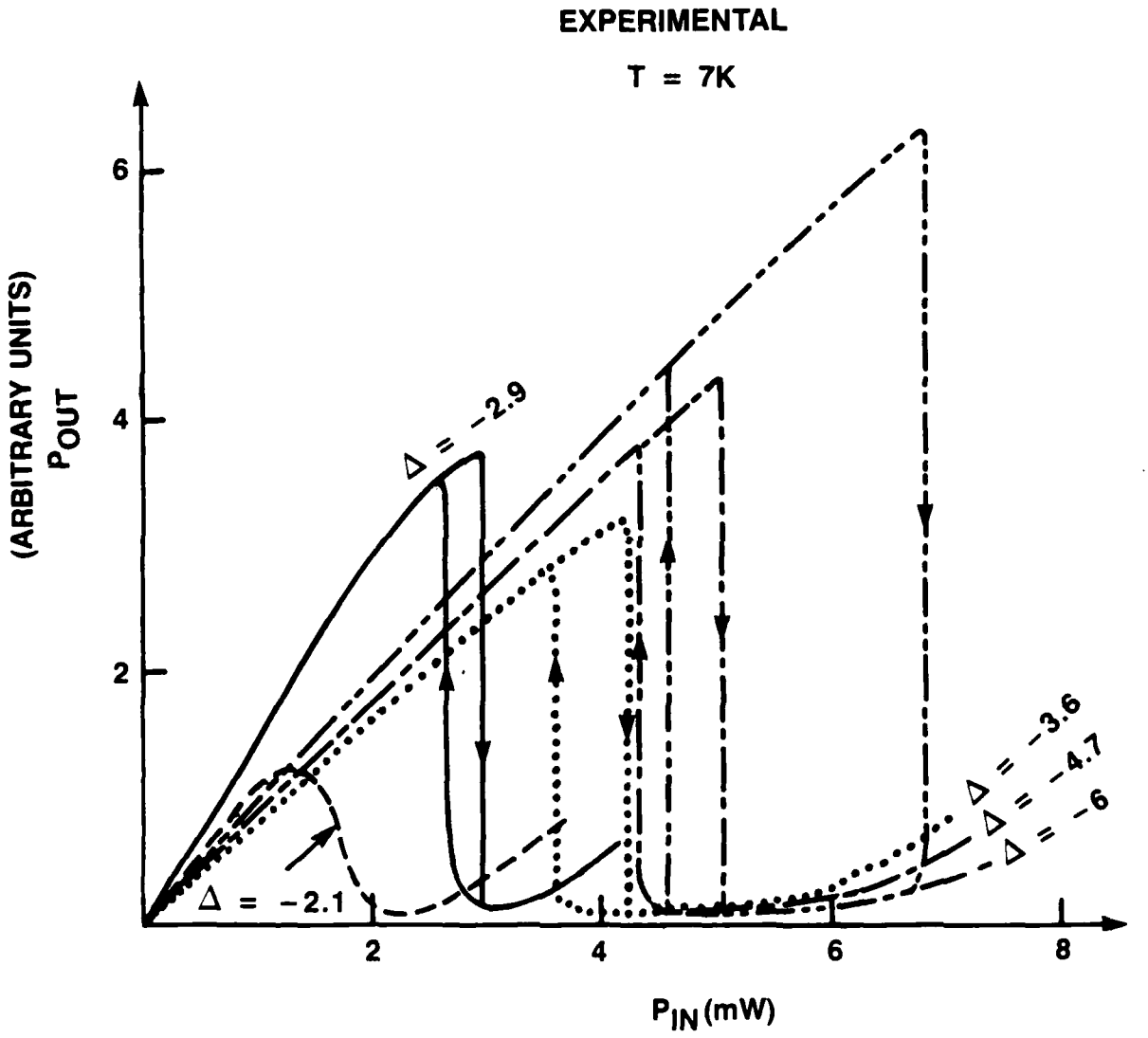

Figure 26. Induced absorption optical bistability near bound excitons.

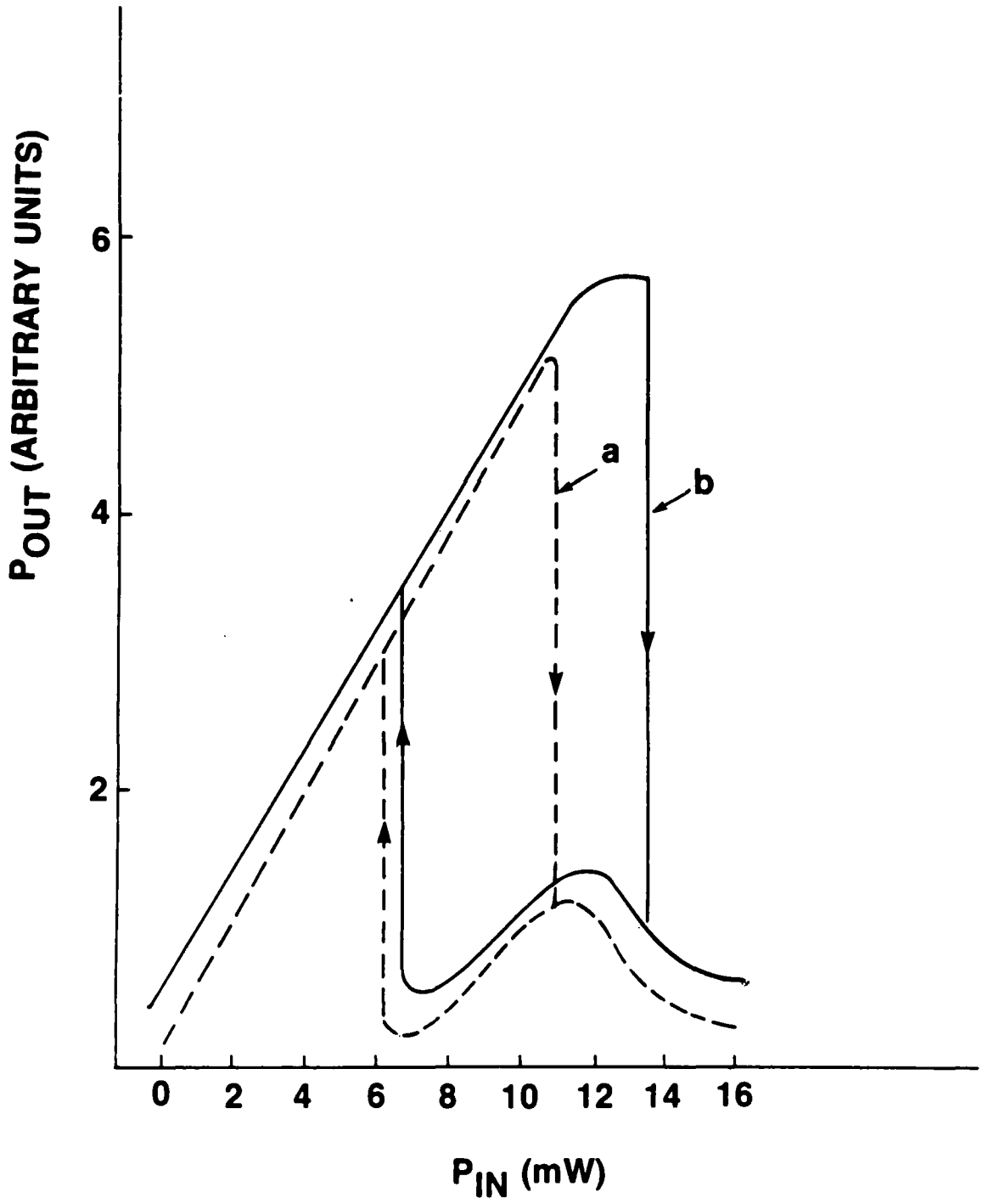

Figure 27 Induced absorption optical bistability due to free excitons: a. $\Delta = -70.6$ cm^{-1}, b. $\Delta = -72.7$ cm^{-1}.

tunings, the bound-exciton absorption becomes significantly broadened as a result of the large increase in temperature. The relative contribution of the bound exciton to the change in sample absorption at its resonant frequency is decreased, and the free exciton is responsible for the bistable behavior. Whole-beam bistability is observed for sample temperatures (with the laser off) as low as 4.2 K and as high as 50 K.

When the sample is illuminated with light whose frequency is less than the bound-exciton resonance, the sample heats up locally owing to absorption in the tail of the free exciton. This causes the resonance to shift to lower energies (the band gap shrinks as the temperature increases). As it shifts toward lower energies, more heat is generated in the sample owing to the increased absorption of the free and bound excitons, and the bound-exciton resonance frequency overshoots the frequency of the laser. The transmission suddenly switches from a high state to a low state because of this rapid shift in the excitonic frequency. The laser is then on the high-energy side of the resonance and is substantially absorbed. This point is a stable point since, if the resonance were to move away from the laser, the absorption would decrease, the sample would cool, and the resonance would have to move back toward the laser (negative feedback). When the intensity is reduced, switching back to a high state is obtained at a much reduced intensity because heat is stored in the sample.

The qualitative features of our results may be understood from the simple model that follows. A more quantitative theory was presented previously. We suppose that the rise in sample temperature ΔT is proportional to the amount of heat absorbed, Q (we neglect diffusion):

$$\Delta T \sim Q. \tag{37}$$

It is assumed here that most of the energy absorbed is dissipated nonradiatively:

$$Q \sim P_{in} - P_{out} = P_{in}(1 - e^{\alpha L}) \sim \alpha P_{in}. \tag{38}$$

Relations (37) and (38) imply that

$$\alpha \sim \Delta T/P_{in}. \tag{39}$$

We also know that, in the case of the bound exciton, α has a resonant line shape that, for simplicity, we assume to be Lorentzian:

$$\alpha \sim \frac{1}{1 + (\omega - \omega_0)^2 T_2^2}, \tag{40}$$

where $\omega_0 = \omega_0(T)$. The solution of relations (39) and (40) is schematically represented in Fig. 28. Using this simple graphic construction, one can easily understand how we can get optical bistability, the shape of the hysteresis loop, and its detuning dependence. Our calculation[12] using a more complete model including diffusion is shown in Fig. 29, and good qualitative agreement is obtained.

This class of bistability based on induced absorption is part of a more general class of bistability. In particular, in CdS it was theoretically predicted that bistability based on an induced absorption that is due to band-gap renormalization should be observed[13]. Recently, power hysteresis with

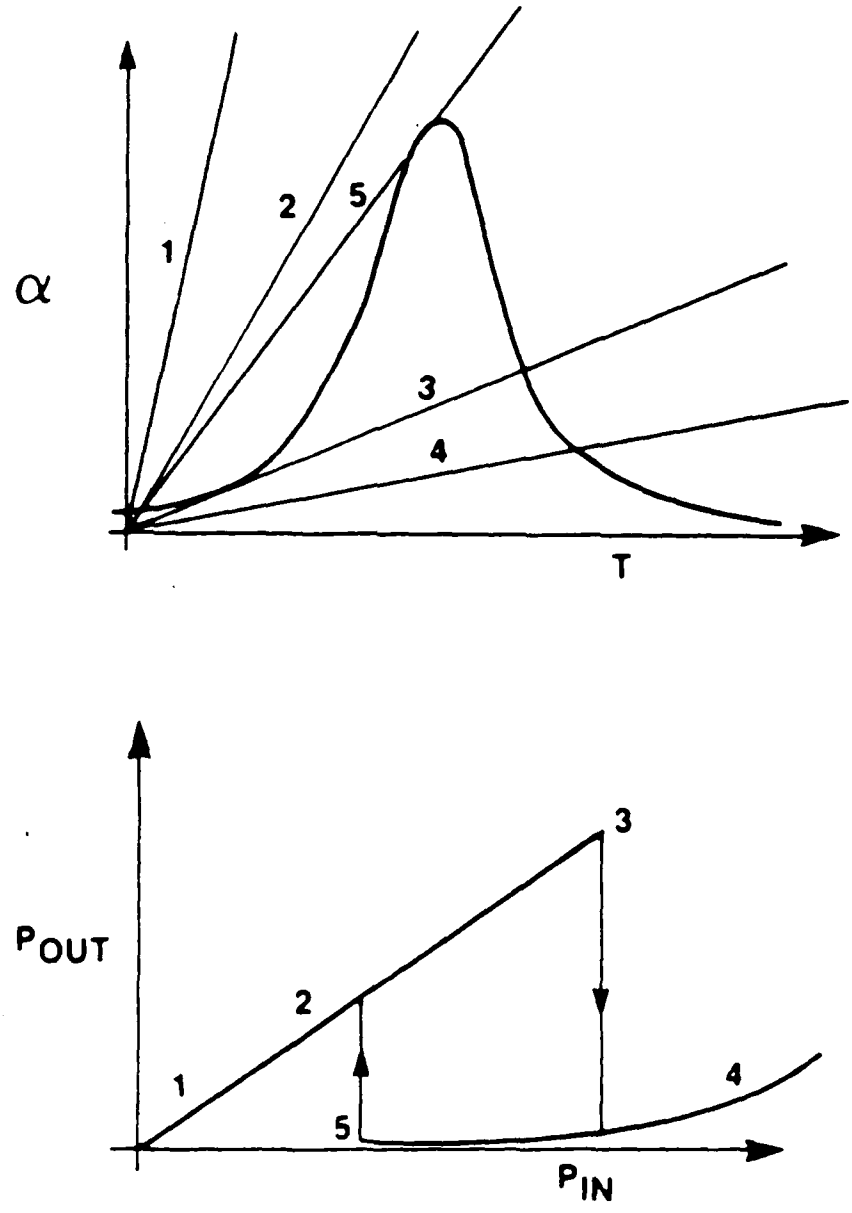

Figure 28. Graphical construction for obtaining optical bistability in the presence of an optically induced absorption. The slope of the straight lines is inversely proportional to the incident intensity. If the intensity is increased to point 3, there are two possible values of the absorption coefficient α, and the transmission switches from a high to a low state. A subsequent decrease in the intensity results in a switch-up at point 5.

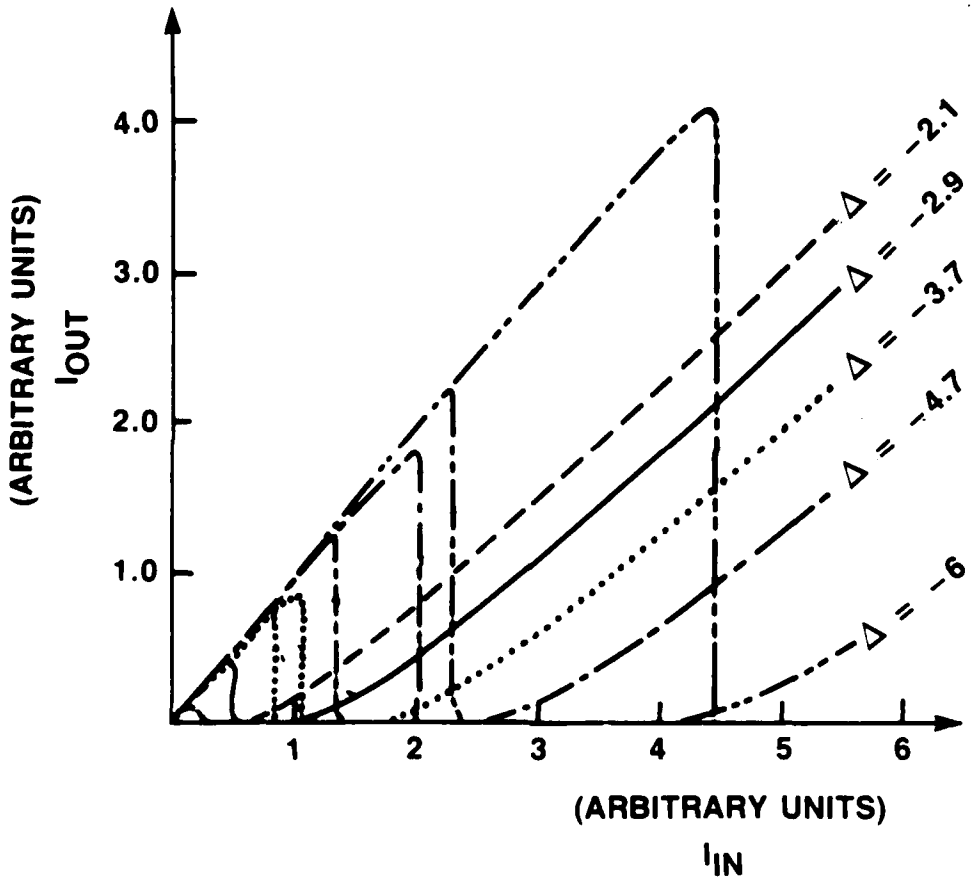

Figure 29. Theoretical simulation of optical bistability due to induced absorption near bound excitons.

≈10 nanosecond pulses was reported in CdS[14], but no clear evidence for switching or optical bistability was presented. Intensities of the order of 1 MW/cm^2 were required. The hysteresis was claimed to be due to the renormalization of the band gap, but thermal effects were not considered. We have a strong suspicion that thermal effects play a significant role in the measurements with input intensities above 1 MW/cm^2, in particular once the induced absorption has set in. The initially induced absorption is probably due to an exciton self-broadening of the transition[15].

4.4 OBSERVATION OF PICOJOULE, SUBNANOSECOND ALL-OPTICAL SWITCHING NEAR BOUND EXCITONS IN CDS

For our observation of quasi-steady-state optical bistability on the nanosecond time scale near the bound exciton[16], we operate a dye laser in a single longitudinal mode. The light is focused to a 20-μm-diameter spot ($1/e^2$) on a high-purity 13-μm-thick sample with a 7.5-cm focal-length lens. The sample is floated strain-free in a cavity immersed in superfluid He. The cavity is formed by a 25-μm-thick spacer with a hole in the center inserted between two 90%-reflecting dielectric mirrors. The single-mode absorption αL at the peak of the bound-exciton resonance is measured to be 4.4. Fabry-Perot fringes with good contrast are observed as the laser frequency is tuned around the bound-exciton resonance. A plot of P_{out} versus P_{in} is obtained by recording both the input and output pulses with a Tektronix (Model 7912AD) transient digitizer. The total time resolution of our system is 2.6 nsec and is limited by our detectors and amplifiers. When the incident laser is tuned in very close proximity ($<0.3\ cm^{-1}$) to the bound-exciton resonance, optical bistability is observed with input powers of less than 8 mW incident upon the nonlinear Fabry-Perot interferometer. For these measurements, we use an electro-optic modulator to generate triangular optical pulses of 80-nsec rise and fall

time at a repetition rate of about 1000 Hz. Figure 30a is a single-shot trace of P_{in} versus time and P_{out} versus time. It also shows P_{out} versus P_{in}. Figure 30b shows a repetitive trace. Very sharp discontinuous switching is observed. The deconvolved switch-up and switch-down times are estimated to be less than 1 and 2 nsec, respectively. Assuming an inhomogeneous linewidth of 6-8 GHz for the bound exciton, it is estimated that changes in the index of refraction as large as 0.01 can be induced when the bound-exciton resonance is saturated. When the laser is detuned by more than 0.3 cm^{-1} from the bound-exciton resonance, no bistability or hysteresis is observed. When bistability is observed, the input pulse (and the duty cycle) can be lengthened by a factor of more than 10 without altering P_{out} versus P_{in} in any significant way (cm Figure 30b). This is clear evidence that heating effects are not important in these measurements. From our measurements, a single-beam-switching energy of less than 4 pJ is determined, which is the lowest value yet reported in a semiconductor. In a two-beam experiment (one holding beam and one switching beam), we expect much lower switching energies for the switching lasers. An important advantage in using bound-exciton nonlinearities is that the switching power can be reduced inversely proportionally to the focused spot area. This is not true for other systems, in which carrier or thermal diffusion is important. By focusing the laser beam to a spot-size diameter of $\approx\lambda/n$ and assuming a switching time of about 500 psec (the radiative lifetime of a bound exciton), we deduce a single-beam switching energy of less than 0.2 fJ. This corresponds to 500 photons. In this regime, statistical fluctuations start becoming important.

We now present a simple calculation demonstrating that a great number of data can be processed in parallel when the I_2 bound exciton in CdS is used as the source of the optical nonlinearity. Let us consider a 1 cm x 1 cm CdS

OBSERVATION OF OPTICAL BISTABILITY NEAR BOUND EXCITONS IN CdS

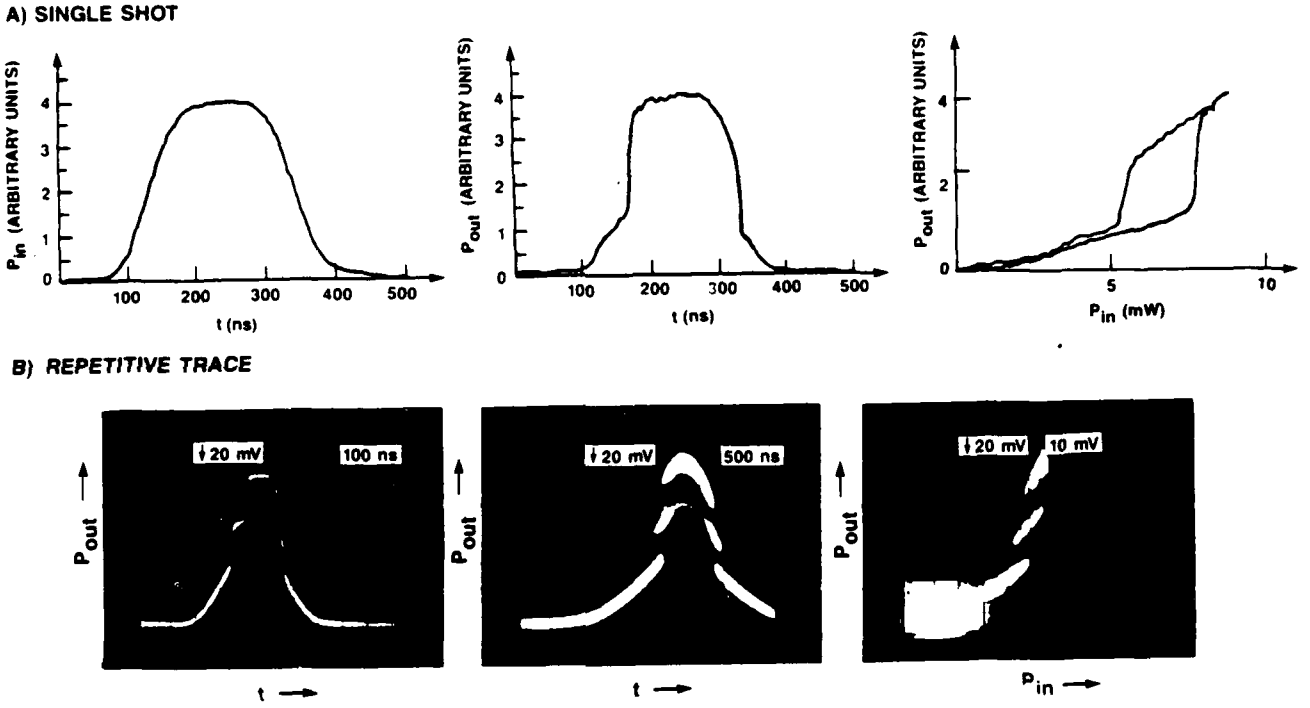

Figure 30

sample and assume a resolvable laser spot size of 2 μm x 2 μm. The total number of addressable spots is then 2.5 x 10^7 spots. We take 10^9 bits/sec as the processing speed of each individual spot, and we assume a duty cycle of 10^{-4} to minimize thermal effects. The total processing rate is evaluated to be 2.5 Tbits/sec. This rate is proportionally increased when the duty cycle is increased. Since the area per bit is 2 μm, we expect that the switching energy will be reduced by a factor of $(20/2)^2$ from what we have measured experimentally. This implies a switching energy of only 80 fJ/bit. At 2.5 Tbits/sec, only 0.2 J would be dissipated in 1 cm^2 of CdS. No heating would result if the sample is appropriately mounted. Since the device works in the visible part of the spectrum, extremely large processing rates appear possible in the area of image processing. Other applications in optical computation and in dynamic interconnections are also possible.

4.5 QUANTUM CONFINED STARK EFFECT OF QUANTUM DOTS

As it was recently discussed in the literature, quantum well materials have very interesting electrical and optical properties[9,17]. In quantum wells, the motion of the free exciton is confined to a two-dimensional plane. Because of this confinement, both the oscillator strength and the binding energy of the free exciton are increased. This leads to the possibility of observing a very clear excitonic absorption peak at room temperature which can be Stark shifted. New modulators based on this concept have recently been demonstrated. Because of the possibility of demonstrating new devices with very interesting properties when the dimensionality of the system is reduced, there is now a new trend. One would now like to confine the exciton motion to one and zero dimensions. One then talks of quantum wires and quantum dots respectively. Since the oscillator strength of the free exciton for molecule is

proportional to the probability of finding both the electron and the hole at the same physical location, there is much to gain in reducing the dimensionality of the system and, by the same token, in increasing the overlap of both the electron and hole wavefunctions. From the point of view of nonlinear optics, the ideal system should have the largest oscillator strength combined with a dephasing time governed by spontaneous decay[18]. This in turn permits the operation of an optical switch at high rates at the minimum switching energy per operation that is physically allowed.

As it was previously discussed, bound excitons can be seen as a Coulomb correlated electron-hole pair (exciton) weakly bound to an impurity center. The bound exciton is then the natural realization of a quantum dot. The confinement by the impurity is over a dimension of the order of the free exciton Bohr radius. Bound excitons have remarkable properties. One of the most interesting ones is the large oscillator strength of the bound excitons. Typically it is of the order of 10.

Because of the possibility of demonstrating new modulation concepts using the "low dimensionality" of the system, we have studied the effect of electric fields in Stark shifting the very sharp ($\simeq$ 8 Ghz) I_2 bound exciton resonance in CdS. Because the electron and the hole in the free exciton are inhibited from splitting apart by the binding impurity potential, we talk about quantum confined Stark effect of quantum dots.

Stark shifting of the n=2 A free exciton in CdS was previously studied by Thomas and Hopfield[19] at electric fields up to 1000 V/cm. The n=1 A free exciton and the bound exciton lines were found to shift less than 10^{-5}eV, the limit of detection, when an electric field of 1000 V/cm was applied parallel to the hexagonal symmetry axis (c-axis). Initial attempts with evaporated

contacts onto the crystal were found unsatisfactory: 1) Strain associated with the contact area broadened the lines, 2) there appeared to be an uneven distribution of the field along the crystal, 3) and the contacts were not always ohmic. Consequently a method was used in which no contacts were made to the crystal. This is also the technique we used. In our case, the electric field was applied in the direction of propagation of the incident laser beam.

Since the crystals are photoconductive, it is necessary to apply a square-wave voltage to the plates with a time interval less than the effective dielectric relaxation time of the crystal to avoid polarization. For the n=1 exciton and for the bound excitons, the Stark effect is dominated by the simple hydrogenic Stark effect in the effective-mass approximation. For an exciton of zero wave vector, all Stark-effect energy shifts are a function only of the absolute value of the electric field. A bipolar square wave electric field of 1.4×10^4 V/cm amplitude was applied to the crystal.' The period of the square wave was 10 μsec and, according to Thomas and Hopfield, was sufficiently short to avoid any screen-out effect by accumulation of charges.

At the maximum applied electric field (1.4×10^4 V/cm), a shift of about 0.1 cm^{-1} was detected. This is shown in Figs. 31 and 32. The incident laser linewidth was assumed to be 0.3 cm^{-1}. The evaluation of the Stark shift from first principles is not an easy task because it is a four-body problem. One can already get an idea of the magnitude of the shift by evaluating the n=1 A free exciton Stark shift. From the well-known expression for the Stark effect of a hydrogen atom[20], an energy shift of ≈ 0.5 cm^{-1} is expected. On theoretical grounds, one might expect that the bound exciton will shift less than the free exciton as the electric field is increased since the bound exciton has a higher binding energy (≈ 34 meV) than the free exciton (≈ 28 meV) as measured

stark shift: 0 v applied

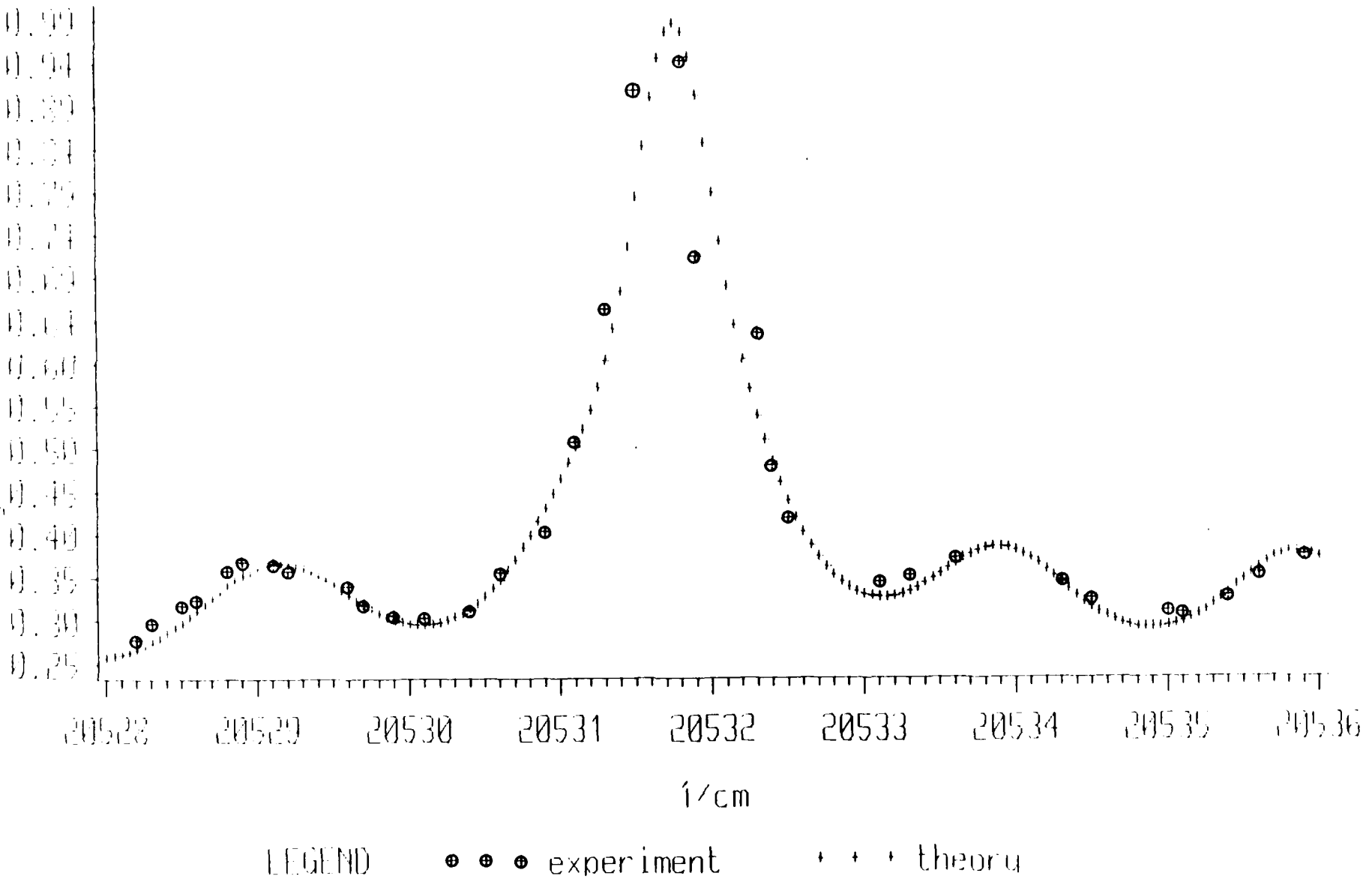

Figure 31(a). Quantum confined Stark effect of quantum dots in CdS. The bound exciton resonance is taken as 20531.75 cm^{-1}.

stark shift: 0 v applied

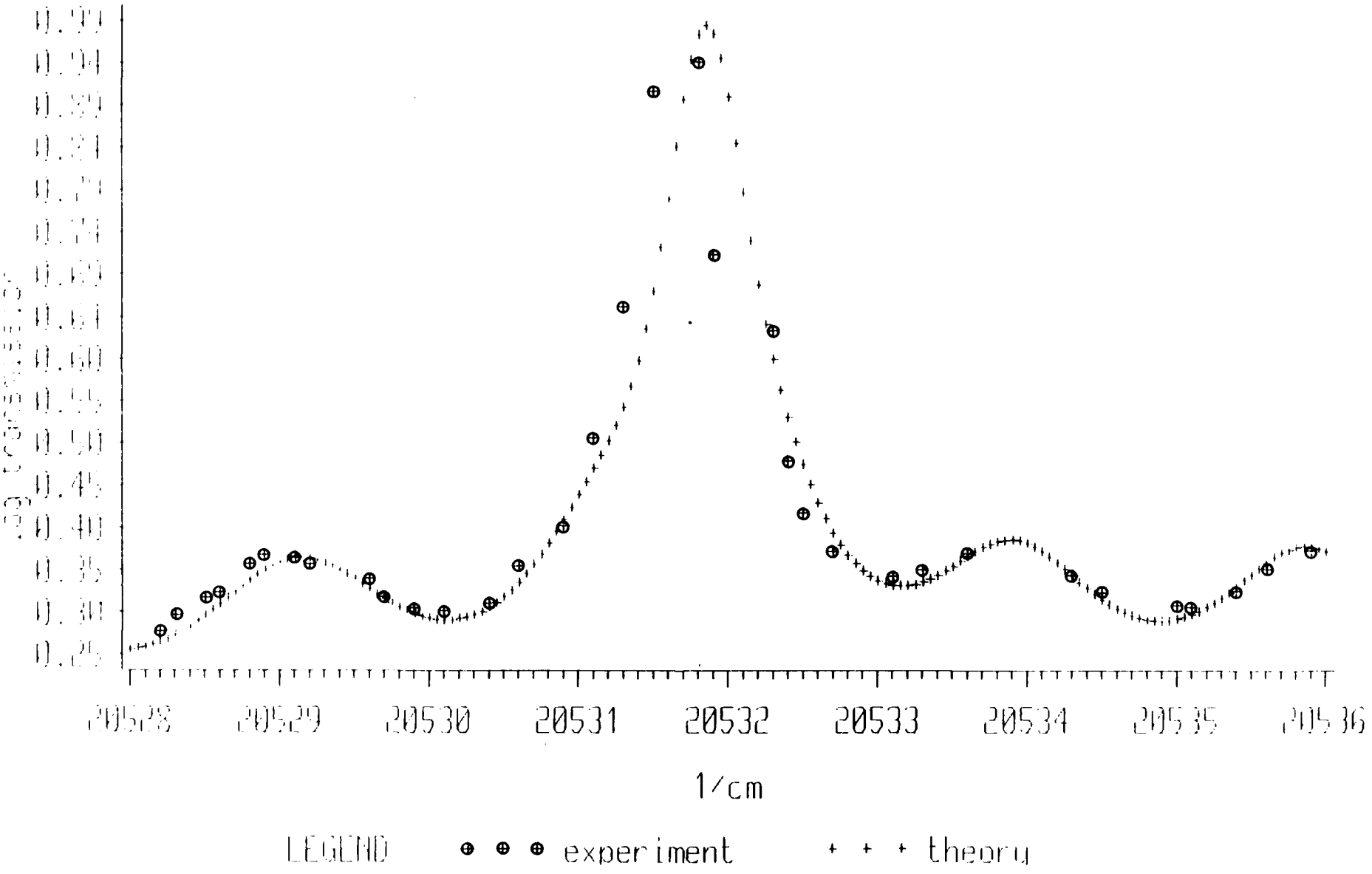

Figure 31(b). Quantum confined Stark effect of quantum dots in CdS. A bound exciton resonance frequency of 20531.85 cm^{-1} gives a much worse fit.

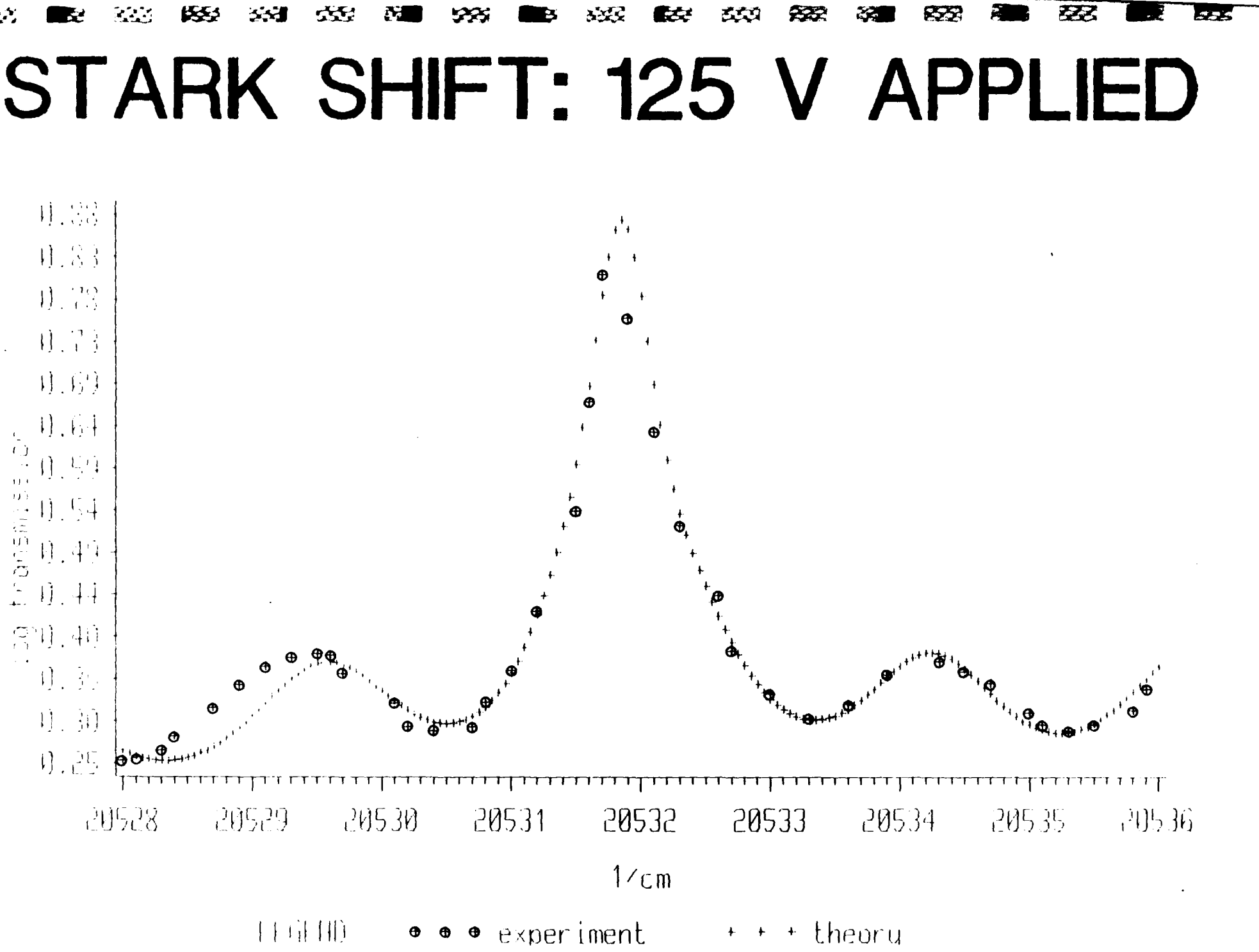

Figure 32(b). Quantum confined Stark effect of quantum dots with E = 1.5 × 10⁴ V/cm. The [illegible] shifted to 20531.85 cm⁻¹.

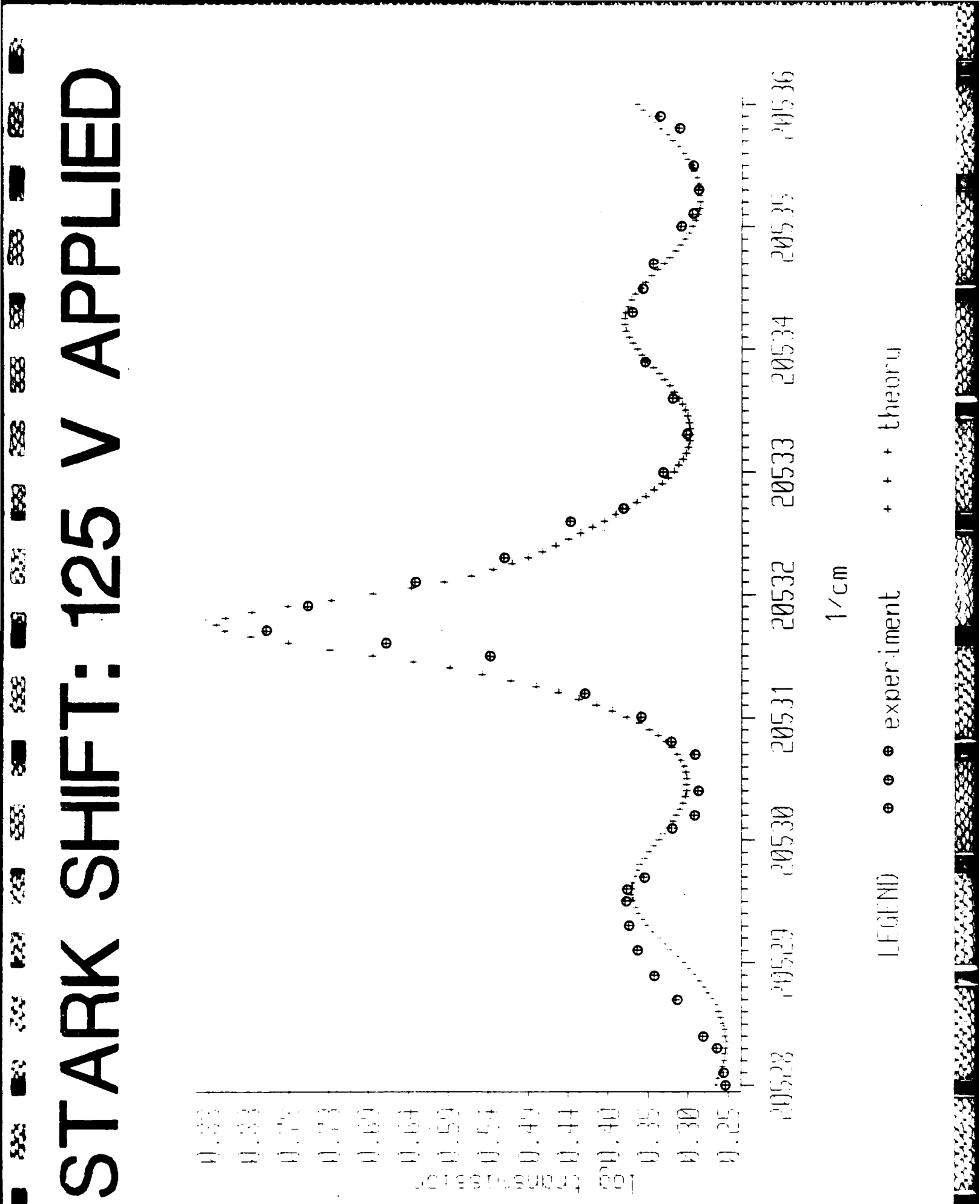

Figure 32(a). Quantum confined Stark effect of quantum dots with E 1.5 x 10^4 V/cm. A bound exciton resonance frequency of 20531.75 cm^{-1} gives a much worse fit.

from the conduction band. This is consistent with the experimental observations. At the electric field used in the experiment, no significant broadening of the bound exciton resonance is detected. By applying slightly larger electric field, the operation of a very efficient modulator would result.

Future work should concentrate on making very good ohmic contacts to the sample. The possible operation of a high speed modulator with less than 10 V drive is anticipated. A new exciting possibility is the operation of new type of SEED device[9,17] based on the bound exciton resonance. This of course would depend on the photoconductivity of the crystal at the bound exciton frequency.

5. OPTICAL NONLINEARITIES NEAR THE A FREE EXCITON IN CDS

5.1 INVESTIGATION OF PERIODIC PULSATIONS AND CHAOS

The transmission characteristics of a CdS platelet immersed in superfluid liquid helium were investigated as the incident intensity of a cw laser tuned below the free exciton resonance was increased. Part of the transmitted beam was monitored through an aperture. At a certain threshold intensity (1-10 kW/cm^2), very regular pulsations of the transmitted intensity in the 10 μs time scale were recorded[21] and are shown in Fig. 33. As the intensity was increased even more, new frequency components appeared and the temporal behavior became very complicated (non-periodic). The intensity spectrum of the transmitted light is also shown in Figure 34 for a different detuning below the free exciton resonance as the intensity increases. Again, periodic pulsations are observed and irregular pulsations appear at high intensities. These pulsations are believed to be thermal in origin. If the whole transmitted beam is collected with a large aperture lens, the pulsation tends to be washed out as a result of averaging across the transverse profile. This appears to be mostly a transverse effect. The spot diameter on the sample was measured to be 20 μm ($1/e^2$ points). Back of the envelope calculations using the heat diffusion equation appear to be consistent with a thermal effect. Pulsations on the same time scale and at similar intensities have also been observed in GaAs. In these measurements, thermal effects were found to play a dominant role[22].

OBSERVATION OF SELF-PULSATION

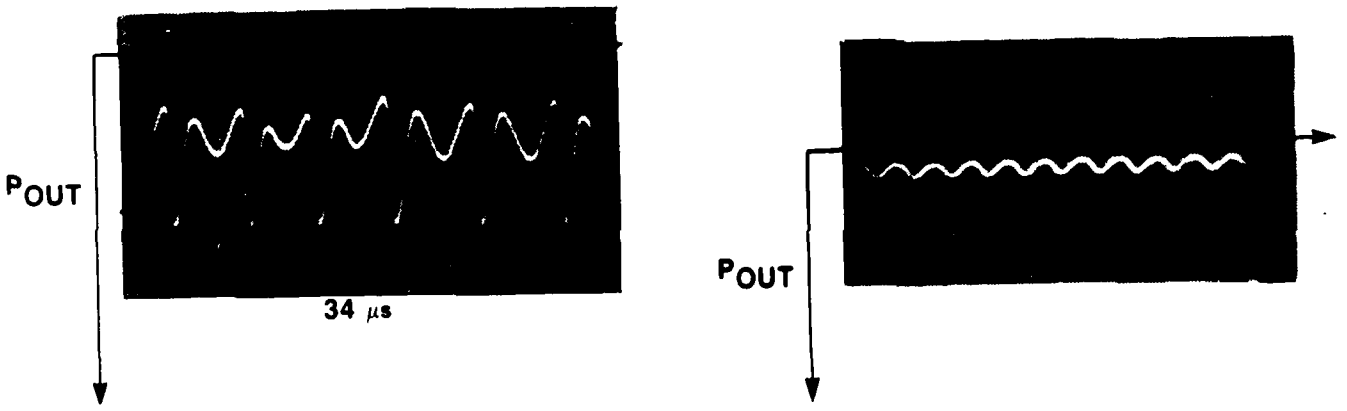

Figure 33. Self-pulsation observed below the A free exciton resonance frequency.

POWER SPECTRA

BEFORE SAMPLE:

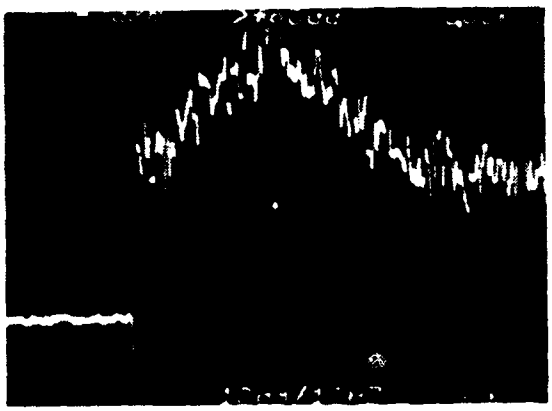

AFTER SAMPLE:

a)

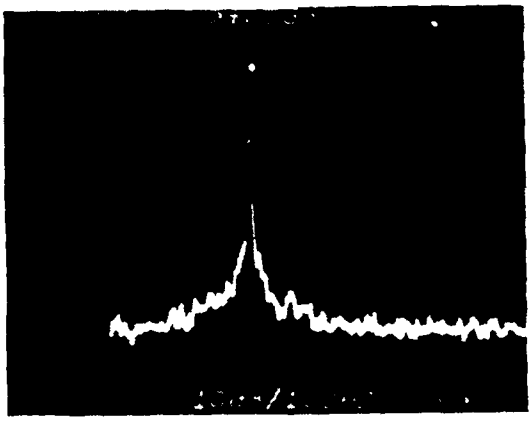

b)

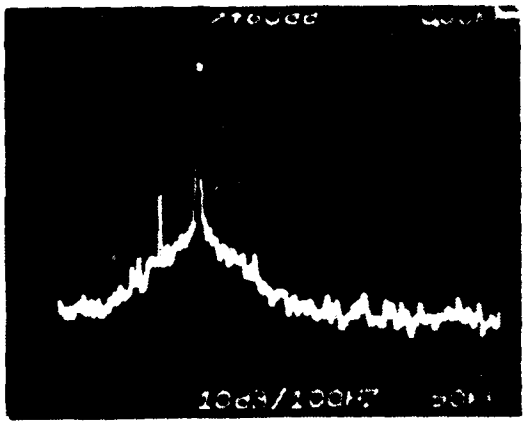

c)

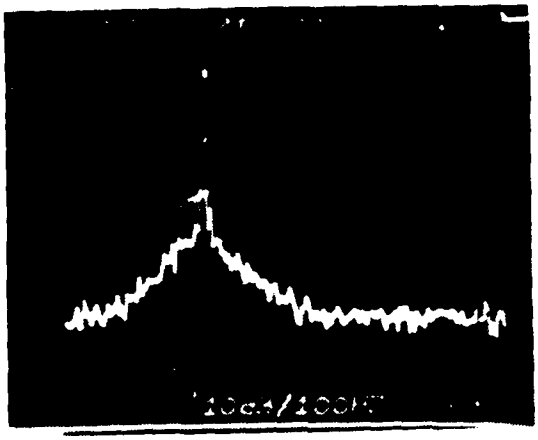

d)

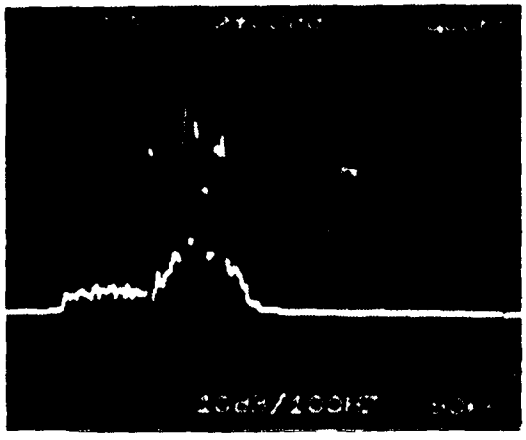

Figure 34 Power spectra of the transmitted light beam tuned below the A exciton resonance as the intensity increases from a to d.

5.2 OPTICAL HYSTERESIS IN TRANSIENT EXPERIMENTS DONE ON THE NANOSECOND TIME SCALE

Two free excitons can collide together and form an excitonic molecule called a biexciton, which is free to move in the crystal. A biexciton can also be formed by direct absorption of two photons. When a large density of free excitons is generated, the free excitons start screening each other (dielectric screening) and one observes a renormalization of the band gap. This renormalization can in principle lead to the possibility of observing optical bistability due to increasing absorption. An enormous amount of work has been published in this area of research[23]. Unfortunately, it is extremely controversial[24]. For instance, many different groups have recently claimed to have observed the biexcitonic resonance in CdS. But no one agrees on the exact position of the resonance. Very implausible assumptions are often made in explaining the details of how a large population of excitonic molecules are created. The details of how an electron-like plasma is generated are also quite controversial and often unreasonable. Clearly, careful work is needed to properly understand the mechanism of formation of a biexciton and of band gap renormalization. Much work remains to be done in the area of electron-hole plasma screening and dielectric excitonic screening. CdS appears to be the ideal candidate for doing such studies.

One important physical mechanism which has most of the time been neglected in high excitation studies on the nanosecond time scale is the mechanism of lattice heating by the incident laser beam. We believe that such a process plays a very important role when nanosecond pulses of 1-10 MW/cm^2 intensities are used on thin CdS samples. These are the typical intensities that were recently used to study electron-hole plasma and also optical bistability due to increasing absorption. We believe that the interpretation of these experiments is incomplete.

Let us consider smooth incident pulses of about 20 ns duration and with peak intensities in the range between $10^5 W/cm^2$ to 10^7 W/cm^2 Let us assume that the laser is detuned below the free exciton by about 20 to 50 cm^{-1}. We will now qualitatively describe what is expected. As the input pulse intensity increases, free excitons are generated. These excitons collide with each other and broaden the free exciton resonance in such a way that a much larger fraction of the incident pulse energy can be absorbed. When the exciton density reaches 5×10^{17} to 1×10^{18}/cc, an appreciable band gap renormalization sets in as excitons screen each other's Coulombic interaction. At the same time, the absorption coefficient in the sample has increased substantially. As a result of this, much of the incident energy is absorbed in a very shallow layer. The carrier lifetime at a density of about 1×10^{18}/cc is about 1 ns. As the density of electron and hole increase above $\approx 5 \times 10^{18}$/cc, the carrier lifetime becomes dramatically shorter because of bimolecular and Auger recombination. It becomes very hard to keep increasing the carrier density. At the same time as all of these processes are happening, heating of the thin layer at the surface of the CdS platelet becomes quite appreciable. Very high temperatures can be reached and even melting can occur at intensities of the order of 10 MW/cm^2. If melting has not occurred, when the input intensity is reduced again, the absorption coefficient does not recover and hysteresis in the curve of P_{out} vs P_{in} is observed. So far, optical bistability using the intrinsic electronic nonlinearity of CdS has not been observed, even though many claims of the contrary can be found in the literature. The following three criteria have been used to determine if a bistable device is truly bistable:

1. Well-defined switch-on and switch-off characteristics are observed;

2. The curve of P_{out} vs P_{in} retraces itself outside the bistability region;

3. Lengthening the incident pulse leads to the same P_{out} vs P_{in} curve.

We will now compare the relative importance of lattice heating compared to the band gap renormalization process. As we have previously seen, excitons can be considered in thermal equilibrium with the lattice for temperatures above 40 to 50 K. If an amount of energy ΔQ is deposited in the lattice, the temperature of the crystal will increase by:

$$\Delta T = \frac{\Delta Q}{C} \tag{41}$$

where C is the specific heat. Since the initial crystal temperature is very low (T_o = 2 K), we can write:

$$\Delta T \simeq T = \frac{\alpha I t}{C} \tag{42}$$

where α is the absorption coefficient and t is time (we are assuming a square optical pulse of constant intensity). But we also have:

$$\omega_{gap} = -aT^2 + \omega_{gap}(T = 0). \tag{43}$$

In the case of band gap renormalization, we can approximate the renormalization by the following equation:

$$\omega_{gap}^{(N)} = -bN^2 + \omega_{gap}\,(N = 0) \quad , \tag{44}$$

where b is chosen in such a way that:

$$\omega_{gap}(N=1x10^{18}) = -bN^2 + \omega_{gap}(N = 0) = \omega_{A\ exciton} \quad . \tag{45}$$

N is the free exciton density and is given by the following expression:

$$N = \frac{\alpha I T}{h\omega} \tag{46}$$

where T is the free exciton lifetime. The ratio of the thermal contribution to the band gap renormalization contribution is given by:

$$\frac{\text{thermal}}{\text{band gap renormalization}} = \frac{a}{b}\left(\frac{\hbar\omega}{c}\right)^2\left(\frac{t}{T}\right)^2 \tag{47}$$

Using a = 0.0105 cm^{-1}/K^2, b = 2.24 x 10^{-34} and C = 2.08 J/ccK, we get:

$$\frac{\text{thermal}}{\text{band gap renormalization}} = 1.7 \times 10^{-6}\left(\frac{t}{T}\right)^2 \tag{48}$$

This expression indicates that in the initial stages of the process, band gap renormalization is much more important than the thermal contribution. At low intensities, we expect the thermal contribution to become important only for times longer than ≈ 1 μsec. At high intensities, we can use a similar ap-

proach to the one we have just presented. We just have to replace the dielectric band gap renormalization by an electron-hole plasma renormalization. We see again that, as the carrier lifetimes get shorter (< 100 ps), thermal effects become again the dominant factor for incident pulses of tens of nanoseconds. This is the regime of validity of our published theoretical transient calculation[25].

5.3 INTRA-CAVITY OPTICAL BISTABILITY DUE TO OPTICALLY INDUCED CHANGES IN ABSORPTION AND REFRACTION

A theoretical and experimental study of optical bistability in a cavity in the presence of both an optically induced absorption and an optically induced index change generated by local heating of a CdS sample was conducted[26]. The laser was tuned in the vicinity of the A-free exciton. Since thermal effects will ultimately impose a speed limitation on two-dimensional optical signal processing, it is important to study in more detail the importance and the role of thermal effects on the operating characteristics of bistable devices in general. Power levels of the order of 5 to 10 mW were sufficient to switch the bistable device on a submillisecond time scale. For detunings above the free exciton resonance, counterclockwise hysteresis loops were predicted and observed as the incident intensity was varied. For detunings below the free exciton resonance, only clockwise hysteresis loops were predicted and observed.

5.4 NONLINEAR ABSORPTION NEAR FREE EXCITONS

The free exciton self-broadening mechanism will now be studied in more detail. Let N be the number of optically generated excitons. We have:

$$N \propto \alpha I \quad , \tag{49}$$

and $$\alpha(N) \propto \frac{T_2(N)}{(\omega-\omega_o)^2 T_2^2(N) + 1} \quad , \tag{50}$$

where $$T_2(N)^{-1} = \Gamma_o + \Gamma_1 N \quad . \tag{51}$$

The dephasing rate T_2^{-1} has a component that comes from impurity and defect scattering (Γ_o) and a component that comes from collision with other excitons (Γ_1). This is a billiard ball model for the collisions. Equations (49) and (50) are two equations of α vs N. The solution is given by the intersection of the two curves. Fig. 35 shows a graphical solution of these two equations for three different intensities and two different detunings. For large detunings, as the intensity is increased, the absorption coefficient just keeps on increasing. For smaller detunings, the absorption coefficient goes through a peak and then decreases again as the intensity increases. This is exactly what was observed experimentally, as shown in Figs. 36 to 38. The duration of the incident pulse (Fig. 39) was chosen long enough ($\simeq$ 60 ns), so that the transmission was measured in a quasi steady state regime, and short enough, so that thermal effects did not have time to set in. The fact that the curve of P_{out} vs P_{in} retraces over itself is an experimental verification that quasi steady state was reached. It should be stressed that our theory does not predict any bistability in a plot of P_{out} vs P_{in}. This is also in agreement with our experimental results and strongly contradicts previous claims toward the experimental observations of optical bistability at similar intensities to ours [27]. We believe that such claims result from the use of a largely fluctuating incident laser pulse. Mode beating leads to large spatial and temporal inhomogenieties. The maximum intensity used in our experiment is $\simeq$ 5 kW/cm^2 Preliminary calculations indicate that the free excito self-broadening param-

NONLINEAR ABSORPTION NEAR FREE EXCITONS

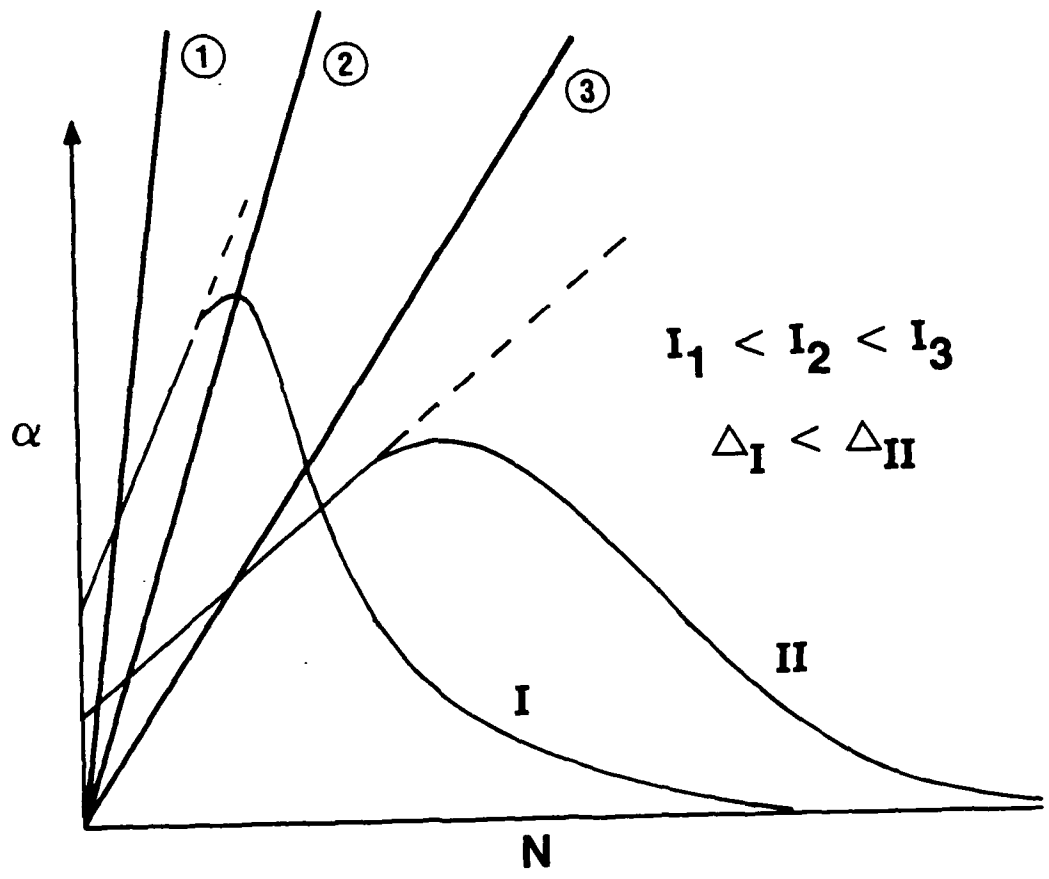

Figure 35. Graphical construction to obtain the absorption coefficient α as the laser intensity increases. The slope of the straight lines is inversely proportional to the input intensity.

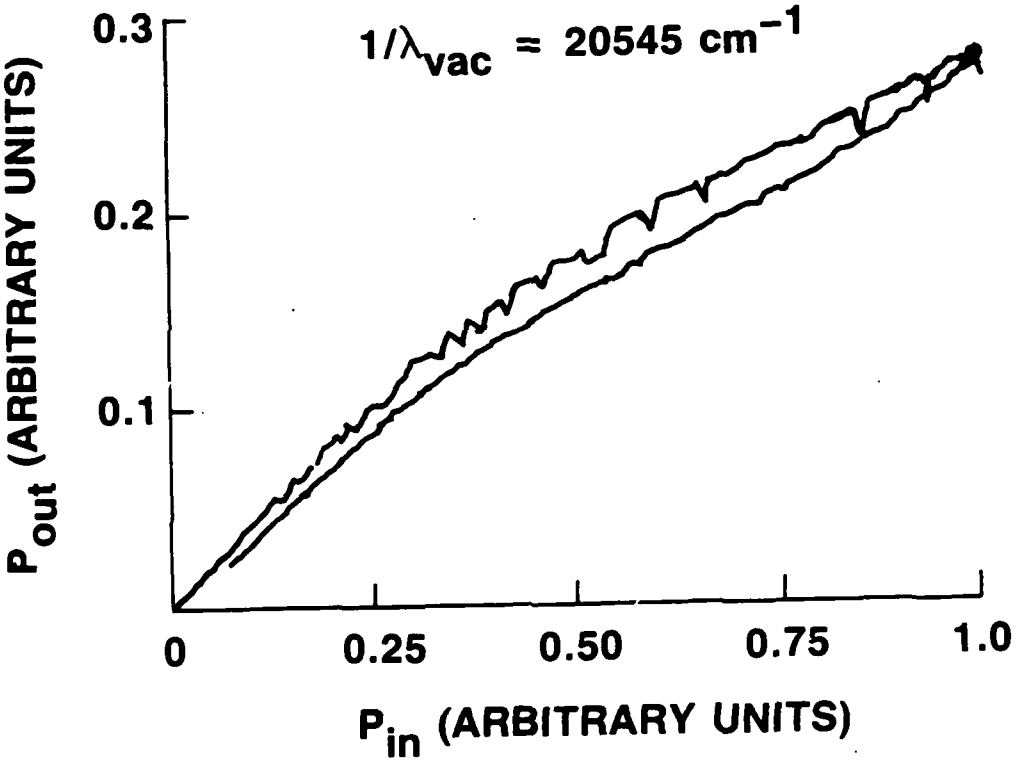

Figure 36. Curve of P_{out} vs P_{in} for a maximum input intensity of ~5 kW/cm^2.

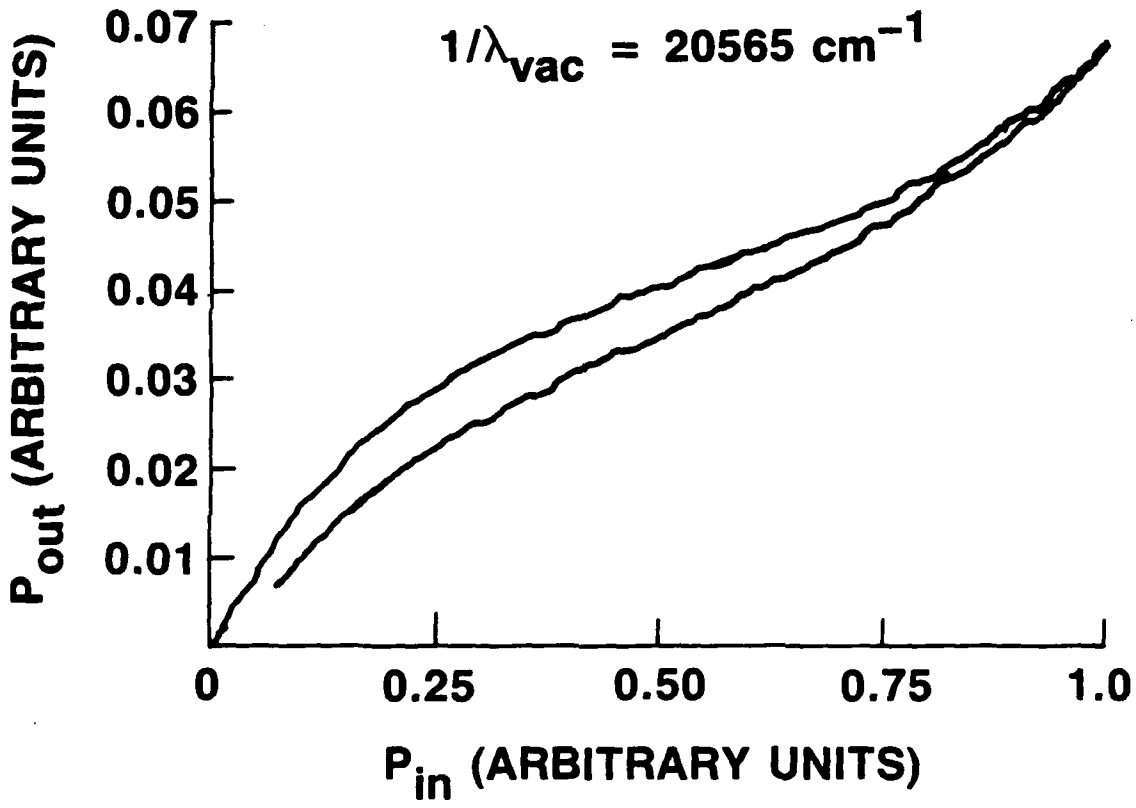

Figure 37. Curve of P_{out} vs P_{in} for a maximum input intensity of ~5 kW/cm².

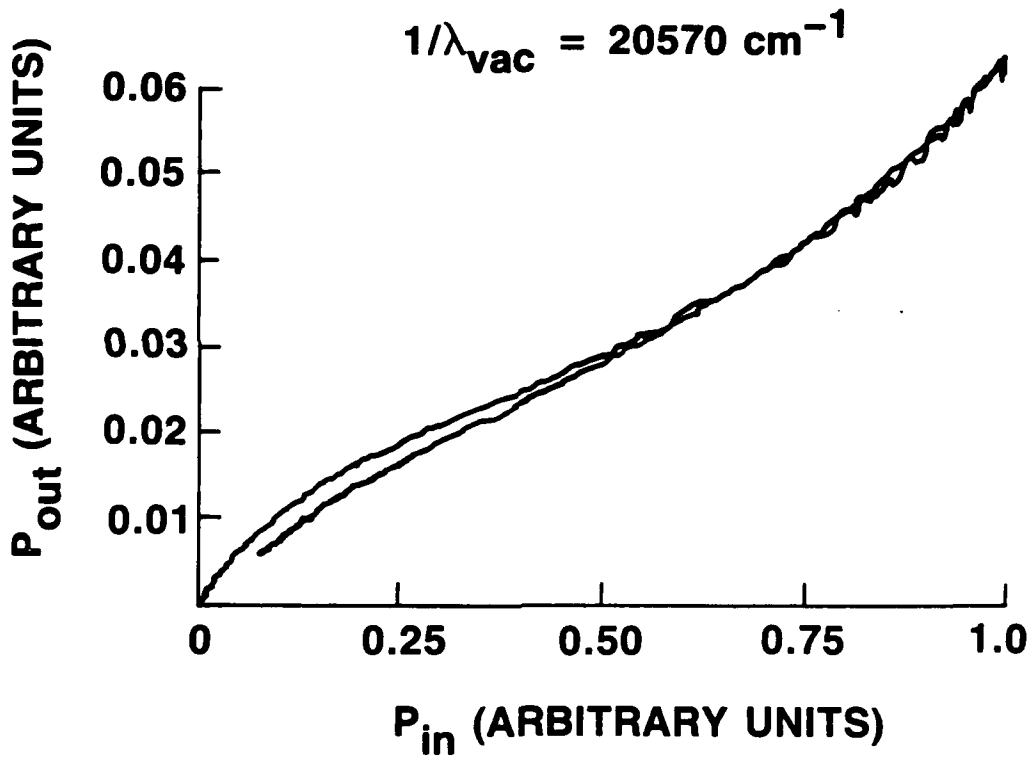

Figure 38. Curve of P_{out} vs P_{in} for a maximum input intensity of ~5 kW/cm².

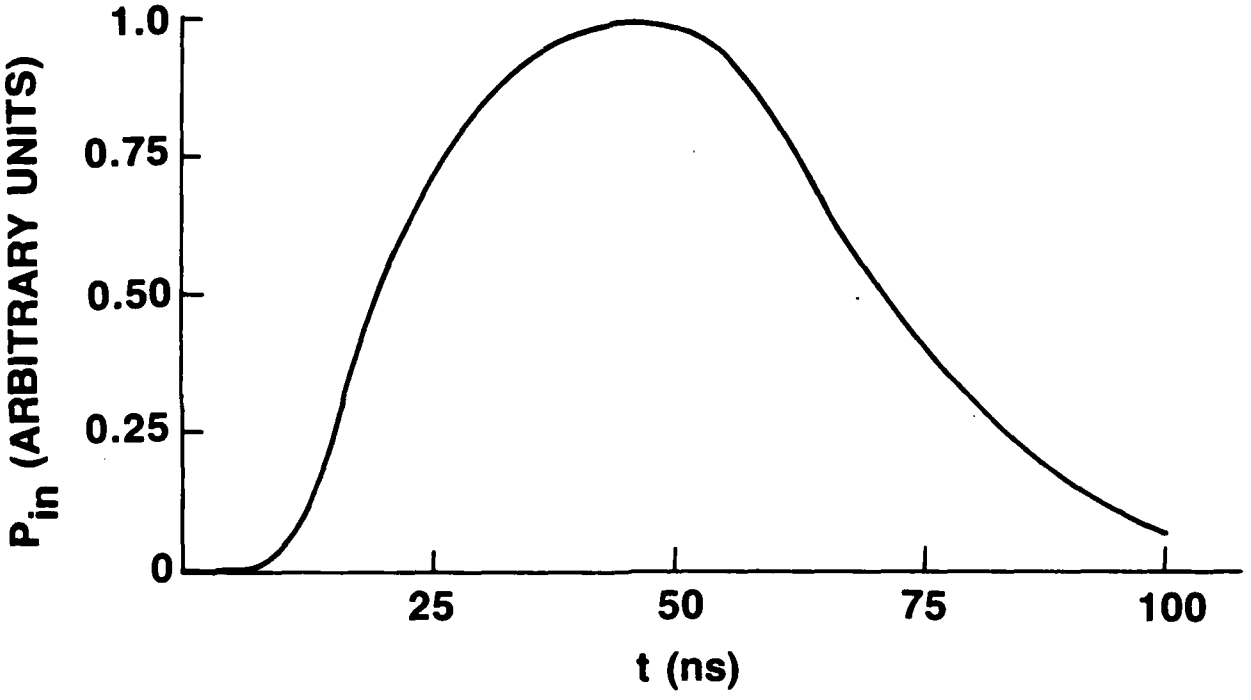

Figure 39. Incident input pulse.

eter is consistent with our previous estimate of this parameter using the technique of ion implantation. A more sophisticated theory is presently being developed to describe the details of these nonlinear transmission measurements.

5.5 TEMPERATURE DEPENDENCE OF NONLINEAR ABSORPTION NEAR FREE EXCITONS

Degenerate four-wave mixing experiments were carried out near the A free exciton in CdS using the apparatus shown in Fig. 40. A four-wave mixing signal was observed up to a temperature of 70 K after which it completely disappeared. The more sensitive technique of nonlinear absorption with a strong pump and a weak probe was then used[28]. These measurements were conducted up to a temperature of 120 K after which the nonlinear signal completely disappeared. The laser beam was modulated at a repetition rate of 10 Khz and at a pulse duration of 2 μs. A typical nonlinear absorption signal is shown in Fig. 41. The oscillations are due to Fabry-Perot interference fringes. Experimentally, it is found that the nonlinear absorption signal shifts much faster with temperature than the band gap does (Fig. 42). This is a clear indication that at the typical intensities used in our experiment (spot diameter at 1/e point = 12 μm, $I<5KW/cm^2$), no evidence for a direct two-photon transition to the biexciton resonance was detected. Since the pulse length and the repetition rate can be arbitrarily varied over a wide range, we were able to determine that the large nonlinear absorption signal near the free exciton resonance has both an intrinsic and thermal contribution. We note that a sample immersed in liquid He can only dissipate the heat generated by laser heating at a rate of $4W/cm^2$. When the sample is not in contact with liquid helium this rate will be orders of magnitude slower. In experiments done at 2K with short pulses (20 to 50 ns) and at intensities of the order 1 KW/cm^2 the ther-

DEGENERATE 4-WAVE MIXING BLOCK DIAGRAM

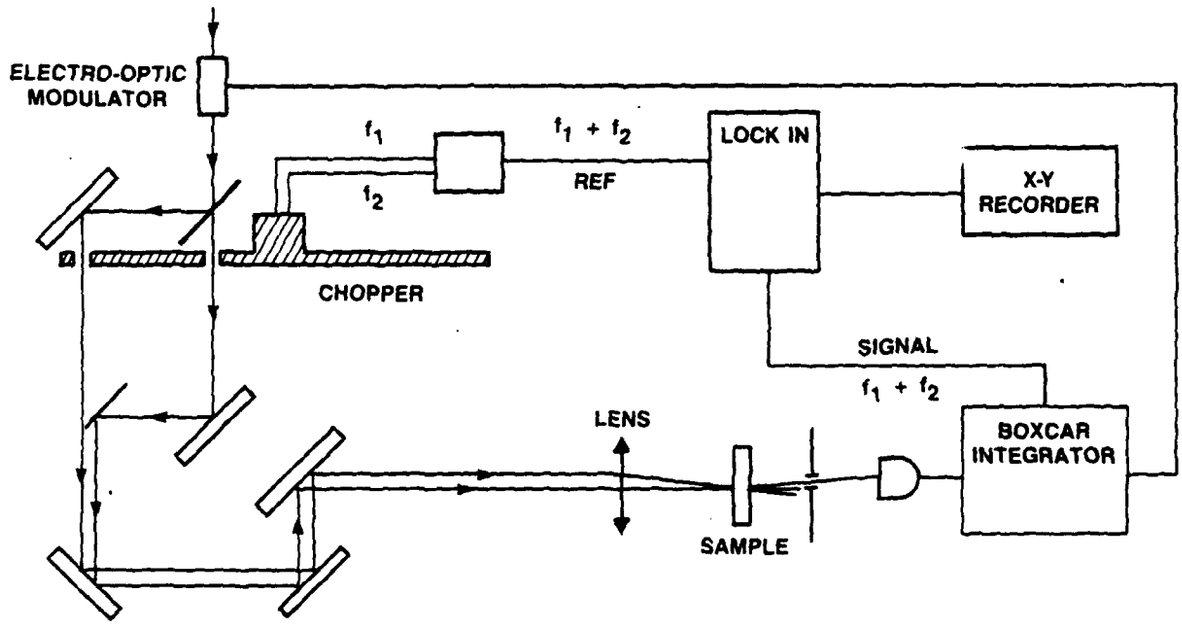

Figure 40

NONLINEAR ABSORPTION NEAR THE A FREE EXCITON IN CdS

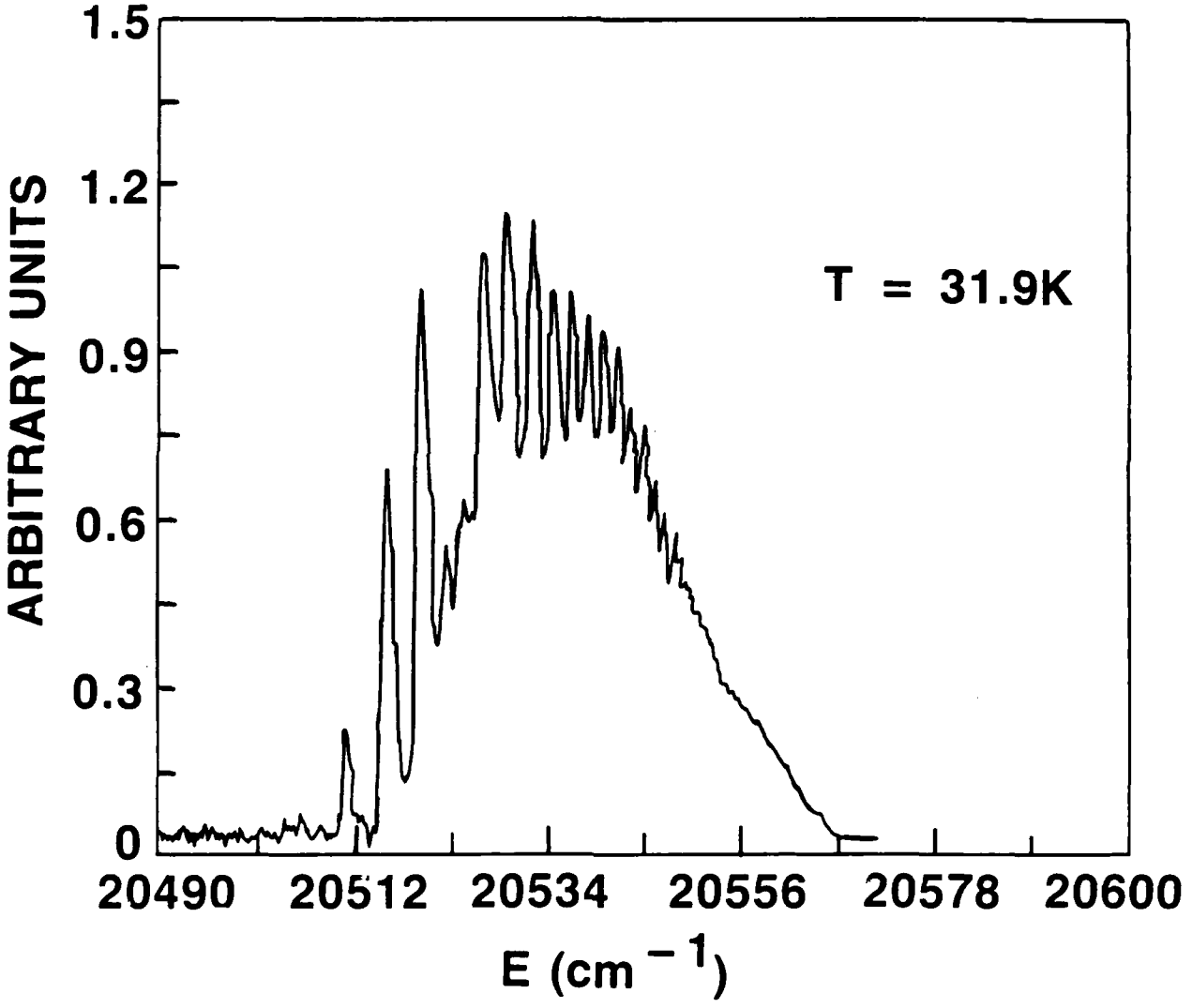

Figure 41(a)

NONLINEAR ABSORPTION NEAR THE A FREE EXCITON IN CdS

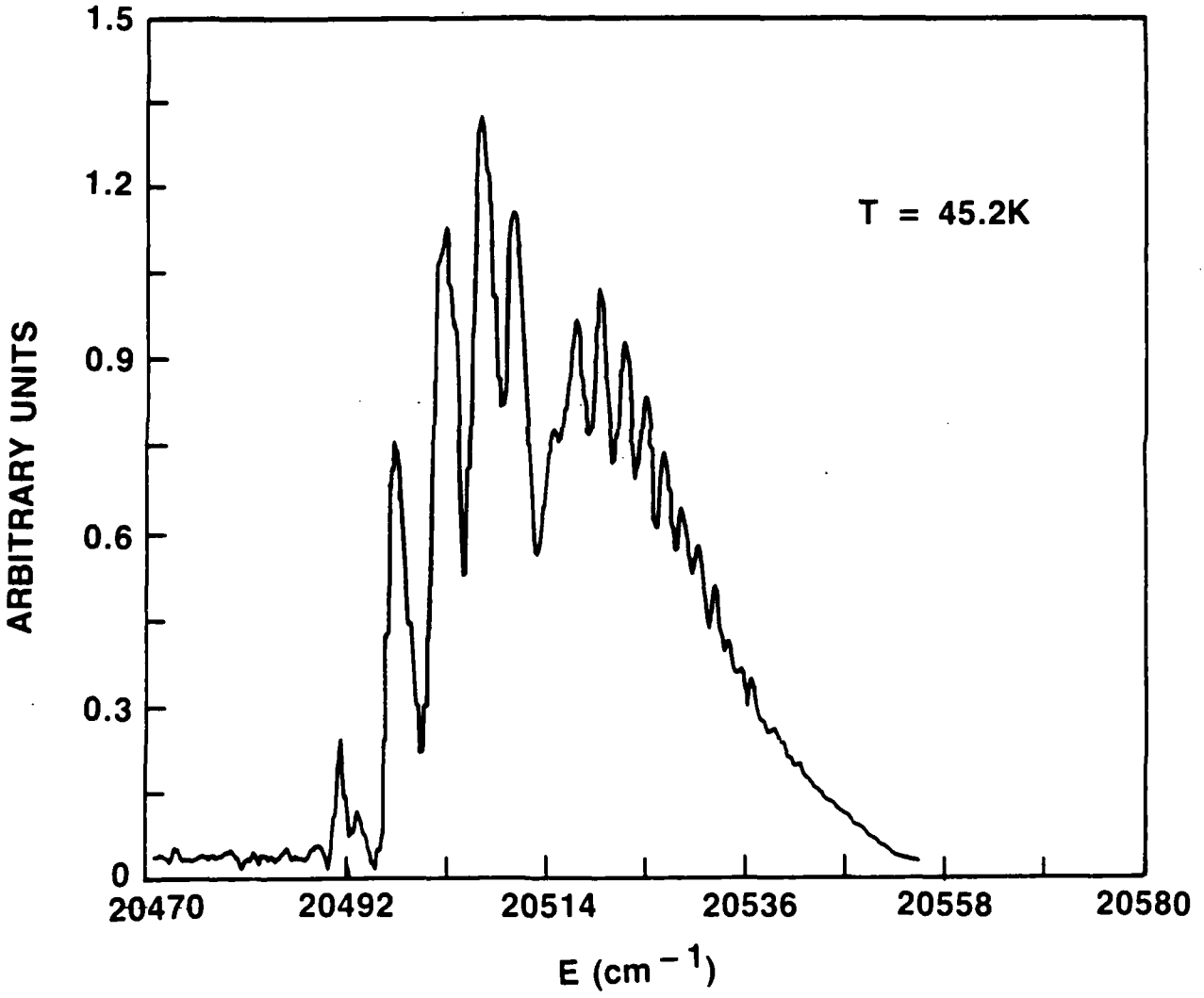

Figure 41(b)

NONLINEAR ABSORPTION NEAR THE A FREE EXCITON IN CdS

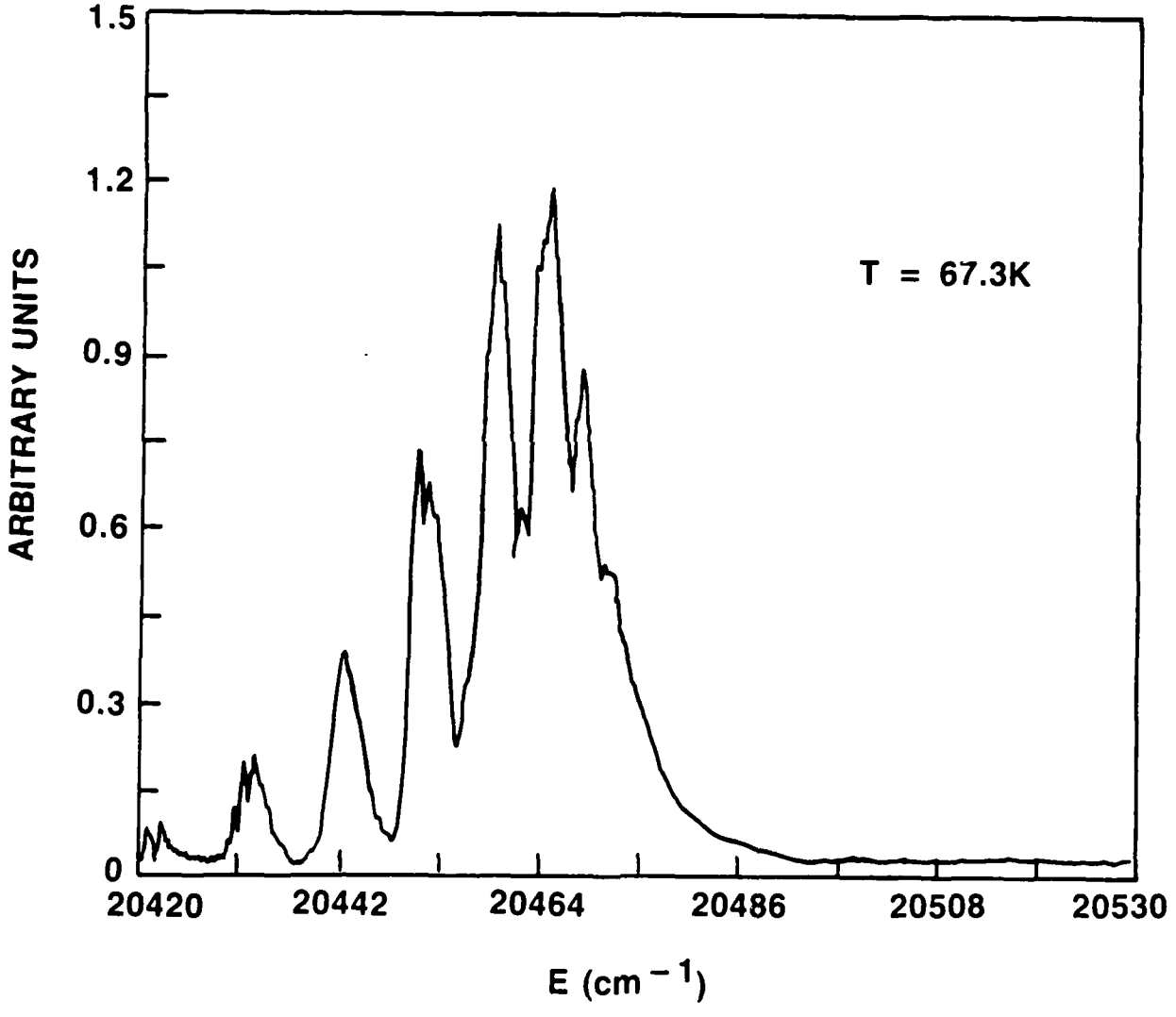

Figure 41(c)

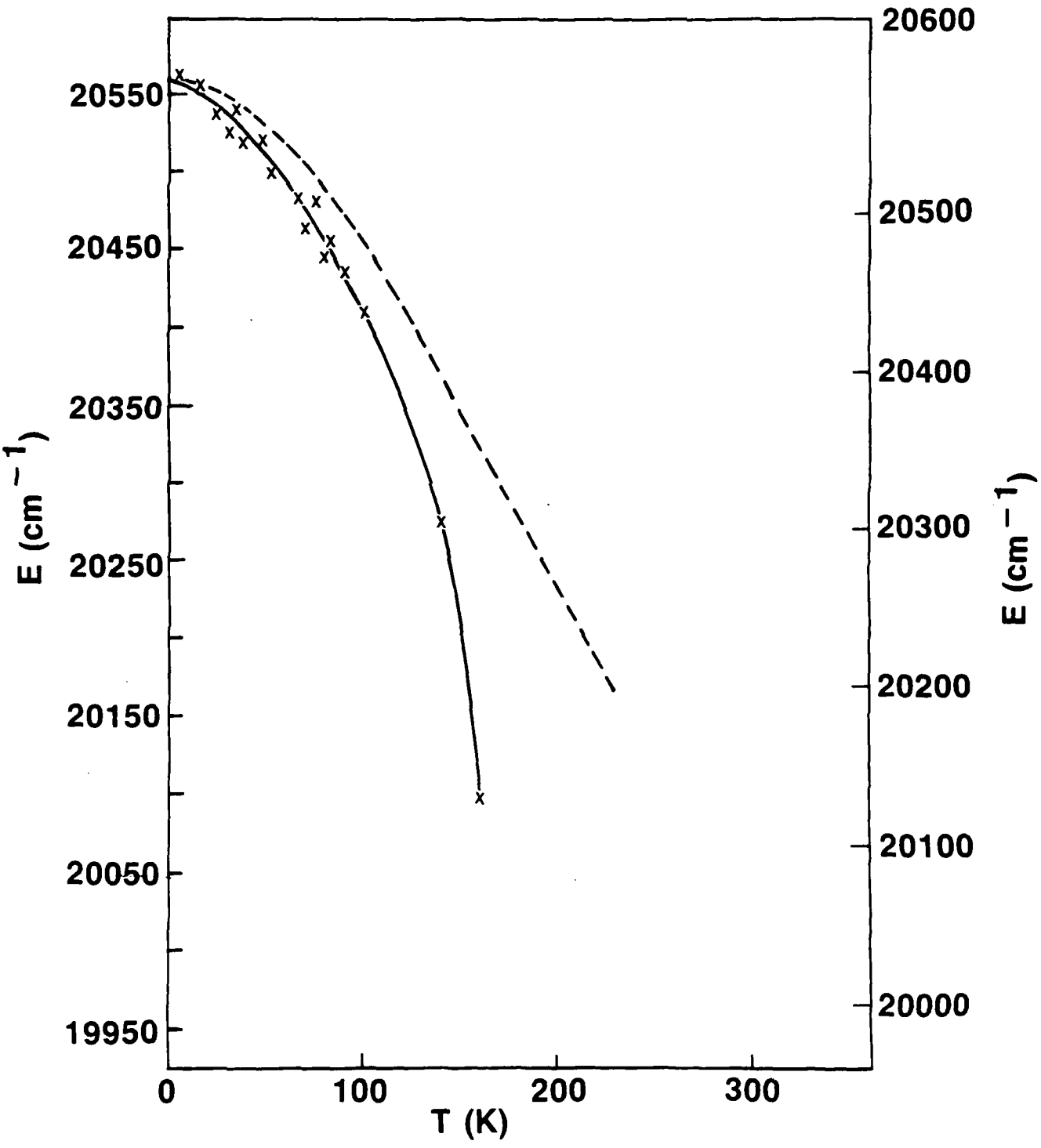

Figure 42. Shift of the nonlinear absorption signal with temperature. The dashed line describes the shift of the bandgap with temperature.

mal contribution can be completely eliminated and the intrinsic nonlinearity due to exciton-exciton collisions is directly measured.

The fact that the nonlinear signal disappears as the temperature increases can be understood by realizing that, as the temperature increases, a substantial amount of LO-phonons contribute to the broadening of the free exciton resonance. This in turn proportionally reduces the importance of the self-broadening due to exciton-exciton collisions. A larger peak intensity is then required to generate the nonlinear signal and thermal effects become more important. For these reasons, optical bistability at room temperature would require much larger powers and thermal effects would play a dominant role in these measurements.

6. CONCLUSIONS AND RECOMMENDATIONS

To optimize optical nonlinear interactions, one should choose as large a transition dipole moment as possible (the shortest t_{spont}) to ensure a fast recovery time of the material, and one should make sure that the radiative decay time t_{spont} is not much different from the energy relaxation time T_1, and that the dephasing time T_2 is as close as possible to 2 T_1[18]. These conditions are closely met in the case of excitons bound to impurities. Bound excitons are known to have a very large oscillator strength, a fast radiative decay and they do not diffuse in the crystal, thus permitting a sharp focussing geometry. Coupling of this strong radiator with the incident laser beam is optimized by working at cryogenic temperatures (T = 2K) since this minimizes the amount of dipole dephasing due to acoustic and optical phonons. Large degenerate four-wave mixing signals and optical bistability was observed near bound excitons. A switching energy of 4 pJ was demonstrated and one of 1 fJ was inferred for a sharp focussing geometry, approaching the fundamental limits. The quantum confined Stark effect of quantum dots was observed for the first time by Stark shifting the bound exciton resonance. New modulator concepts are envisioned.

In nonlinear absorption measurements near the free exciton, the collisional broadening of the free exciton was studied as a function of intensity, detuning and temperature. Linear measurements indicate the very rapid broadening of the free exciton resonance by LO phonons above 50 K and explain why the nonlinear absorption signal near the free exciton grows smaller as the temperature rises. The detuning dependence of the exciton-polariton broadening was studied for the first time.

AD-A174 492 HIGH SPEED LOW POWER NONLINEAR OPTICAL SIGNAL PROCESSING(U) GTE LABS INC WALTHAM MA M DAGENAIS ET AL 15 SEP 86 AFOSR-TR-86-1093 2/2

UNCLASSIFIED F490620-84-C-0052 F/G 20/6 NL

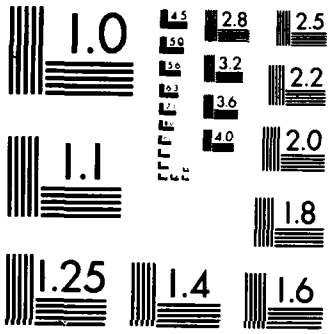

Future fundamental work on CdS is required. One should establish for good the existence or non existence of biexcitons in CdS. If this nonlinear resonance is found, its position should be measured accurately. For intensities less than 10 kW/cm^2, we feel that nonlinear interactions in CdS are well understood. For intensities above 10 kW/cm^2, the situation is reversed and very controversial. One should study in a systematic way the mechanism of e-h plasma screening and of dielectic excitonic screening in CdS. The bimolecular and Auger coefficients should be measured with accuracy.

From the point of view of applications, the switching energy of optical bistable devices based on the bound exciton should be optimized by adjusting the mirror reflectivity, the sample thickness and the bound exciton concentration. The technique for making good ohmic contacts to CdS should be developed and the operation of a very efficient modulator based on Stark shifting the bound exciton resonance should be demonstrated. Fabry-Perot optical bistability using the intrinsic nonlinearity due to free excitons in CdS is not likely to be demonstrated at any power since thermal effects cannot be avoided. We predict that intensities about 2400 times larger than needed in GaAs will be required for observing optical bistability in the vicinity of the free exciton in CdS. A speed improvement of about 30 is also expected. Switching energies about 80 times larger than in GaAs are then anticipated. These predictions use a GaAs Bohr radius of $130A^{o}$ and a carrier lifetime of 30 ns for GaAs and 1 ns for CdS and assume that saturation of the free exciton resonance is required for observing bistability. At these intensities, it is dubious that thermal effects can be avoided. For room temperature operation, III-V materials with their small band gaps appear to be the material of choice for the demonstration of new optical modulators and new optical switching devices. But very interesting physics remain to be understood in large band gap II-VI

materials and might lead to new types of devices. We recommend continued support of large band gap II-VI nonlinear optical material research.

REFERENCES

1. M. Dagenais and W. F. Sharfin, J. Opt. Soc. Am. B2, 1179 (1985).
2. E. I. Rashba and G. E. Gurgenishivili, Sov. Phys. Solid State 4, 759 (1962).
3. C. H. Henry and R. Nassau, Phys. Rev. B1, 1628 (1970) E. J. Rashba, in Excitons at High Density, H. Haken and S. Nikitine, eds. (Springer-Verlag, New York, 1975), Vol. 73, p. 151.
4. G. D. Sanders and Y. C. Chang, Phys. Rev. B28, 5887 (1983) B. Stebe and G. Munschy, Sol. State Comm. 43, 841 (1982) M. Suffczynski and W. Gorzkowski, Phys. Rev. B4, 512 (1971).
5. D. F. Nelson, J. D. Cuthbert, P. J. Dean, and D. G. Thomas, Phys. Rev. Lett. 17, 45 (1966) P. J. Dean and D. C. Herbert in Exitons, K. Cho, ed. (Springer Verlag, New York, 1979), p. 170.
6. T. Takagahara, Phys. Rev. B31, 8171 (1985) T. Shigenari, X. Z. Lu, and H. Z. Cummins, Phys. Rev. B30, 1962 (1984).
7. M. Dagenais, B. S. Elman and W. F. Sharfin, J. Appl. Phys. 58, 1067 (1985).
8. D. G. Thomas and J. J. Hopfield, Phys. REv. 175, 1021 (1968).
9. D. S. Chemla and D. A. B. Miller, J. Opt. Soc. Am. B2, 1155 (1985).
10. M. Dagenais, Appl. Phys. Lett. 43, 742 (1983).
11. See Chapter 8 in A. Yariv, Quantum Electronics (Wiley, New York, 1975).
12. M. Dagenais and W. F. Sharfin, Appl. Phys. Lett. 45, 210 (1984).
13. H. E. Schmidt, H. Haug and S. W. Koch, Appl. Phys. Lett. 44, 787 (1984).
14. K. Bohnert, H. Kalt, and C. K. Klingshirn, Appl. Phys. Lett. 43, 1088 (1983) K. Bohnert, F. Fidorra, and C. Klinghshirn, Z. Phys. B 57, 263

(1984) ; F. Fidorra, M. Wegener, J. Y. Bigot, B. Honerlage, and C. Klingshirn, Jnl. of Luminescence 35, 43 (1986).

15. Hoang Yuan Nguyen ane R. Zimmermann, Phys. Status Solidi (b) 124, 191 (1984).

16. M. Dagenais and W. F. Sharfin, Appl. Phys. Lett. 46, 230 (1985).

17. D. A. B. Miller, J. S. Weiner, and D. S. Chemla, IEEE J. Quantum Electron OE-22, 1816 (1986).

18. M. Dagenais and W. F. Sharfin, Opt. Eng. 25, 219 (1986).

19. D. G. Thomas and J. J. Hopfield, Phys. Rev. 124, 657 (1961).

20. H. E. White, Introduction to Atomic Spectra (McGraw-Hill, New York, 1934), p. 402; L. I. Schiff, Quantum Mechanics (McGraw-Hill, Tokyo, 1968), p. 263.

21. M. Dagenais and H. G. Winful, in Optical Bistability 2, edited by C. M. Bowden, H. M. Gibbs and S. L. McCall (Plenum, 1984), p. 267.

22. J. L. Jewell, H. M. Gibbs, S. S. Tarng, A. C. Gossard and W. Wiegmann, Appl. Phys. Lett. 40, 291 (1982).

23. See for instance: Ref. 13; F. Fidorra, M. Wegener, J. Y. Bigot, B. Honerlage, and C. Klingshirn, Jnl. of Luminescence 35, 43 (1986) and references therein ; F. Henneberger and H. Rossmann, Phys. Stat. Sol. 121, 685 (1984) ; Ref. 14.

24. R. F. Leheny, J. Shah, and G. Carina Chiang, Solid State Comm. 25, 621 (1978) H. Schrey, V. G. Lyssenko, and C. Klingshirn, Solid State Comm. 32, 897 (1979) ; Ref. 15; Ref. 16; A. Kuroiwa, H. Saito, and S. Shionoya, Solid State Comm. 18, 1107 (1976) R. Planel and C. Benoit a la Guillaume, Phys. Rev. B15, 1192 (1977) M. V. Lebedev and V. G. Lysenko, Sov. Phys. Solid State 25, 682 (1983) R. Baumert, I. Broser, and K. Buschick, IEEE J. of Quantum Electr. QE-22, 1539 (1986) H. Kalt, V. G.

Lyssenko, R. Renner, and C. Klingshirn. J. Opt. Soc. Am. B2, 1188 (1985) ; H. Kalt, R. Renner, and C. Klingshirn, IEEE J. Quantum Electr. QE-22, 1312 (1986) ; V. Nozue, T. Itoh and M. Ueta, Jnl. of Physical Society of Japan 44, 1305 (1978) A. Maruani, D. S. Chemla, E. Batifol, Sol. State Commun. 33, 805 (1980) I. Abram, J. Opt. Soc. Am. B2, 1204 (1985) H. Saito and E. O. Gobel, Phys. Rev. B31, 2360 (1985) ; E. O. Gobel in Nonlinear Optics: Materials and Devices, edited by C. Flytzanis and J. L. Oudar (Springer, 1986), p. 104.

25. M. Dagenais, Appl. Phys. Lett. 45, 1267 (1984).
26. M. Dagenais, A. Surkis, W. F. Sharfin, and H. G. Winful, IEEE J. Quantum Electron QE-21, 1458 (1985).
27. F. Fidorra, M. Wegener, J. Y. Bigot, B. Honerlage and C. Klingshirn, Jnl. of Luminescence 35, 43 (1986).
28. M. Dagenais and W. F. Sharfin in Optical Bistability III, edited by H. M. Gibbs, P. Mandel, M. Peyghambarian and S. D. Smith (Springer, 1986), p. 122.

ACKNOWLEDGEMENTS

The authors of this report wish to thank Mr. John Greene, Jr. and Mr. Peter Ketteridge for their expert technical assistance. The authors would also like to acknowledge many useful discussions with Drs. H. G. Winful, Dr. E. Koteles, and Dr. Boris Elman, and the enthusiastic support of the program manager, Dr. Robert J. Seymour. Further thanks go to Dr. D. C. Reynold from Wright-Patterson Air Force Base for having supplied the high optical quality CdS crystals used in these studies.

AFOSR Contract Conference Papers

1. "Low Switching Energy Optical Bistable Devices", M. Dagenais and W. F. Sharfin, Invited paper, Annual Meeting, Opt. Soc. of Am., Seattle, WA (October 1986).
2. "Linear and Nonlinear Optical Properties of Free Excitons in CdS", M. Dagenais and W. F. Sharfin, IQEC '86, San Francisco, CA (June 1986).
3. "Fast Response and Low Power Optical Switching in CdS and Laser Amplifiers", M. Dagenais and W. F. Sharfin, NSF Meeting, Tucson, AZ (May 1986).
4. "Extremely Low Optical Switching Energy Nanosecond Response Bistable Devices", M. Dagenais and W. F. Sharfin, SPIE OE Lase '86, Los Angeles, CA (January 1986).
5. "Fast All-Optical Switching at Extremely Low Switching Energy in CdS Platelets", M. Dagenais and W. F. Sharfin, Optical Soc. of America Topical Meeting on Optical Bistability, Tucson, AZ (December 1985).
6. "Giant Nonlinearities with Fast Response: Ion Implementation of Bound Excitons in CdS and Applications in Bistable Devices", M. Dagenais, W. F. Sharfin, and M. Prise, 1985 Materials Research Symposium, Boston, Dec. 1985.
7. "Forward Degenerate Four-Wave Mixing Near Bound Excitons in CdS", M. Dagenais, M. Prise, and W. F. Sharfin, 1985 Annual Meeting of the Optical Society of America, Washington, DC, Oct. 1985.
8. "Intracavity Optical Bistability in the Presence of an Optically Induced Absorption", M. Dagenais, A. Surkis, W. F. Sharfin, and H. G. Winful, 1985 Annual Meeting of the Optical Society of America, Washington, DC, Oct. 1985.

9. "Nonlinear Properties of Free and Bound Excitons in CdS", M. Dagenais, W. F. Sharfin, S. Eddins and B. Elman, Invited Paper, Gordon Conference on Nonlinear Optics, Wolfeboro, NH (July 1985).

10. "Picojoule, Subnanosecond All-Optical Switching in a CdS Etalon", M. Dagenais and W. F. Sharfin, CLEO '85, Baltimore, MD (May 1985).

11. "Commutations Rapides a Basse Energie et Bistabilite-Optique dans CdS", M. Dagenais and W. F. Sharfin, Conference on "Aspects Temporels des Phenomenes Nonlineares et Commutations Cptiques Ultrarapides", Orsay, France (March 1985).

12. "Low Power Optical Bistability Near the Band Gap in Cadmium Sulfide", W. F. Sharfin and M. Dagenais, 7th International Conference on Lasers and Applications, San Francisco, CA (Nov. 1984).

13. "Low Power Optical Bistability in Cadmium Sulfide Platelets", M. Dagenais and W. F. Sharfin, IQEC '84, Anaheim, CA (June 1984).

14. "Giant Bound Exciton Nonlinearities and Observation of Transverse Bistability and Self-Pulsation in Cadmium Sulfide", (with M. Dagenais and H. G. Winful), Gordon Research Conference on Nonlinear Optics and Lasers, Wolfeboro, NH (August 1983).

Patents

1. "Optical Bistable Devices Based on Bound Exciton Nonlinearity," M. Dagenais and W. F. Sharfin, patent pending.

Publications

1. "Extremely Low Optical Switching Energy Nanosecond Response Bistable Devices," M. Dagenais and W. F. Sharfin, Proc. SPIE, Opt. Comput. 625, p. 94 (1986).
2. "Fast All-Optical Switching at Extremely Low Switching Energy in CdS Platelets," M. Dagenais and W. F. Sharfin, in Optical Bistability III, H. M. Gibbs, P. Mandel, N. Peyghambarian, and S. D. Smith, Eds., Springer-Verlag, NY, p. 122 (1986).
3. "Extremely Low Switching Energy Optical Bistable Devices," M. Dagenais and W. F. Sharfin, Opt. Eng. 25, p. 219 (1986).
4. "Giant Nonlinearities with Fast Response: Ion Implantation of Bound Excitons in CdS and Applications in Bistable Devices," M. Dagenais, M. Prise, and W. F. Sharfin, in Nonlinear Optical Materials - Proc. Mater. Res. Conf., D.A.B. Miller, Ed. (1985).
5. "Generation of New Bound Exciton Lines by Lithium Implantation of CdS," M. Dagenais, B. S. Elman, and W. F. Sharfin, J. Appl. Phys. 58, p. 1067 (1985).
6. "Very Fast, Picojoule Optical Switching in a CdS Etalon," W. F. Sharfin and M. Dagenais, Proc. Int. Conf. on Lasers '84, p. 187 (1985).
7. "Intra-Cavity Optical Bistability Due to Thermally Induced Changes in Absorption and Refraction," M. Dagenais, Alisa Surkis, W. F. Sharfin, and H. G. Winful, IEEE J. Quantum Electron 21, p. 1458 (1985).
8. "Linear and Nonlinear Optical Properties of Free and Bound Excitons in CdS and Applications in Bistable Devices," M. Dagenais and W. F. Sharfin, J. Opt. Soc. Am. B2, (1985).
9. "Picojoule, Subnanosecond, All-Optical Switching Using Bound Excitons in CdS," M. Dagenais and W. F. Sharfin, Appl. Phys. Lett. 46, p. 230 (1985).

10. "Optical Hysteresis in Fast Transient Experiments Near the Band Gap of Cadmium Sulfide," M. Dagenais, Appl. Phys. Lett. 45, p. 1267 (1984).

11. "Giant Nonlinearities and Low Power Optical Bistability in Cadmium Sulfide Platelets," M. Dagenais, Phil. Trans. R. Soc. Lond. A313, p. 265 (1984).

12. Cavityless Optical Bistability Due to Light Induced Absorption in Cadmium Sulfide," M. Dagenais and W. F. Sharfin, Appl. Phys. Lett. 45, p. 210 (1984).

Manuscripts in Preparation:

1. M. Dagenais and W. F. Sharfin, "Quantum Confined Stark Effect of Quantum Dots in CdS"
2. M. Dagenais and W. F. Sharfin, "Measurement of the Exciton-Polariton Damping Dispersion in CdS"
3. M. Dagenais and W. F. Sharfin, "Temperature Dependence of the Exciton-Polariton Damping Dispersion in CdS"
4. M. Dagenais and W. F. Sharfin, "Nonlinear Optical Absorption and Free Exciton Self-Broadening in CdS"
5. M. Dagenais and W. F. Sharfin, "Time Dependence of an Optically Induced Free Exciton Self-Broadening in CdS"
6. M. Dagenais and W. F. Sharfin, "Free Exciton Broadening by Impurities and Defects in CdS"

END

12-86

DTIC